THE ROLE OF INVERTASES IN ANTHER DEHISCENCE

Marie Komrsová BSc

Thesis submitted to the University of Nottingham for the degree of Master of Philosophy

August 2022

Abstract

The opening of anthers to release pollen (anther dehiscence) is a complex, regulated process. One of the mechanisms contributing to anther dehiscence is the active removal of water from anthers. Invertases are plant enzymes which cleave sucrose into glucose and fructose, changing the osmotic potential, suggesting they may have a role in water movement in the anthers. Invertase expression has been investigated by qRT-PCR in *A. thaliana* buds of different developmental stages to determine which genes are upregulated as dehiscence happens. As jasmonic acid has been shown to regulate water movement in anther dehiscence, the expression of invertases in a *dad1*, the *A. thaliana* mutant which does not produce jasmonic acid, and the phenotypes of *A. thaliana* invertase KO mutants have also been investigated. Invertase isoforms *INVH, INVD, CWINV2,* and *CWINV4* are upregulated in *A. thaliana* buds during late stages but downregulated in the absence of JA, while *CINV2* and *VACINV* are upregulated in absence of JA. Single knockout mutants in these genes however did not show a striking phenotype, but the expression patterns of closely related genes indicate they may be acting redundantly. Double mutant *cwinv2cwinv4* did not have an impaired phenotype, so CRISPR/Cas9 gene targets were instead explored as an option to produce quadruple mutant *cwinv1cwinv2cwinv4cwinv5.* β-glucuronidase reporter constructs have been prepared to investigate the localization of *INVH, INVD, CWINV2, CWINV4, CINV2 and VACINV* throught flower development in WT and in *dad1*.

List of abbreviations

- µg: microgram
- µl: microlitre
- A/N-Inv: Alkaline/neutral invertases
- cDNA: Complementary Deoxyribonucleic acid
- CW-Inv: cell wall bound invertase
- DAD1: Defective Anther Dehiscence 1
- DAPI: 4',6-diamidino-2-phenylindole
- DNA: Deoxyribonucleic acid
- dNTP: Deoxynucleotide Triphosphate
- EtOH: Ethanol
- GA: Gibberellic acid
- GUS: β-glucuronidase
- h: hour(s)
- HCl: Hydrochloric acid
- Het: Heterozygous
- Hm: Homozygous
- JA: Jasmonic acid
- Kb: kilobase pair
- l: Litre
- LB: Luria Broth
- m: metre
- M: molar
- min: minute(s)
- ml: millilitre
- mM: millimolar
- mRNA: Messenger Ribonucleic acid
- MS: Murashige and Skoog Basal Medium
- ng: nanogram
- OE: Overexpression
- PCR: Polymerase Chain Reaction
- PIP: Plasma Membrane Intrinsic Protein
- PMI: Pollen Mitosis I
- PMII: Pollen Mitosis II
- qRT-PCR: Quantitative Reverse-Transcriptase Polymerase Chain Reaction
- RNAi: RNA interference
- RT: Room Temperature
- s: second(s)
- T-DNA: Transfer DNA
- v: volume
- Vac-Inv: Vacuolar invertase
- w: weight
- wt: Wild type

List of figures

List of tables

Contents

Chapter 1: Introduction

1.1 Anther and pollen development in A. thaliana

Pollen is formed within organs called anthers on plant stamens. Stamen and anther anatomy varies across angiosperms and is often used as a taxonomic tool. Many species have developed diverse additional functions to their stamens; however, the development and overall structure are conserved (Åstrand et al., 2021).

Arabidopsis thaliana (family *Brassicaceae*) is a widely used model plant. Its flowers are representative of a typical eudicot flower with its organs arranged in four concentric whorls arising from the floral meristem according to the ABCDE model (Robles and Pelaz, 2005). The outermost whorl contains four sepals, the next four petals, the third whorl contains four medial (long) and two lateral (short) stamens and at the centre of the flower is a gynoecium with two carpels (Fig. 1-1).

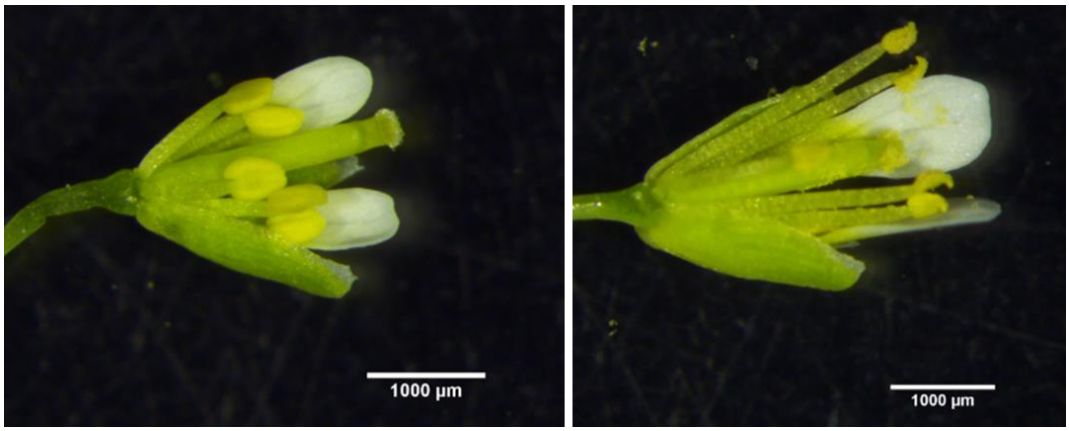

Figure 1-1. Anther dehiscence and pollen release in *A. thaliana* flower

maturing flower (left); flower after dehiscence (right)

1.1.1 Anther structure and development

Anthers are supported at the apex of the stamen by a filament. Anthers have two locules, each containing two lobes separated in the middle by the septum. Each lobe contains sporogenous cells in the centre, surrounded by four maternal cell layers: epidermis, endothecium, middle layer, and tapetum.

Mature pollen is released from the anthers in a process termed anther dehiscence. Similar to silique dehiscence and release of seeds, this process involves the structure splitting open along a specific site of weakness termed stomium.

The synchronized development of the anther layers, the anther, and of pollen itself has been characterized in 14 stages describing the major developmental events by Sanders *et al*. and shown in Table 1-1 below (Sanders et al., 1999).

Table 1-1 Anther developmental stages in *A. thaliana* (adapted from Sanders *et al*., 1999)

Ar, archesporial; C, connective; E, epidermis; En, endothecium; L1, L2, and L3, the three cell layers of the stamen primordia; MC, meiocyte; ML, middle layer; MMC, microspore mother cell; MSp, microspore; 2°P, secondary parietal layer; PG, pollen grains; Sm, septum; Sp, sporogenous cells; St, stomium; T, tapetum; Tds, tetrads; V, vascular

Anther stage	Major events and morphological markers	Tissues present		
1	Stamen primordia emerge, consisting of three cell layers.	L1	L2	L3
2	Archesporial cells arise in layer 2 of stamen primordia.	E	Ar	
3	Primary parietal and primary sporogenous layers derived from archesporial cells. Further divisions of each layer generate the secondary parietal layers and sporogenous cells, respectively.	E	2°P, Sp	
4	Four-lobed anther pattern with two developing stomium regions present. Vascular region initiated.	E	En, ML, T, Sp,	C, V
5	Four clearly defined locules established. All anther cell types present, and pattern of anther defined. Microspore mother cells appear.	E	En, ML, T, MMC	C, V
6	Microspore mother cells enter meiosis. Middle layer is crushed and degenerates. Tapetum becomes vacuolated and the anther undergoes a general increase in size.	E	En, ML, T, MC	C, V
7	Meiosis completed, generating tetrads of haploid microspores. Remnants of middle layer present.	E	En, ML, T, Tds	C, V
8	Callose wall surrounding tetrads degenerates and individual microspores released.	E	En, T, MSp	C, V
9	Growth and expansion of anther continue. Microspores generate an exine wall and become vacuolated. Septum cells can be distinguished.	E	En, T, MSp, Sm	C, V
10	Tapetum degeneration initiated.	E	En, T, MSp, Sm	C, V
11	Pollen mitotic divisions occur. Tapetum degenerates. Expansion of endothecial layer. Secondary thickenings or “fibrous bands” appear in endothecium and connective cells. Septum cell degeneration initiated. Stomium differentiation begins.	E, St	En, T, PG, Sm	C, V
12	Anther contains tricellular pollen grains. Anther becomes bilocular after degeneration and breakage of septum below stomium. Differentiated stomium.	E, St	En, PG	C, V
13	Breakage along stomium. Anther walls retract, locules are open and pollen is released.	E	En, PG	C, V
14	Senescence of stamen. Shrinkage of cells and anther structure.	E	En	C, V
15	Stamen falls off senescing flower.			

1.1.2 Opening of anther

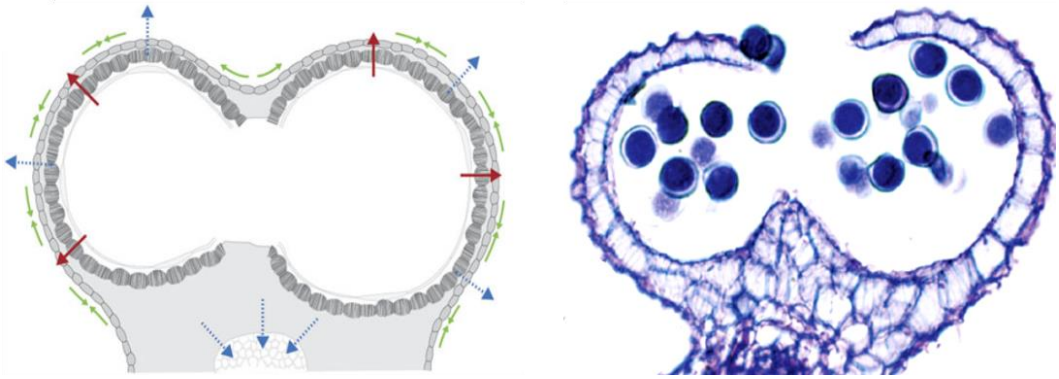

Figure 1-2 Diagram of forces involved in dehiscence and a transverse section of *A. thaliana* anther.

Green arrows: shrinkage of epidermal cells; red arrows: pressure from expanding pollen; blue arrows: movement of water evaporating via stomata and active transport. Adapted from Wilson *et al*., 2011

The opening of the anther involves several mechanisms working together to increase tension on the stomium, leading to the rupture of the anther wall (Fig. 1-2). Initially the secondary thickening of the endothecium and expansion of the pollen, along with the enzymatic lysis of the septum, lead to the breakage of the septum and the anther forming a single locule. The subsequent shrinkage of the anther wall caused by dehydration leads to further increase of tension at the stomium, finally leading to stomium breakage and anther opening (Wilson et al., 2011)

1.1.2.1 Secondary thickening of endothecium

Secondary thickening of the endothecium refers to deposits of fibrous bands, which appear in stage 11 of anther development in *Arabidopsis*. These bands consist of lignin and cellulose and are deposited along the endothecium except at the stomium and the septum (Dawson et al., 1999). As the locule expands with expanding pollen and the swelling of the epidermis and the endothecium adjacent to the septum, the secondary endothecial thickening restricts this expansion. This causes the locule walls to bend inwards, and along with enzymatic lysis contributes to the breakage of the septum (Wilson et al., 2011).

Afterwards, the epidermis becomes dehydrated and contracts. The endothecium stays relatively stiff, and this interplay of mechanical forces leads to the locule walls bending outward and the anther opening (Nelson et al., 2012).

The requirement for endothecium thickening has been demonstrated in mutants in *MYB26/MALE STERILE35* (Dawson et al., 1999) and *NST1* (*NAC SECONDARY WALL THICKENING PROMOTING FACTOR 1*) and *NST2* (Mitsuda et al., 2005). The lack of secondary thickening in these *myb26* and *nst1nst2* mutants leads to their non-dehiscence and sterility, despite their pollen being viable. Overexpression of *MYB26* (Yang et al., 2007b) and *NST1*, *NST2* (Mitsuda et al., 2005) causes an ectopic secondary thickening phenotype. MYB26 protein is localized specifically to the

anther endothecium nuclei, and it up-regulates both *NST1* and *NST2* expression (Yang et al., 2017). This suggests that the downstream pathways involved in secondary endothecium thickening (lignin and cellulose biosynthesis) are conserved between floral and vegetative tissues.

1.1.2.2 Stomium split

Stomium breakage from tension generated by bending of locule walls also involves the degeneration of cells to create a site of weakness through enzymatic cell wall breakdown of the septum and tapetal programmed cell death at the septum and stomium (Wilson et al., 2011).

Tapetal development and breakdown involves regulation by transcription factors *DYSFUNCTIONAL TAPETUM1* (*DYT1*) (Zhu et al., 2015), *DEFECTIVE IN TAPETAL DEVELOPMENT AND FUNCTION1* (*TDF1*) (Lou et al., 2018), *MALE STEILITY1* (*MS1*) (Yang et al., 2007a), *ABORTED MICROSPORES* (*AMS*) (Ferguson et al., 2017; Xu et al., 2014a), *MYB80* (Xu et al., 2014b), *MYB2* (Guo et al., 2022).

1.1.2.3 Anther wall dehydration

It has been suggested that anther dehydration is facilitated by evaporation through stomata, since it can be affected by relative humidity as observed on the anthers in *G. verrucosa* (Keijzer, 1987). Research in tomato anther dehiscence suggests that transpiration does not play a major role because tomato anthers lack stomata; instead, water is thought to be exported from anthers along an osmotic gradient established by conversion of starch to sugars (Bonner and Dickinson, 1990). In *Allium triquetrum*, it is reported that while anther opening does not require evaporation and seems to be due to dehydration through water movement, the subsequent outward bending of the anther wall was facilitated by evaporation (García et al., 2006).

1.2 Water movement

Water movement in plants is influenced by several factors. On the most basic level, water movement is driven by differences in osmotic potential between compartments permeable to water. Between cells, water can travel through water channels in the plasma membrane: aquaporins, intercellular cytoplasmic junctions: plasmodesmata, and at a low rate also directly across the cell membrane (Beauzamy et al., 2014).

1.2.1 Aquaporins

Aquaporins localized on the plasma membrane are termed PIPs (plasma membrane intrinsic proteins). The extent to which PIPs are required for anther dehiscence seems to vary between different plant species. In tobacco, silencing of aquaporins of the *PIP2* class by RNA interference led to a delay in anther dehiscence and slower efflux of water from the anthers as compared to wild type (Bots et al., 2005). *Arabidopsis* double and triple KO mutant lines *pip1;2pip2;1* and *pip1;2pip2;1pip2;6* showed reduced seed set compared to wild type (Dennis, 2017). In these cases, fertility was only reduced. By contrast, in lily, silencing of *LoPIP2* prevented anther dehiscence completely (Tong et al., 2013). In a comparative transcriptome analysis

of fertile and sterile eggplant lines, aquaporins *PIP2-1* and *PIP1-1* were identified as downregulated among the differentially expressed genes in anthers (Yuan et al., 2021).

1.2.2 Osmoregulation

The osmotic potential can be actively modulated in the plant by changing the concentrations of osmotically active ions, carbohydrates or amino acids (Beauzamy et al., 2014).

1.2.2.1 Ions

Ion flux across cell plasma and intracellular membranes is modulated by ion transporters such as H+-pumps and cation/H+ antiporters. The class of antiporters most relevant to water transport are Na+/H+ antiporters (NHXs), which pump H+ out of the vacuole and Na+ as well as K+ into the vacuole, which then drives water movement into the vacuole (Beauzamy et al., 2014).

Arabidopsis antiporters NHX1 and NHX2 have been shown to have a role in dehiscence. Double knock-out plants *nhx1nhx2* had significant defects in cell elongation, including failure to elongate their filaments enough to reach the stigma for pollination to occur and failure in stomia rupture (Bassil et al., 2011). Bassil et al. propose that the lack of filament extension could be the due to insufficient K+ accumulation in the vacuole of filament cells, which is necessary for filament extension (Heslop-Harrison and Heslop-Harrison, 1996). The *nhx1nhx2* phenotype could be partly rescued by application of Na+ (by watering the plants with NaCl solution) but not with K+, suggesting that other vacuolar transporters were able to compensate for the K+ accumulation requirement with Na+ (Bassil et al., 2011).

1.2.2.2 Carbohydrates

Carbon captured in photosynthesis is transported from source tissues in the form of sucrose and stored in the form of polysaccharides. Changes in the concentration of a carbohydrate through its import or export can drive water movement. It has been suggested that in *A. thaliana*, an osmotic gradient required for anther dehiscence is established by the sucrose transporter *AtSUC1* (Stadler et al., 1999).

Osmotic potentials can alternatively be influenced by breakdown of a complex carbohydrate. To be utilized in the sink tissues by the plant, sucrose (a disaccharide) must be hydrolysed either irreversibly by invertase, or reversibly by sucrose synthase (Barratt et al., 2009). Sucrose synthase (SUS) functions predominantly in storage sinks and cleaves sucrose into fructose and UDP-glucose. Invertase cleaves sucrose into glucose and fructose, and operates in growing sinks, such as elongating stems and roots (Sergeeva et al., 2006). In *Petunia*, water is retracted from anthers to the nectaries during dehiscence, possibly due to conversion of starch to sugars involving *NECTARY1* (*NEC1*) and *NEC2*, which build up the necessary osmotic pressure (Ge et al., 2000, 2001).

1.3 Project aims

The aim of this project is to investigate the potential role of invertases in anther dehiscence. Their proposed role is in establishing the osmotic gradient required for anther dehydration by creating a high-solute environment outside of the anther wall by the irreversible hydrolysis of sucrose. The resulting hexoses require more water molecules to hydrate them than the original sucrose, and this change in osmotic potential can then drive water movement.

The expression patterns of *Arabidopsis* invertases in time and in space were investigated using data in published literature and qRT-PCR analysis; and GUS-reporter constructs were generated (Chapter 3).

The function of *Arabidopsis* invertases was investigated in T-DNA insertional knock-out plants by expression analysis using qRT-PCR, as well as examining their vegetative and reproductive phenotype. Redundancy of closely related invertase isoforms was addressed by generating a double knock-out mutant by crossing (Chapter 4). The hormonal regulation of *Arabidopsis* invertases in the context of anther dehiscence was investigated in plants deficient in jasmonic acid by expression analysis using qRT-PCR (Chapter 5).

Chapter 2: Materials and Methods

2.1 Plant Material

2.1.1 General Growth Conditions

Arabidopsis thaliana seeds were sown in Levington M3 compost (Everris). Plants were grown either in the growth room under a 16h photoperiod with day/night temperatures of 23/18°C (+/- 2°C); or in the glass house under a 16h photoperiod with day/night temperatures of 24/18°C (+/- 7°C).

2.1.2 *A. thaliana* T-DNA insertion lines

Seeds for T-DNA insertion lines were obtained from the Nottingham *Arabidopsis* Stock Centre. The presence of the T-DNA was confirmed in samples collected using the sucrose buffer method for DNA extraction (Section 2.2.4) by PCR (RedTaq PCR, Section 2.2.1, with annealing temperature of 56°C) using sequence-specific primers (Table 2-1).

Table 2-1 . Primers used to confirm presence of the T-DNA insert in KO lines.

Gene	Primer Name	Primer Sequence	Amplicon size: Forward and Reverse Primer (base pairs)	Amplicon Size: Forward and T-DNA Primer (base pairs)
T-DNA SAIL lines	LB3	TAGCATCTGAATTTCATAACCA ATCTCGATACAC	-	-
T-DNA SALK lines	LBb1.3	ATTTTGCCGATTTCGGAAC	-	-
BFRUCT3 AT1G62660	SALK_015898_F	GTCGAAGACTCAGCTCAATGG	1128	527-827
	SALK_015898_R	ACATGATCTTCCACCTTGTGC		-
CINV1 AT1G35580	SAIL_637_CO2F	GTCTCCCTGTCTTAATGCACG	1096	477-777
	SAIL_637_CO2R	CTTCATGGCTTTGAGATCTGC		-
CWINV1 AT3G13790	SALK_091455_F	TCTTCCCTATATTTGCAAGCG	1105	499-799
	SALK_091455_R	TGGTTTCAAGATGGACGGTAC		-
CWINV2 AT3G52600	SALK_068113_F	TTACAGGCCAGACGGTTACAC	1070	448-748
	SALK_068113_R	TTTGCACCTTGGTTCATCTTC		-
CWINV4 AT2G36190	SALK_094878_F	TTGGTTTTGTGAAGTGATTTCC	1129	539-839
	SALK_094878_R	CGATGCTAGACCGTACGTTTC		-
DAD1 AT2G44810	SALK_138439_F	AACTTTGGTGATGACGTCGTC	1063	530-830
	SALK_138439_R	CTCTCTTTCTCCCGTACGTCC		-
INVA AT1G56560	SALK_015233_F	CGTTGCAAGAGAGAGAACCAC	1138	514-814
	SALK_015233_R	CAAAGCAGAAGGCACAAAATC		-
INVC AT3G06500	SALK_080181_F	AAACTAACGGAACTGGCAAGG	1042	511-811
	SALK_080181_R	TGATTCCGATTCCATTAGCTG		-
INVE AT5G22510	SALK_138953_F	CATCCAAAATCAATCCACACC	1057	635-935
	SALK138953R2	TTTAAGAAGAAAGGCGATCCC		-
INVH AT3G05820	SALK_016378_F	TGTGTTGTGGTTCCAGAGTTG	1012	448-748
	SALK_016378_R	TTGGTTCTGTTTTGGTGTTCC		-
VACINV AT1G12240	SAIL_1256_C02_F	TGGATCGACCTACTAATCATCG	1083	472-772
	SAIL_1256_C02_R	CACAACACACAATCCACGTTG		-

2.1.3 Staging of *A. thaliana* flower buds

A. thaliana buds were collected and divided into four developmental stages based on size and position in the inflorescence. In stage 1 (youngest) buds, the anther stage (Sanders et al., 1999) is approximately 9-10; the flower stage (Smyth et al., 1990) is 10-11. Stage 2 buds contain bicellular pollen (anther stage 11; flower stage 11-12). Stage 3 buds contain tricellular pollen (anther stage 12; flower stage 11-12). Finally, the pollen in stage 4 buds is mature (anther stage 12; flower stage 12).

2.1.4 Phenotyping

2.1.4.1 Measurements

Plant age is given in days from sowing. Length of leaf was the measurement of the longest rosette leaf. Plant height was the length of the main stem from the base of the plant to the main inflorescence. Silique measurements and counts were taken from the main stem only, with the 1st silique being the oldest. Average silique length is given by calculating the mean length of the first 6 siliques. For plants sown in the Growth Room II experiment, silique measurements were taken at 35 days. For other measurements, the times they were taken are stated individually. Floral organ lengths were measured from photographs using ImageJ (Schindelin et al., 2012)

2.1.4.2 Statistical analysis

As the sample sizes and variances differed between samples, Welch's unequal variances *t*-test was used (rather than Student's *t*-test) for observations with normal distribution: leaf length, stem length, number of siliques. The observations for silique length and proportion of sterile siliques were not normally distributed, and they were analysed using the non-parametric Wilcoxon Rank-Sum test. Due to time constraints, in the Growth room III. experiment, silique length and proportion of sterile siliques were analysed using Welch's unequal variances *t*-test also.

2.1.5 Methyl Jasmonate (MeJA) treatment to restore *dad1* fertility

To rescue the *dad1* mutant (T-DNA insertion line SALK_138439) and restore its fertility, siliques and open flowers were removed from the inflorescence and the remaining buds were dipped into 500 µM MeJA dissolved in in 0.05% aqueous Tween 20. The plants were covered with a plastic sleeve for 1d, then left to finish flowering. This procedure was adapted from (Ishiguro et al., 2001a; Sanders et al., 2000)

2.2 DNA extraction, purification, and amplification

2.2.1 RedTaq PCR

A single reaction contained 5µl of RedTaq DNA Polymerase (VWR International), 0.3µl (10 pmol/µl) forward and reverse primers, and 5µl molecular grade water (Sigma-Aldrich). The PCR conditions were: 3 min at 94°C, 28-35 cycles of 30 s at

94°C, 30 s at primer-specific annealing temperature, 30 s/kb at 72°C; and a final extension of 4 min at 72°C.

2.2.2 Phusion High Fidelity PCR

A single reaction contained 0.2µl (2.5mM) dNTPs, 0.15µl Phusion High Fidelity Polymerase (Thermo Scientific), 2 µl 5 x HF buffer, 0.3µl 100% DMSO (Thermo Scientific), 0.23µl (10pm/µl) forward and reverse primers and 6.64µl molecular grade water (Sigma-Aldrich). The PCR conditions were: 30 s at 98°C, 35 cycles of 30 s at 98°C, 30 s at primer-specific annealing temperature, 30s/kb at 72°C; and a final extension of 6 min at 72°C. 1µl of loading buffer (Bioline) was added to PCR products before gel electrophoresis.

2.2.3 Gel Electrophoresis

PCR products were resolved by electrophoresis (45-60 min at 100-120 V) in 0.5 x TBE buffer (45mM Tris-borate, 1mM EDTA), using an agarose gel (1-2% w/v, depending on PCR product size) stained by 500µg/ml ethidium bromide (Sigma-Aldrich) with a suitable ladder (Bioline). The results were visualized with the Ingenius^3 UV illuminator (Syngene).

2.2.4 Sucrose buffer DNA Extraction

Small samples (<5mm in diameter) of young leaves were placed into 100 µl of Sucrose buffer (Tris-Cl 50 mM, pH7.5, NaCl 300 mM, sucrose 300mM), crushed with a pipette tip and heated to 100°C for 10 min. The samples were stored at -20°C. 1µl of supernatant was used for DNA amplification in a 10µl PCR (Section 2.2.1). (Adapted from Berendzen et al. (Berendzen et al., 2005))

2.2.5 PCR product purification

PCR products were purified using QIAquick purification kit (Qiagen) according to the manufacturer's instructions. Purified DNA was eluted in 25µl of molecular grade water (Sigma-Aldrich).

2.2.6 Colony PCR

Bacterial colonies were screened for presence of insert by RedTaq PCR (Section 2.2.1) using relevant vector-specific primer R and primer F2 (Table 2-3). Cells from single isolated colonies were transferred on a new plate with a sterile pipette tip. The same tip was then used to pick up the remaining colony and add it to each PCR tube directly.

2.3 Expression analysis

2.3.1 RNA Extraction

Plant material collected for RNA extraction was flash-frozen in liquid nitrogen and stored at -80°C. RNA was extracted using the RNeasy Plant Mini Kit (Quiagen), with several modifications to the manufacturer's protocol "Purification of Total RNA from Plant Cells and Tissues and Filamentous Fungi". The incubation at 56°C after the addition of buffer RLT was extended to 5 min. The time of centrifugation of lysate in the QIAshredder column was extended to 10 min. The optional DNase

Digestion was performed with an RNase-free DNase Set (Qiagen). The on-column digestion was extended to 45 min and performed twice. In the final step, 30µl of water (Sigma-Aldrich) was used to elute the RNA. The concentration of the resulting RNA was measured with NanoDrop Spectrophotometer 2000 (Thermo Scientific).

2.3.2 cDNA Synthesis

cDNA was synthesized using 1.5ng of total RNA, 1µl (0.5 µg/µl) oligo(dT), 1 µl (10mM) dNTP and water (Sigma-Aldrich) to a total volume of 13 µl. The samples were heated to 65°C for 5 min and immediately incubated on ice for 1 min. Then, 4 µl of 5x First Strand Buffer, 1 µl (0.1M) DTT, 1 µl (40 units/µl) RNase OUT and 1 µl (200 units/µl) Superscript3 (all Life Technologies) were added to each sample. The reaction was incubated at 50°C for 1 hour, then inactivated by heating to 70°C for 15 min.

2.3.3 qRT-PCR

qRT-PCR was performed using SYBR Green (Fermentas) and sequence-specific primers with the LightCycler480 (Roche) in a 384 well reaction plate. The conditions were 10 min at 95°C, then 45 cycles of 30 s at 95°C, 30 s at annealing temperature (primer specific: Table 2-2) and 1 min at 72°C. The reactions were performed in triplicate and expression levels were normalized to the house-keeping gene *PP2A-3* (*PROTEIN PHOSPHATASE 2A-3*; AT2G42500).

Table 2-2 Primers used for qRT-PCR.

Gene	Primer Name	Primer Sequence	Annealing Temperature Used (°C)	Amplicon Size (base pairs)
BFRUCT3 AT1G62660	qBFRUCT3_465F	GAGCAACGACGGGGTTTGGA	62	205
	qBFRUCT3_669R	GTCACCCCACACAGCTGCAT		
CINV1 AT1G35580	CINV1_F	TGGTACTCTTGCCGCGGTTG	60	300
	CINV1_R	TCTACAGGAGCCACACGTCCA		
CINV2 AT4G09510	CINV2_F	CAATGTAAGCCCGGCCCGTA	60	300
	CINV2_R	GGCCGTCCAGTCTTGATGCA		
CWINV1 AT3G13790	qCWINV1_173F	CCGTAAACCAGCCCTACCGG	62	145
	qCWINV1_317R	ACGATGTTACCCCACACGGC		
CWINV2 AT3G52600	qCWINV2_240F	CACTTTCAACCTCCCCGCCA	62	221
	qCWINV2_460R	GCTGAACCGGACCATGTACCG		
CWINV4 AT2G36190	qCWINV4_589F	ACCGGACGATAACCCGATTGC	62	192
	qCWINV4_780R	ACCGGGTGCTTAGCTTTGACC		
DAD1 AT2G44810	qDAD1_1415F	GCCACGCTGACTCATCTCCC	60	274
	qDAD1_1688R	CGGTAACCATAGGCGCACGT		
INVA AT1G56560	INVA_F	GGCGGCGAATGATCCTGGAG	60	299
	INVA_R	CCACAGGAGCAACACGACCA		
INVB AT4G34860	INVB_F	ACCTTTGGCCGTTTCGTCTCT	60	150
	INVB_R	TGCCCTTATGAATCCAGCGTCG		
INVC AT3G06500	INVC_F	GCCATTGGACGTGTTAGCCCT	60	274
	INVC_R	GAGCACAACGGAGAGCGGAG		
INVD AT1G22650	INVD_F	GGAACGGTGGGAGGAGTTGG	60	263
	INVD_R	TCCCGTCGTAGTACTCCGGC		
INVE AT5G22510	INVE_F	ACGTGTTGCCCCGGTTGATT	60	295
	INVE_R	TGACCCGTCCTCTGGCGTAA		
INVH AT3G05820	INVH_65F	TGCCTGCGAGTTTCAAAGTCAGA	60	150
	INVH_214R	TCCCGTATGCCCTCAACAAGA		
VACINV AT1G12240	qVACINV_691F	ACAAAGCGGTGCAGGTCCAA	60	145
	qVACINV_835R	GCAGTCGTTGGGTCACGGAA		
PP2A-3 AT1G13320	PP2A3F	TCCGTGAAGCTGCTGCAAAC	60	323
	PP2A3R	CACCAAGCATGGCCGTATCA		

2.4 Promoter-GUS Fusion Constructs

2.4.1 DNA Amplification

A. thaliana (accession Columbia) genomic DNA was extracted using the Isolate II Plant DNA Kit (Bioline) according to the manufacturer's instructions. Promoter sequences of selected genes were amplified by Phusion High Fidelity PCR (Section 2.2.2). The PCR conditions were 30 s at 98°C, 35 cycles of 30 s at 98°C, 30 s at annealing temperature (primer-specific: Table 2-3), 3 min at 72°C; a final extension of 6 min at 72°C. Primers F1 and R1 were used to amplify promoter sequences, Vector-specific primer R and primer F2 were used for colony PCR (Section 2.2.6).

Table 2-3 Primers used for cloning.

Gene	Primer Name	Primer Sequence	Annealing Temperature Used (°C)	Amplicon Size (base pairs)
Vector Specific	M13F	TGTAAAACGACGGCCAG	59	-
	M13R	CAGGAAACAGCTATGAC		
Vector Specific	GUSpGWB3_138 R	AGCAATTGCCCGGCTTTCTT	59	-
CINV2 (promoter) AT4G09510	CINV2pro_F1	TGTTCACTGTCTCTTACGAA	59	2000
	CINV2pro_R1	GGGACTTGTTAAGAGACCG		
	CINV2pro_F2	TGACTGGAGACCGATAAAAT	59	-
CWINV2 (promoter) AT3G52600	CWINV2_pro_F1	GGTGTGGAGAGTAACTTACA	62	1932
	CWINV2_pro_R1	AGAGGAGGGAAAAGTAGAG		
	CWINV2_pro_F2	TCCTGCTCTCCAATTGACGT	59	-
CWINV4 (promoter) AT2G36190	CWINV4_pro_F1	GATGGTTTGTGATATGTGCA	62	1931
	CWINV4_pro_R1	AAGTGGAAGTAGTTTGTTGTAAT		
	CWINV4_pro_F2	CAAACCGCCGACCAAACATA	59	-
INVD (promoter) AT1G22650	INVD_pro_F1	GGCGACACGAAGCTGTGTGT	62	1840
	INVD_pro_R1	GGACCTTAATTACGACGGAGAGA		
	INVD_pro_F2	TCTCTACGACCCTTCATGCC	59	-
INVH (promoter) AT3G05820	INVH_pro_F1	TAACAATGCATTCGACCAGA	62	1920
	INVH_pro_R1	GACCTAAGATTACAAAAGGC		
	INVH_pro_F2	TGCGATCAAATTAGCGGTAAACT	59	-
VACINV (promoter) AT1G12240	VACINV_pro_F1	GAGGGAGACAGAGCACGTGG	62	1855
	VACINV_pro_R1	GACACGAGAAAGAGCAAATGTC		
	VACINV_pro_F2	CGAAGCAGGAGACAGTAAAAGG	59	-

2.4.2 Overhanging Reaction and TOPO® TA-Gene Cloning

15 µl of purified (Section 2.2.5) PCR product was incubated with 1.5 µl of 10x standard *Taq* reaction buffer (New England Biolabs), 0.5 µl (2.5 mM) dATP and 0.3 µl (500 units/ml) *Taq* DNA Polymerase (New England Biolabs) for 15 min at 72°C. 4 µl of the product was added with 1µl PCR8/GW/TOPO vector (Life Technologies), 1 µl salt solution (Life Technologies) and water (Sigma-Aldrich) to a final volume of 6 µl. The reaction was incubated overnight at room temperature.

2.4.3 Transformation of *Escherichia coli* by heat shock

Chemically competent *E.coli* (One Shot® Mach1, Invitrogen) were incubated on ice for 30 min with relevant solution containing the desired insert. The cells were heat shocked for 1 min 30 s at 42°C and transferred to ice for 1 min. 250 µl of room-temperature SOC medium (Section 2.6.3) was added and the cells were incubated at 37°C for 1 h 30 min with horizontal shaking at 200 rpm.

2.4.4 Transformation of entry vector into *Escherichia coli*

The overnight solution of the TOPO® TA-Gene Cloning reaction (section 2.4.2) was used to transform E. coli (section 2.4.4). The cells were plated on LB agar plates (Section 2.6.2) with a spectinomycin selection (50µg/ml) and incubated overnight at 37°C. Successfully transformed colonies (checked with colony PCR, Section 2.2.6) were used to set up liquid cultures 30ml sterile tubes containing 10 ml LB media and spectinomycin (50 µg/ml). These were incubated overnight at 37°C with shaking at 200 rpm.

2.4.5 Plasmid Extraction

The overnight cultures were pelleted by centrifugation and the pellet was used for plasmid purification with the Gen Elute Plasmid Miniprep Kit (Sigma-Aldrich). The plasmids were eluted using 50µl of water (Sigma-Aldrich). Their concentrations were measured with NanoDrop Spectrophotometer 2000 (Thermo Scientific). The plasmids were checked by sequencing by Eurofins MWG Operon, using 100 ng of plasmid, 1.5 µl of vector-specific primer, and water (Sigma-Aldrich) to a final volume of 15 µl.

2.4.6 LR Reaction

50 ng of entry vector PCR8/GW/TOPO containing the gene of interest was incubated with 100 ng of destination vector pGWB3, 1.5 µl LR clonase (Life Technologies), and water (Sigma-Aldrich) to a final volume of 7 µl, for 18 h at 25°C. 1.5 µl Proteinase K (Life Technologies) was then added and the reaction was incubated at 37°C for 10 min.

2.4.7 Transformation destination vector into *E.coli*

The LR solution was used to transform *E. coli* (section 2.4.4). Transformed cells were plated onto LB agar plates (Section 2.6.2) with kanamycin (50 µg/ml) and incubated overnight at 37°C. Colony PCR (Section 2.2.6) was performed to check the presence and orientation of inserts. Colonies were also plated onto LB agar plates with a spectinomycin selection (50µg/ml) to confirm they do not still contain the entry vector. Overnight cultures were set up from successful colonies in 30ml sterile tubes containing 10 ml LB media (Section 2.6.2) and kanamycin (50 µg/ml). These were incubated overnight at 37°C with shaking at 200 rpm.

2.4.8 Plasmid Extraction

The destination vector was extracted same as the entry vector. The plasmids were verified by sequencing by Eurofins MWG Operon, using 100 ng of plasmid, 1.5 µl of vector-specific primer, and water (Sigma-Aldrich) to a final volume of 15 µl.

2.4.9 Transformation of *Agrobacterium tumefaciens* by electroporation

Agrobacterium strain GV3101 electrocompetent cells (40µl) were placed in a chilled 2mm electroporation cuvette with 100 ng of destination vector containing the desired insert. The cells were electroporated using Gene Pulser (Bio-Rad) set at 2.5 kV, 25 mFd, 400 Ohms; with a 6 ms pulse. 1 ml of LB media (Section 2.6.2) was added, and the cells were incubated for 3 h at 28°C, then plated onto LB agar plates

(Section 2.6.2) with kanamycin (50 µg/ml) and rifampicin (30 µg/ml) selection and incubated at 28°C for 3-4 days.

2.4.10Glycerol Stock for storage of bacteria

A single colony was used to inoculate a 10 ml overnight liquid culture with the appropriate antibiotic selection. These were incubated overnight (*A. tumefaciens*; 28ºC, *E. coli*; 37ºC) with shaking at 200 rpm. 750 µl of the resulting culture was added to 250 µl sterile 80% glycerol in a 2ml cryo-Eppendorf tube, frozen in liquid nitrogen and stored at -80°C.

2.4.11*Agrobacterium* Culture for Floral Dip

In a 30ml tube, 5 ml of LB media (Section 2.6.2) with kanamycin (50 µg/ml) and rifampicin (30 µg/ml) was inoculated from glycerol stock and incubated at 28°C with shaking at 200 rpm until near saturation. This starter culture was used to inoculate 100ml LB media with kanamycin (50 µg/ml) and rifampicin (30 µg/ml), and this was incubated at 28°C with shaking at 200 rpm until the optical density (at the wavelength of 600 nm) was between 0.8-1.2.

2.4.12 Transformation of *A. thaliana* by floral dip

2.5 g of sucrose and 50 µl (0.05% w/v) Silwet L-77 were added to the *Agrobacterium* liquid culture. Inflorescences of 4–6-week-old *A. thaliana* plants were dipped into the solution for 15 s. The plants were covered by plastic sleeves to retain humidity and placed into a shaded area. After 24 h, they were moved back into direct light and the sleeves were opened to allow flowering to finish.

2.4.13 Screening of transformed seeds

Seeds collected from transformed plants were washed three times in a 1.5ml microcentrifuge tube with 70% (v/v) ethanol with 5 min of agitation using a vortex mixer. Afterwards, the seeds were briefly suspended in 100% (v/v) ethanol before tipping them onto a sterile filter paper in a laminar air flow cabinet to dry. The seeds were spread evenly onto plates of ½ MS media (Section 2.6.1) with 50µg/ml kanamycin for selection and sealed with micropore tape. The plates were placed in a growth room with a 16 h photoperiod for two weeks. Transformed plantlets were identified by their more robust growth, transferred to pots of Levington M3 compost (Everris) in the glasshouse (section 2.1.1) and covered with plastic sleeves for 3 days to retain humidity.

2.5 Staining methods

2.5.1 DAPI Staining

Anthers of staged Arabidopsis buds (section 2.1.3) were placed on a microscopy slide and stained by adding 30µl of 3µg/ml 4',6-diamidino-2-phenylindole (DAPI) solution. A cover slip was placed on top of the anther and pressed down to release pollen grains into the DAPI solution. The samples were incubated in the dark for 5 minutes and examined with a Leica DM5000B fluorescence microscope.

2.5.2 β-glucuronidase (GUS) Staining

Whole inflorescences of Arabidopsis thaliana GUS lines were incubated overnight at 37°C in 150µl of β-glucuronidase substrate solution (Table 2-4) in a 0.6ml microcentrifuge tube covered in foil.

Table 2-4 Components and quantities used to make solutions for β-glucuronidase (GUS) staining.

Solution	Components	Quantity of components
Solution A (50ml)	1 M K_2HPO_4	3.59ml
	water	50ml
Solution B (50ml)	1M KH_2PO_4	1.24ml
	water	50ml
Phosphate Buffer (0.05M PO_4, pH 7.2) (150ml)	Solution A	30.5ml
	Solution B	19.5ml
	Water	100.0ml
β-glucuronidase substrate solution (5ml)	0.05M PO_4 buffer pH 7.2	4.245ml
	33 mg/ml $K_3Fe(CN)_6$ in 0.05M PO_4 buffer pH7.2	250µl
	43 mg/ml $K_4Fe(CN)_6.3H_2O$ in 0.05M PO_4 buffer pH 7.2	250µl
	10 mg/ml X-Gluc staining solution	250µl
	Triton X-100	5µl

The samples were then clarified in a series of incubations in 150µl of the following solutions: 20% acidified methanol (HCl/methanol/water 4:20:76 (v/v)) at 55°C for 15 min, 7% (w/v) sodium hydroxide in 70% (v/v) ethanol at room temperature (RT) for 15 min, 40% (v/v) ethanol at RT for 20 min, 20% (v/v) ethanol at RT for 20 min, 10% (v/v) ethanol at RT for 10 min. The samples were stored in 50% (v/v) glycerol until use.

2.6 Media

2.6.1 ½ MS (Murashige and Skoog) Medium Agar Plates

Components (table 2-5) were dissolved in 500ml distilled water, adjusted to pH5.8 and sterilised by autoclaving.

Table 2-5 components used to make 500ml ½ MS (Murashige and Skoog) media

Component	Quantity (g) for 500ml
Murashige and Skoog Basal medium (MS)	1.23
Agar	3.5
Sucrose	2.5

2.6.2 LB Medium and LB Agar Plates

Components (table 2-6) were dissolved in 1L distilled water, adjusted to pH7.5 and sterilized by autoclaving. For LB agar plates 15g/L Bacto Agar was added before autoclaving.

Table 2-6 components used to make 1L LB media

Component	Quantity (g) for 1L
Bacto Tryptone	10
Bacto-yeast extract	5
NaCl	10

2.6.3 Super Optimal broth with Catabolite repression (SOC) Medium

Components (Table 2-7) were dissolved in 900ml distilled water and adjusted to pH7.5. Water was added to 980ml and autoclaving was used to sterilise. After cooling the medium to less than 50°C, 20ml of filter-sterilized 20% (w/v) glucose solution was added.

Table 2-7 Components used to make 1L SOC (Super Optimal broth with Catabolite repression) medium

Component	Quantity for 1L (g)
Yeast Extract	5
Bacto Tryptone	20
NaCl	0.584
KCl	0.186
$MgSO_4$	2.4

Chapter 3: Localisation of Invertases

3.1 Introduction

3.1.1 *Arabidopsis* invertase classification

Invertases, or β-fructofuranosidases (EC 3.2.1.26), are plant enzymes responsible for the irreversible hydrolysis of sucrose into the hexoses glucose and fructose. Invertases can therefore influence the sugar composition in plant tissues, as well as metabolic fluxes and osmoregulation. Based on their catalytic pH optima, invertases are usually classified into two groups: alkaline/neutral invertases and acid invertases. Alkaline/neutral invertases can be further divided into two sub-types: α (mitochondrion or plastid-targeted) and β (cytosolic). Acid invertases can be subdivided into extracellular (or cell wall bound: CW-Inv) and vacuolar (Vac-Inv).

There are 15 invertase isoforms which have been identified in *Arabidopsis*. Initially, invertase isoforms were reported based on sequence homology and named *Atbfructl1-4* for soluble isoforms (Haouazine-Takvorian et al., 1997; Mercier and Gogarten, 1995; Schwebel-Dugue et al., 1994) and *AtcwINV1-6* for cell wall bound isoforms (Sherson et al., 2003a). Later, genes named *AtcwINV3* and *6* were shown to not have invertase activity, and instead classified as fructan exohydrolases (de Coninck et al., 2005). Alkaline/neutral invertases were not extensively studied until more recently (Vargas and Salerno, 2010). Initially they were called *InvA-K* (Vargas et al., 2003), but the names *CINV1* and *2* became more popular for the two most highly expressed cytosolic isoforms (Barratt et al., 2009; Lou et al., 2007). This explains the somewhat inconsistent nomenclature of *Arabidopsis* invertase genes seen in literature and summarised in Table 3-1 below.

Table 3-1. *A. thaliana* invertase classification.

Alternative names: (1) (Vargas et al., 2003), (2) (Schwebel-Dugue et al., 1994), (3) (Mercier and Gogarten, 1995) (4), (Haouazine-Takvorian et al., 1997), (5) (Tarkowski et al., 2020), (6) (Vu et al., 2020)

		Locus	**Name**	**Alternative names**	Location (from TAIR (Berardini et al., 2015))
Alkaline/neutral invertases	α (mitochon-drion or plastid-targeted)	AT1G56560	*INVA*	*INVB* (1)	mitochondria
		AT3G06500	*INVC*		mitochondria
		AT5G22510	*INVE*		chloroplast
		AT3G05820	*INVH*		chloroplast
	β (cytosolic)	AT4G34860	*INVB*	*INVK* (1)	cytosol
		AT1G22650	*INVD*		cytosol, nucleus
		AT1G72000	*INVF*		cytosol
		AT1G35580	*CINV1*	*INVG* (1), AtNIN2 (5)	cytosol, nucleus
		AT4G09510	*CINV2*	*INVI* (1) *INVJ* (1)	cytosol
Acid invertases	Extra-cellular	AT3G13790	*CWINV1*	*Atβfruct1* (2)	apoplast, cell wall, extracellular region, plasma membrane
		AT3G52600	*CWINV2*	*Atβfruct2* (3)	apoplast, cell wall, extracellular region
		AT2G36190	*CWINV4*		apoplast, cell wall, extracellular region
		AT3G13784	*CWINV5*		extracellular region
	Vacuolar	AT1G12240	*VACINV*	*Atβfruct4* (4), VI2 (6)	vacuole
		AT1G62660	*BFRUCT3*	*Atβfruct3* (4), VI1 (6)	vacuole

3.1.1.1 Alkaline/neutral Invertases

Alkaline/neutral invertases (A/N-Invs) have not been extensively studied until recently and their role in plant metabolism has been thought to be of little importance (Vargas and Salerno, 2010). Several A/N-Inv isoforms have however been shown to play a part in root and/or shoot development, and oxidative stress

defence, in *A. thaliana* (Barratt et al., 2009; Martín et al., 2013a; Xiang et al., 2011a). Compared to acid invertases, their activity is highly specific to sucrose only and not other β-fructose-containing substrates (Vargas and Salerno, 2010), suggesting their role may be in more subtle sucrose signalling rather than just sucrose catabolism.

3.1.1.1.1 MITOCHONDRION- AND PLASTID- TARGETED A/N-INVS

INVA and *INVC* are the two *Arabidopsis* invertase isoforms located in mitochondria. *INVA* KO mutants have a severe growth defect in root and leaf development (Martín et al., 2013a; Xiang et al., 2011a), increased levels of mitochondrial reactive oxygen species (Xiang et al., 2011a, 2011b) and their flowering is delayed (Martín et al., 2013a). In *INVC* KO mutants, shoot growth is severely impaired but root development is not affected. Flowering and germination are delayed (the latter can be rescued by exogenous GA application) (Martín et al., 2013a).

The chloroplast-located *INVE* has been reported to have a role in the development of the photosynthetic apparatus and the assimilation of nitrogen in *Arabidopsis* seedlings (Tamoi et al., 2010), specifically in plastid signalling to regulate greening and carbon-nitrogen balance (Maruta et al., 2010). While *INVE* is transcribed in roots, leaves, and flowers, the other plastidic invertase, *INVH*, is only transcribed in flowers (Vargas et al., 2008). The fact that they are not expressed only in photosynthetic tissue may point to their involvement in other plastids, such as amyloplasts (Vargas et al., 2008). *INVH* is highly expressed in guard cells and upregulated in response to ABA; and may be involved in modulation of sucrose metabolism in guard cells (Yoshida et al., 2019).

3.1.1.1.2 CYTOSOLIC A/N-INVS

INVB, *INVD* and *INVF* are cytosolic *Arabidopsis* invertase isoforms expressed at much lower levels than *CINV1*. Unlike *cinv1* KO mutant, individual mutants *invb*, *invd* and *invf* did not have impaired root development (Pignocchi et al., 2021). In a KO mutant in *ICE1*, which plays a key role in stomatal differentiation and its mutants are indehiscent, *INVF* was the only invertase isoform among the differentially expressed genes in comparison with wild-type, along with genes associated with water transport and ion exchange. (Wei et al., 2018).

Single mutations in cytosolic invertases *CINV1* and *CINV2* do not severely affect the plant phenotype due to their mutual redundancy, however, the growth of double mutants *cinv1cinv2* was stunted and particularly their root cell expansion was strongly inhibited. This phenotype could be partially rescued by addition of exogenous glucose (Barratt et al., 2009; Pignocchi et al., 2021).

CINV1 along with *CINV2* appear to control the entry of carbon from sucrose into cellular metabolism. Their activity is controlled by a glucose feed-forward loop they are a key part of the sucrose signalling pathway which regulates transition from juvenile to vegetative phase in *Arabidopsis* (Meng et al., 2021).

CINV1 is a key modulator of glucose-mediated root cell elongation (Lou et al., 2007; Meng et al., 2020), and is involved in the inhibition of root growth under osmotic stress (Qi et al., 2007). The defect in root elongation of *cinv1cinv2* double mutants is mostly due to loss of CINV1. *cinv1cinv2* plants also had smaller leaf area and a higher density of stomata (Pignocchi et al., 2021).

CINV1 may also be involved in mitochondrial reactive oxygen species homeostasis (Xiang et al., 2011a, 2011b). *Arabidopsis CINV1* and the homologous invertase in cyanobacterium *Anabaena* are similar both in sequence and in protein structure, suggesting that they are highly conserved during evolution (Tarkowski et al., 2020).

3.1.1.2 Acid invertases

3.1.1.2.1 EXTRACELLULAR INVERTASES

Extracellular invertases are involved in assimilate partitioning (by regulating apoplasmic phloem unloading), in the response to pathogen infection and abiotic stress, and are regulated by many phytohormones (Roitsch et al., 2003). Single KOs for extracellular invertase genes are not reported as showing abnormal phenotype (Sherson et al., 2003a).

CWINV1 is involved in mechanical wounding response by facilitating carbon supply to wounded tissue (Quilliam et al., 2006). During seed germination, *CWINV1* is induced by gibberellin in response to red light along with vacuolar invertases (Mitsuhashi et al., 2004)

CWINV2 and *CWINV4* are predominantly expressed in the reproductive tissues of *Arabidopsis*. Silencing of *CWINV2* by anther specific RNA interference was demonstrated to produce male sterile plants in *A. thaliana* due to its role in carbohydrate supply for pollen development, and similar results were also achieved in *N. tabacum* (Hirsche et al., 2009a). *MYB21* has been shown to regulate *CWINV2* expression in anthers, along with *ARF6* and *ARF8*, which were shown to directly bind at the *CWINV2* promoter (Li et al., 2021).

CWINV4 was shown to be required for nectar production by Ruhlmann et al. They suggest that *CWINV4* may have a key role in establishing a high-solute environment within nectary cells which draws in water required for nectar production (Ruhlmann et al., 2010a). Similar to *CWINV2*, *ARF6* and *ARF8* were shown to regulate *CWINV4* directly and *MYB21* indirectly in nectaries, anthers, and petals (Li et al., 2021).
CWINV2 and *CWINV4* are also expressed at ovule primordia. Ovule-specific silencing of *CWIN2* and *CWIN4* impacted ovule initiation by disrupting sugar signalling (Liao et al., 2020).

3.1.1.2.2 VACUOLAR INVERTASES

The expression of both vacuolar invertase isoforms is correlated with germination and early seedling growth (Mitsuhashi et al., 2004)

VACINV has a role in *A. thaliana* root elongation through osmotic independent pathways (Sergeeva et al., 2006; Wang et al., 2010). There is evidence for the role of *VACINV* in stomatal opening: its activity is much higher in guard cells than in other epidermal cells, and KO mutants have lower stomatal aperture than wild type (Ni, 2012a). It must be noted, however, that this observation was made in leaves, and the phenotype of stomata on the anther may not always match the phenotype of leaf stomata.

In a study of *Arabidopsis* response to drought, *VACINV* was significantly repressed during water deficit, whereas that of *BFRUCT3* was not (Slawinski et al., 2021). Mutants suppressing both vacuolar invertases were impaired in development and survival under dark conditions (Vu et al., 2020).

3.2 Results

3.2.1 Phylogeny alignment

The division of invertases into two classes based on their catalytic pH optima (alkaline/neutral invertases and acid invertases) corresponds with the two distinct evolutionary branches of invertases in *Arabidopsis* (Fig 3-1).

The Acid invertase branch contains three pairs of closely related genes. *VACINV* and *BFRUCT3* are the two vacuolar invertases. *CWINV2* and *CWINV4* are expressed in reproductive organs. *CWINV1* and *CWINV5* are both situated close together on chromosome 3.

Among alkaline/neutral invertases, cytosolic invertases are in a distinct, evolutionarily more recent group.

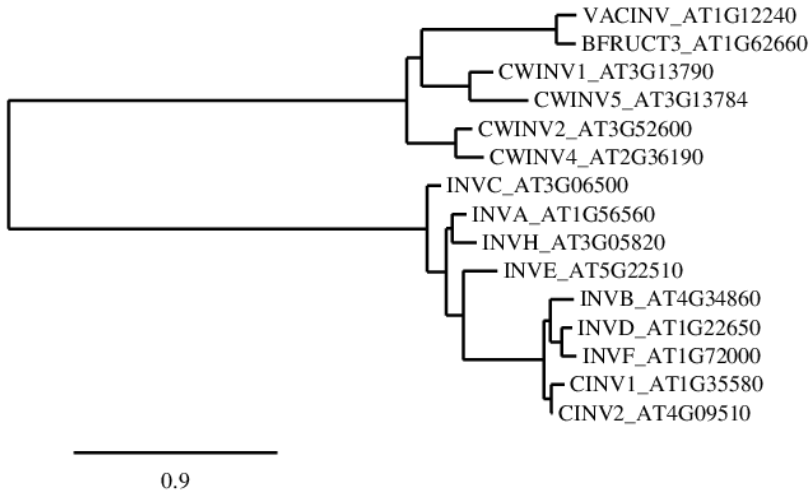

Figure 3-1. Phylogenic tree showing the evolutionary relationships of *A. thaliana* invertases.

Each node represents the most recent common ancestor, and the branch lengths correspond to the amount of evolutionary change. Constructed from invertase protein sequence alignment using the BLAST-Explorer tool at http://www.phylogeny.fr (Dereeper et al., 2008)

3.2.2 Identification of genes of interest *in silico*

In addition to literature survey, microarray data available in the FlowerNet gene expression network resource (Pearce et al., 2015) was analysed as initial investigation of genes of interest to this work. This resource contains collections of anther and flower expression data, which were screened with two criteria: does the gene expression change over the course of floral development; and does the gene expression change in response to jasmonic acid treatment (this is explored in more detail in Chapter 5, Section 5.2.1). Genes upregulated in late flower stages approaching dehiscence, and genes responding to JA, the main regulator of water transport during dehiscence, are outlined in Table 3-2. The isoforms which are both upregulated during flower development and respond to JA are *INVE*, *INVH*, *INVD*, *CWINV2*, *CWINV4*, *CWINV5*, *VACINV* and *BFRUCT3*.

Table 3-2. Invertase expression in flower development.

Data obtained from FlowerNet (http://www.cpib.ac.uk/anther) (Pearce et al., 2015)

Gene code	Gene name	Upregulated in late flower stages	Responds to jasmonic acid (Fig.5-2)
AT1G56560	*INVA*	yes	no
AT3G06500	*INVC*	yes	no
AT5G22510	*INVE*	yes	yes
AT3G05820	*INVH*	yes	yes
AT4G34860	*INVB*	no	yes
AT1G22650	*INVD*	yes	yes
AT1G72000	*INVF*	no	no
AT1G35580	*CINV1*	no	no
AT4G09510	*CINV2*	no	no
AT3G13790	*CWINV1*	yes	no
AT3G52600	*CWINV2*	yes	yes
AT2G36190	*CWINV4*	yes	yes
AT3G13784	*CWINV5*	yes	yes
AT1G12240	*VACINV*	yes	yes
AT1G62660	*BFRUCT3*	yes	yes

3.2.3 Expression Analysis during flower development

3.2.3.1 Stages of Arabidopsis flower development

To investigate invertase expression during flower development, *A. thaliana* buds were collected and divided into four developmental stages. This staging method was based on size and position of buds in the inflorescence (More detail in Chapter 2 Section 2.1.3) and confirmed by imaging their pollen using the fluorescent stain DAPI (4',6-diamidino-2-phenylindole) (Fig 3-2). DAPI binds to centromeric heterochromatin and labels the nucleus with blue fluorescence when excited by

ultraviolet light, thus enabling identification of different stages of pollen development.

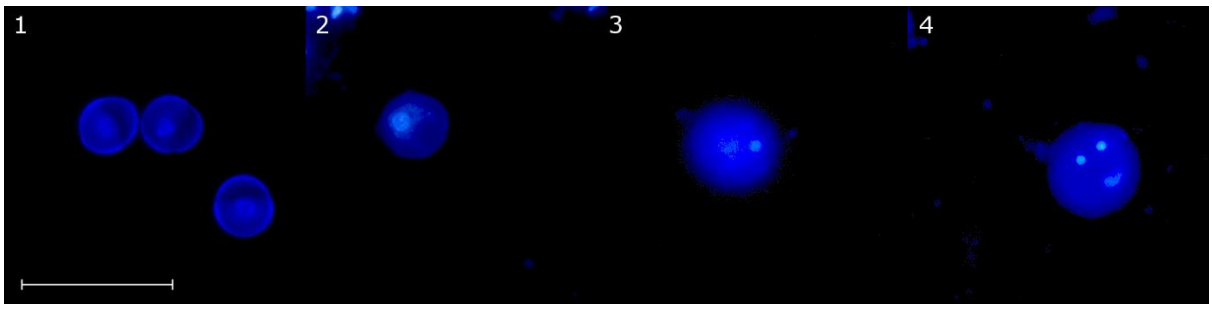

Figure 3-2 *A. thaliana* wild type pollen visualised with DAPI stain.

Bar=250µm. 1. stage 1 (youngest) buds; 2. Stage 2 buds: bicellular pollen; 3. Stage 3 buds: tricellular pollen; 4. Stage 4 buds: mature pollen

3.2.3.2 Alkaline/neutral Invertase Expression WT Background bud series

The expression of alkaline/neutral invertases in staged *A. thaliana* (ecotype *Landsberg*) grown in the glass house was assessed by qRT-PCR, with methods described in Section 2.3 of Chapter 2. The two biological replicates are shown in Fig. 3-3 (normalized to *PROTEIN PHOSPHATASE 2A-3* (*PP2A3)* and shown relative to the average at stage 4 – buds containing mature pollen).

The overall trends which the expression follows seem to be consistent between the two replicates, especially in *INVB* (decreasing), *INVD* and *INVH* (increasing). The precise expression levels were however quite different between the replicates, particularly in *INVC*, *CINV1* and *CINV2*.

More biological replicates would be desirable to accurately assess invertase expression, and at least three biological replicates would be necessary to perform statistical analysis. The differences observed between biological replicate 1 and biological replicate 2 in Fig. 3-3 could be explained by inconsistency in growing conditions in the glass house which unfortunately get influenced by outside weather (e.g., temperature fluctuations of +/- 7°C, as described in Section 2.1.1).

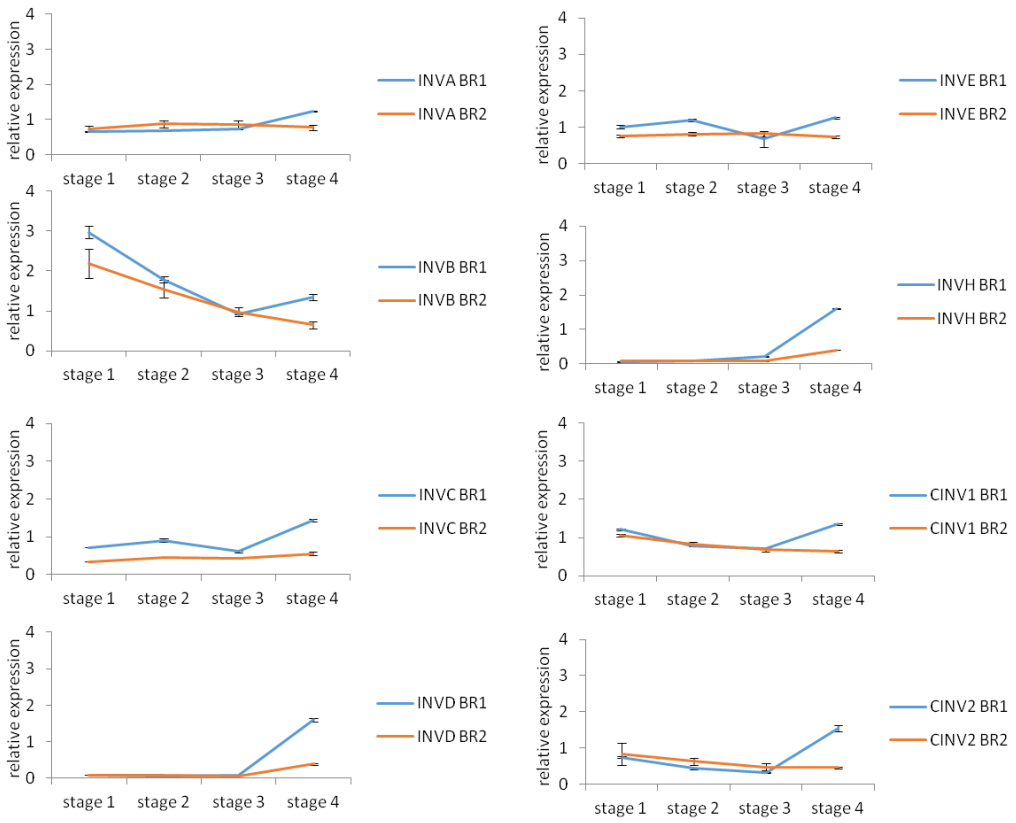

Figure 3-3 Alkaline/neutral invertase expression in WT background.

Expression was assessed by qRT-PCR in *A. thaliana* (ecotype *Landsberg erecta*) buds divided into four developmental stages, based on size and position in the inflorescence, from stage 1 (youngest buds) to stage 4 (buds containing mature pollen, before dehiscence). The values are normalized to the expression of the house-keeping gene *PP2A3* and shown relative to the average at stage 4, +/- standard error of the mean. BR1 = biological replicate 1, BR2 = biological replicate 2.

3.2.3.3 Acid Invertase Expression in WT Background bud series

The expression of acid invertases in WT background (ecotype *Landsberg*) was assessed in staged buds by qPCR. The qRT-PCR expression data is shown in Fig. 3-4 normalized to *PP2A3* and shown relative to expression at stage 4 (buds containing mature pollen). Only one biological replicate was performed. Except for *CWINV1*, acid invertases are upregulated in older buds.

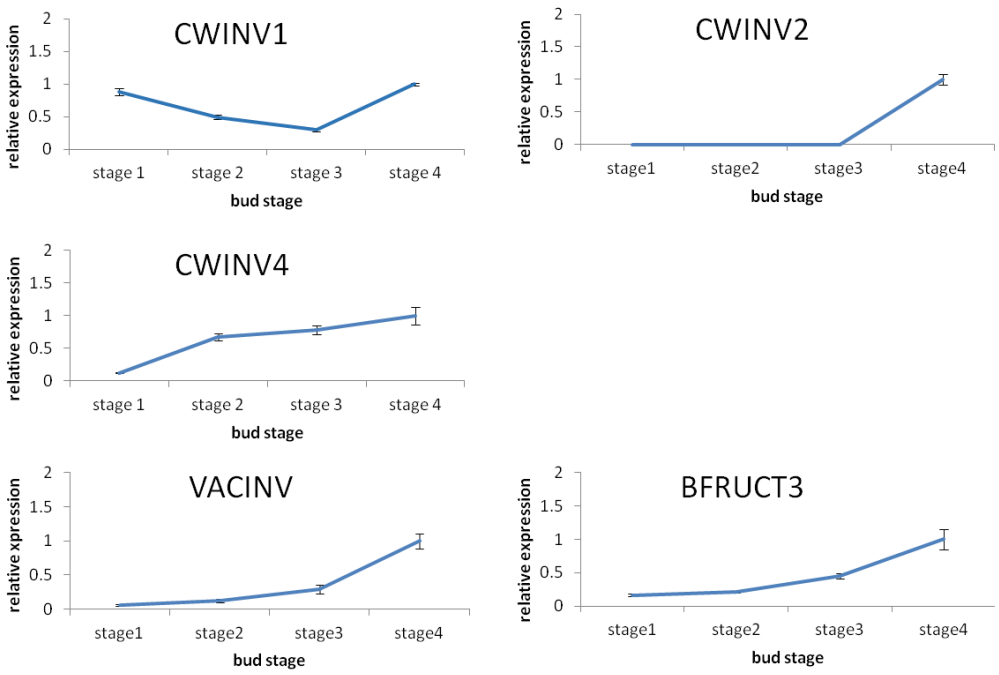

Figure 3-4 Acid invertase expression WT background.

Expression was assessed by qRT-PCR in *A. thaliana* (ecotype *Landsberg erecta*) buds were divided into four developmental stages, based on size and position in the inflorescence, from stage 1 (youngest buds) to stage 4 (buds containing mature pollen, before dehiscence). The values have been normalized to the expression of the house-keeping gene *PP2A3* and shown relative to the average at stage 4, +/- standard error of the mean.

3.2.4 Promoter-GUS fusions

To analyse invertase expression pattern in floral tissues further, promoter-GUS fusion constructs were generated (Chapter 2, Materials and Methods; Section 2.4). Based on the information gathered from microarray data (Section 3.2.2) and expression analysis (Section 3.2.3), genes were selected for which are summarized in Table 3-3. In addition to expression data from the four flower development stages presented above, data from analysis of expression in JA deficient mutant *dad1,* presented in Chapter 5 (Section 5.2.2), was also included. Constructs were generated and transformed into *Arabidopsis;* however no transformed plants were obtained.

Table 3-3 Genes selected for promoter-GUS fusion

Locus	Gene Name	Microarray data from FlowerNet (Pearce et al., 2015)	Expression data
AT3G05820	*INVH*	High expression in late stamen stages and pollen, increase during JA time course	Expression increased in stage 4 buds in WT, but decreased in *dad1*
AT1G22650	*INVD*	High expression in late stamen stages and pollen, increase during JA time course	Expression increased in stage 4 buds in WT, but decreased in *dad1*
AT4G09510	*CINV2*	Decreasing expression across flower stages	Expression increased massively in stage 4 *dad1* buds
AT3G52600	*CWINV2*	High expression in late stamen stages and pollen, increase during JA time course	Expression increased in stage 4 buds in WT, but decreased in *dad1*
AT2G36190	*CWINV4*	Increase across flower stages, high expression in stage 12 stamen	Expression increased in stage 4 buds in WT, but decreased in *dad1*
AT1G12240	*VACINV*	High expression in late flower and stamen stages, increase during JA time course	Expression increased in stage 4 buds in WT and increased in stage 4 *dad1*

3.3 Discussion

To identify genes of interest, expression patterns of invertases in time and space were investigated. Several invertase isoforms were detected by qRT-PCR analysis which are upregulated in *A. thaliana* buds during late stages, suggesting their potential involvement in dehiscence: *INVH*, *INVD*, *CINV2*, *CWINV2*, *CWINV4*, *VACINV*.

Unfortunately, the number of replicates in which the expression analysis in Section 3.2.3 was performed is fewer than desirable. The plants were grown in the glass house, potentially leading to inconsistency in growing conditions between replicates. Considering this, three further replicates of plants were grown in the growth room where growth conditions are more consistent, and samples were collected (Appendix: Table 8 1). However, due to time constraints this material has not been analysed.

Invertases involved in dehiscence would be expected to be localized in floral organs, especially stamen filament or nectary, to drive water transport out of anther. *CWINV2* and *CWINV4* have been described previously to be regulated by transcription factors which mediate flower development (*ARF6*, *ARF8* and *MYB21*). *CWINV2* is expressed in anthers and *CWINV4* in nectaries, anthers, and petals (Li et al., 2021). *CWINV4* has been shown to be required for nectar production (Ruhlmann et al., 2010a). This may have an indirect role in anther dehiscence, as it has been suggested, in a study using *Petunia*, that water is retracted from anthers to the nectaries during dehiscence (Ge et al., 2000).

Closely related genes may have some degree of redundancy. In the case of *CWINV2* and *CWINV4*, they are suspected to play complementary or additive roles in ovule initiation (Liao et al., 2020). Vacuolar invertases can also compensate for loss of one isoform to some degree. While *VACINV* provides the majority of vacuolar invertase activity, both genes need to be suppressed to achieve significant alteration to vacuolar sugar homeostasis (Vu et al., 2020; Weiszmann et al., 2018). Similarly, in the case of *CINV1* and *CINV2*, *CINV1* is the primary cytosolic invertase isoform, but *CINV2* is able to compensate for loss of *CINV1* (Meng et al., 2021; Pignocchi et al., 2021). However, deficiency in vacuolar invertase does not seem to be compensated cytosolic invertase (Weiszmann et al., 2018).

Chapter 4: Function of invertases

4.1 Introduction

A direct approach to investigating the function of genes in an organism is to utilise null mutations, also termed gene knockout (KO). In the Chapter 3, several genes were identified with differential expression during flower development (Chapter 3; Table 3-2), however whether they have a specific role in floral development particularly dehiscence is not known. In this chapter, the function of invertase genes in flower development is explored by analysis of *Arabidopsis* KO mutants.

4.1.1 Approach to *Arabidopsis* KO

A common approach in investigating gene function in *Arabidopsis* KO mutants is to utilise the available collections of insertional mutants. These have been created by indexing transferred DNA (T-DNA) insertion events, which occur via infection with *Agrobacterium tumefaciens* (Alonso et al., 2003). T-DNA inserts randomly and can be an effective gene disrupting mutagen, while also having the advantage of a known DNA sequence which can then be mapped through sequencing and targeted using tools such as T-DNA Express (http://signal.salk.edu/cgi-bin/tdnaexpress) (O'Malley et al., 2015). T-DNA insertional mutants have been utilised in the majority of invertase KO studies (Table 4-1).

Alternative specific approaches include the use of artificial microRNA under a constitutive promoter (Vu et al., 2020), or a specific promoter (Hirsche et al., 2009a; Liao et al., 2020), or using the CRISPR/Cas9 system. In the case of invertases, gene KO study can also be complemented by expressing a proteinaceous invertase inhibitor, although this has been reported as not very efficient in *Arabidopsis* (Hirsche et al., 2009a).

4.1.2 Invertase KO lines described in the literature

Published literature has been searched for mentions of invertase knock-outs in *Arabidopsis* and descriptions of their phenotype. The information is summarised in Table 4-1.

Table 4-1 Phenotype of *Arabidopsis* invertase knock-outs described in literature

Gene code	Gene name	KO phenotype	KO approach
AT1G56560	*INVA*	Severe growth defect in root and leaf development. Increased levels of mitochondrial reactive oxygen species (Xiang et al., 2011a)	T-DNA insertion
		Reduced root and shoot growth, late flowering (Martín et al., 2013b)	T-DNA insertion
AT3G06500	*INVC*	Severely impaired shoot growth (root development is not affected), late flowering. Delayed germination which can be rescued by exogenous GA application (Martín et al., 2013b)	T-DNA insertion
AT5G22510	*INVE*	--	--
AT3G05820	*INVH*	--	--
AT4G34860	*INVB*	normal root development (Pignocchi et al., 2021).	T-DNA insertion
AT1G22650	*INVD*	normal root development (Pignocchi et al., 2021).	T-DNA insertion
AT1G72000	*INVF*	normal root development (Pignocchi et al., 2021).	T-DNA insertion
AT1G35580	*CINV1*	Appeared identical to WT (Barratt et al., 2009); impaired root and leaf growth (Xiang et al., 2011a); impaired root development (Pignocchi et al., 2021)	T-DNA insertion
AT4G09510	*CINV2*	Appeared identical to WT. No severe effect due to redundancy with CINV1 (Barratt et al., 2009)	T-DNA insertion
	Double mutant *CINV1*, *CINV2*	Stunted growth, smaller leaf area and a higher density of stomata, root cell expansion was strongly inhibited. (Barnes and Anderson, 2018; Barratt et al., 2009; Pignocchi et al., 2021).	T-DNA insertion
AT3G13790	*CWINV1*	Normal phenotype (Sherson et al., 2003a).	T-DNA insertion
AT3G52600	*CWINV2*	Normal phenotype (Sherson et al., 2003a).	T-DNA insertion
		Anther-specific silencing disrupted carbohydrate supply for pollen development leading to sterility (Hirsche et al., 2009a).	RNA interference, invertase inhibitor
AT2G36190	*CWINV4*	Normal phenotype (Sherson et al., 2003a)	T-DNA insertion
		Lack of nectar production (Ruhlmann et al., 2010b)	T-DNA insertion
	CWINV2 and *CWINV4*	Ovule-specific silencing of CWIN2 and CWIN4 impacted ovule initiation by disrupting sugar signaling (Liao et al., 2020).	RNA interference
AT3G13784	*CWINV5*	Normal phenotype (Sherson et al., 2003a).	T-DNA insertion
AT1G12240	*VACINV*	Short root phenotype (Sergeeva et al., 2006; Wang et al., 2010) Lower stomatal aperture (Ni, 2012b)	T-DNA insertion
AT1G62660	*BFRUCT3*	--	--
	VACINV and *BFRUCT3*	Mutants suppressing both vacuolar invertases were impaired in development and survival under dark conditions (Vu et al., 2020).	RNA interference

4.2 Results

4.2.1 Selecting insertional KO mutant lines

T-DNA insertional lines to be used in this work were selected using the T-DNA Express online tool (http://signal.salk.edu/cgi-bin/tdnaexpress) (O'Malley et al., 2015). Lines where T-DNA was in the exon, preferably at the start of the gene, were picked, as they would have the highest likelihood of the gene being disrupted. In some cases, lines used here were already described in published literature, namely *inva* (SALK_015233), *invc* (SALK_080181), *invf* (SALK_131881) (Martín et al., 2013a; Pignocchi et al., 2021; Xiang et al., 2011c). In other cases, lines used previously were not available, or a different line was selected which fit the T-DNA location criteria better (Table 4-2).

Table 4-2 Arabidopsis T-DNA insertional KO mutant lines used in this work

Locus	Name	KO line name	T-DNA insert location	KO confirmed (Section 4.2.2.1)	Approach used in published literature
AT1G56560	***inva***	SALK_015233	Exon 1	Yes	SALK _109830 (Martín et al., 2013a; Xiang et al., 2011c) SALK _015233 (Xiang et al., 2011a)
AT3G06500	***invc***	SALK_080181	Exon 1	No	SALK_080181 (Martín et al., 2013b)
AT5G22510	***inve***	SALK_138953	Exon 2	Yes	
AT3G05820	***invh***	SALK_016378	Exon 4	Yes	
AT4G34860	***invb***	--	----	--	SALK_097137 (Pignocchi et al., 2021)
AT1G22650	***invd***	--	----	--	WiscDSLox466C11 (Pignocchi et al., 2021)
AT1G72000	***invf***	SALK_131881	Exon 3	No	SALK_131881 (Pignocchi et al., 2021)
AT1G35580	***cinv1***	SAIL_637_C02	Exon 5	No	SALK _095807 (Barratt et al., 2009; Pignocchi et al., 2021; Xiang et al., 2011a)
AT4G09510	***cinv2***	--	----	--	Sail_518_D02 (Barratt et al., 2009)
AT3G13790	***cwinv1***	SALK_091455	Exon 4	Yes	Unspecified insertional KO mutant (Sherson et al., 2003a; Thorneycroft et al., 2001)
AT3G52600	***cwinv2***	SALK_068113	Exon 4	Yes	CWINV2-antisense construct under CWINV2 promoter; proteinaceous invertase inhibitor under CWINV2 promoter (Hirsche et al., 2009a). Unspecified insertional KO mutant (Sherson et al., 2003a; Thorneycroft et al., 2001)
AT2G36190	***cwinv4***	SALK_094878	Exon 6	Yes	SALK_130163 and SALK_017466C (Ruhlmann et al., 2010b) Unspecified insertional KO mutant (Sherson et al., 2003a; Thorneycroft et al., 2001)
AT3G13784	***cwinv5***	GK-849H10-025838	Exon 2	no	
AT1G12240	***vacinv***	SAIL_1256_C02	Exon 3	Yes	SALK_100813 (Ni, 2012a; Sergeeva et al., 2006; Wang et al., 2010)
AT1G62660	***bfruct3***	SALK_015898	Exon 5	yes	artificial microRNA (targeting VACINV and BFRUCT3 simultaneously) under constitutive promoter

4.2.2 Expression Analysis in KO Lines

4.2.2.1 Expression analysis to confirm KO

Expression analysis by qRT-PCR (Chapter 2, Section 2.3) was performed to verify the relevant gene was knocked out in each T-DNA insertional line. Samples of whole inflorescence (containing all unopened buds) were pooled from several plants from each line in which the presence of T-DNA was verified by PCR (Chapter 2, Section 2.1.2). Most of the lines shown in Figure 4-1 and Figure 4-2 have the relevant gene knocked out or at least down to less than 0.5 of its normal expression level in WT, except *invc* and *invh. INVC* showed increased expression in the in *invc* insertion line SALK_080181, so although this is based on only one replicate and line SALK_080181 has been used as a KO mutant before (Martín et al., 2013a), it cannot be considered a verified knock-out. The expression level of *INVH* in *invh* (SALK_016378) is 0.66 of that of WT, so it can be considered a knockdown.

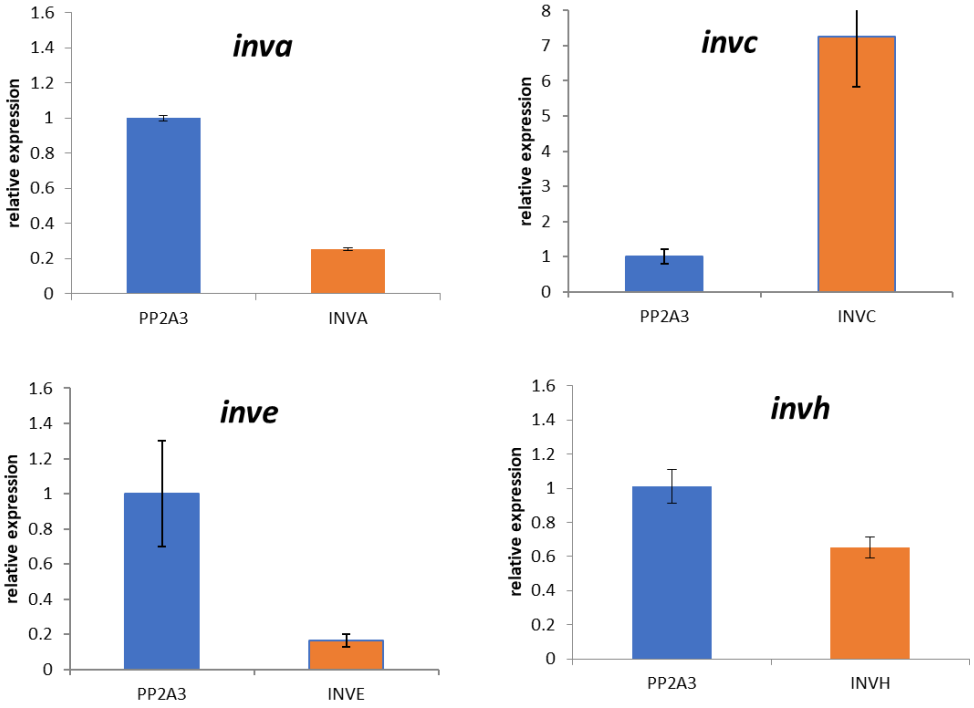

Figure 4-1 . Expression of alkaline/neutral invertase genes in KO lines.

Expression was assessed by qRT-PCR in *A. thaliana* T-DNA insertion mutant lines and in wild-type (*invc*, *inve*, Ler; *inva*, *invh,* Col) using whole inflorescence samples. Expression of invertases in each line is shown relative to their expression in WT, +/- standard error of the mean (three technical replicates), n=1. The values are normalized to the expression of the house-keeping gene *PP2A3*.

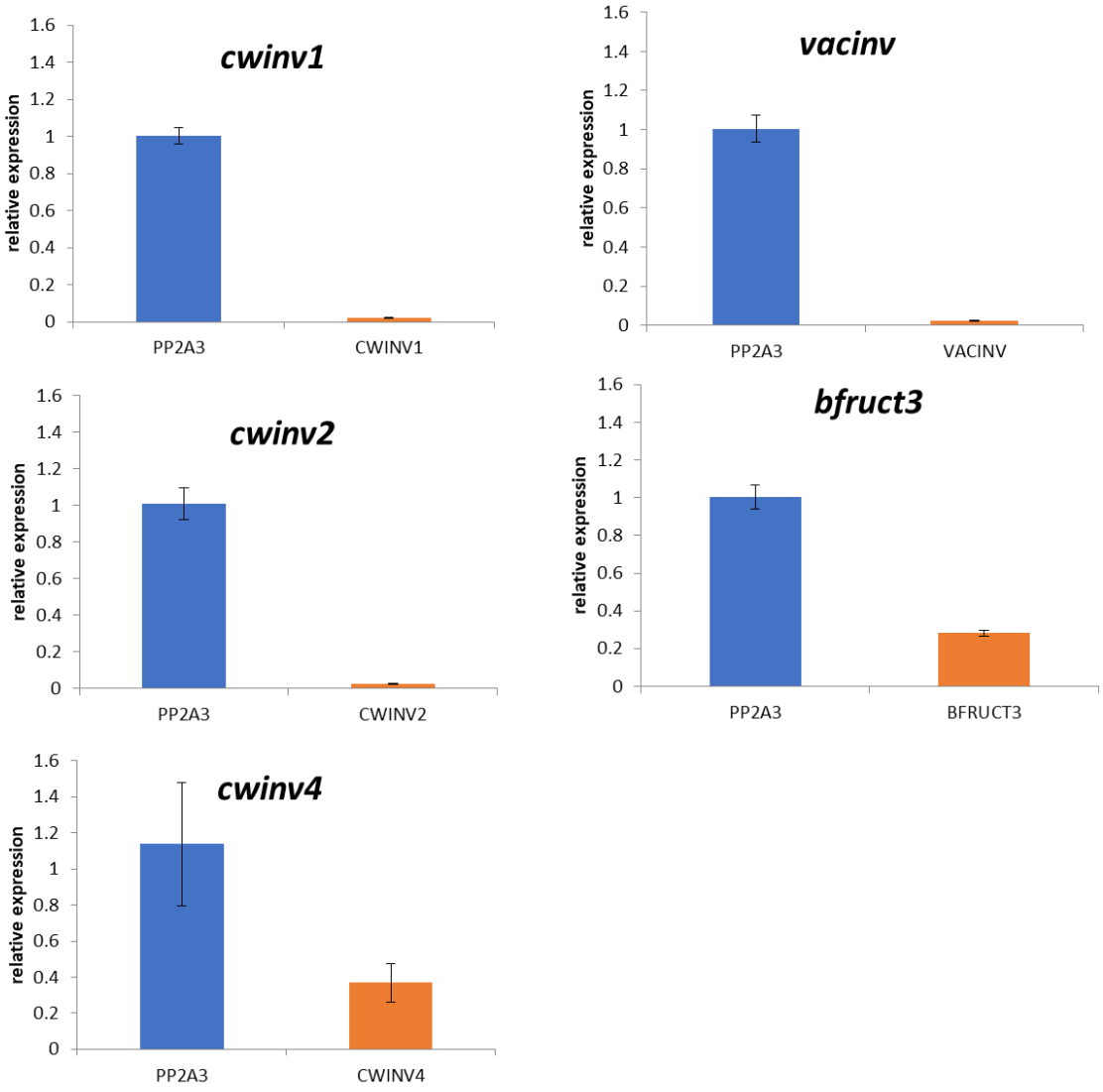

Figure 4-2 Expression of acid invertase genes in KO lines.

Expression was assessed by qRT-PCR in *A. thaliana* T-DNA insertion mutant lines and in wild-type (Col) using samples of the whole inflorescence. Expression of invertases in each line is shown relative to their expression in WT, +/- standard error of the mean (three technical replicates), n=1. The values are normalized to the expression of the house-keeping gene PP2A3.

4.2.2.2 Acid invertase expression profile

Expression analysis by qRT-PCR (Chapter 2, Section 2.3) was performed to investigate the expression of closely related isoforms (Chapter 3, Section 3.2.1) in a KO mutant background. Samples of whole inflorescence (containing all unopened buds) were pooled from several plants from each line in which the presence of T-DNA was verified by PCR (Chapter 2, Section 2.1.2).

CWINV1, *CWINV2* and *CWINV4* seem to be acting in a complementary way: when one is knocked out, the other two are upregulated. This is also true in *vacinv* and

bfruct3, particularly *CWINV1* is massively upregulated in the *bfruct3* mutant (Fig. 4-3).

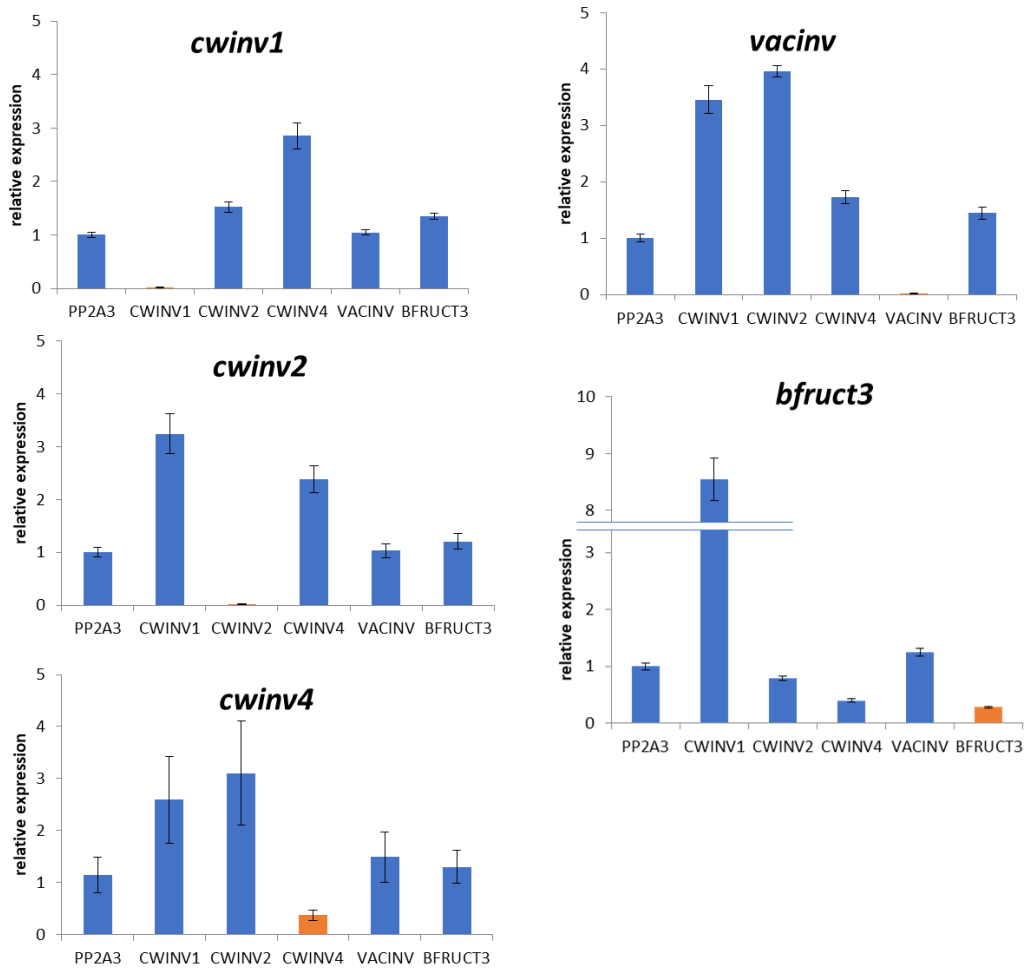

Figure 4-3 Expression of acid invertase genes in KO lines.

Expression was assessed by qRT-PCR in *A. thaliana* T-DNA insertion mutant lines and in wild-type (Col) using samples of the whole inflorescence. Expression of invertases in each line is shown relative to their expression in WT, +/- standard error of the mean (three technical replicates), n=1. The gene which is knocked out in each line is shown in orange. The values are normalized to the expression of the house-keeping gene *PP2A3*.

4.2.3 Phenotype of invertase KO plants

4.2.3.1 Plant vegetative phenotype

To assess the general phenotype of KO plants, they were grown on compost in a growth room with a 16h light cycle. For a general impression of KO line phenotype, measurements were taken of vegetative tissue throughout plant development. Rosette leaf size was measured at 14, 21 and 30 days after sowing, stem length at maturity (30 d) and in senescing plant (over 40 days since sowing) were also measured. The observations are summarised in Table 4-3.

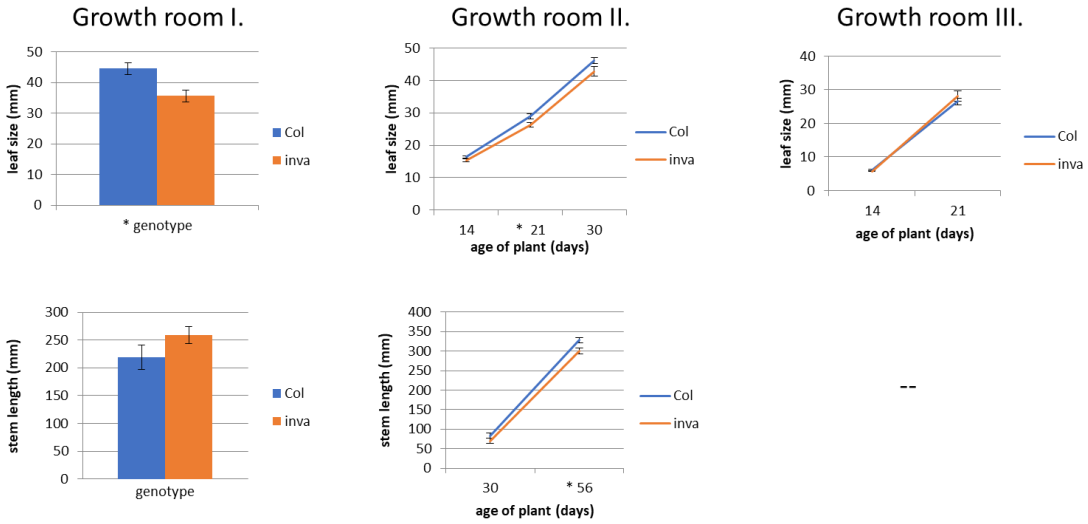

Figure 4-4 Vegetative tissue measurements of *inva* and WT (Col).

Mean values shown +/- standard error. Asterisks indicate significant difference (* P<0.05, ** P<0.001).

inva was grown in three separate experiments (Figure 4-4). In Growth room I. experiment, the leaves of *inva* were significantly shorter than WT leaves (t=3.22, n_1=14, n_2=16, P=0.003). There was no significant difference in plant height (measured at 40 days). In Growth room II. experiment, the leaves of *inva* were significantly shorter at 21 days (t=2.78, n_1=27, n_2=28, P=0.007), but no significant difference was observed at 14 days or at 30 days. The stem length did not differ at 30 days, but at 56 days, *inva* plants were significantly shorter (t=2.78, n_1=26, n_2=23, P=0.008). No significant differences were observed in Growth room III. experiment.

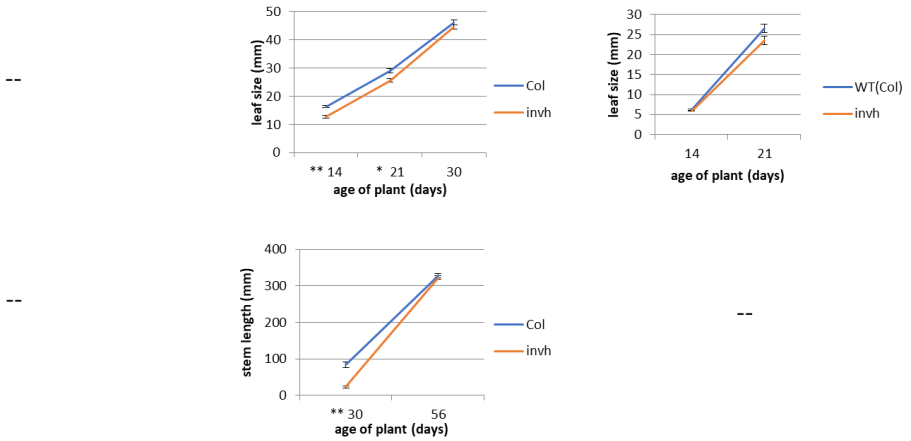

Figure 4-5 Vegetative tissue measurements of *invh* and WT (Col)

Mean values shown +/- standard error. Asterisks indicate significant difference (* P<0.05, ** P<0.001)

invh was grown in two separate experiments (Fig. 4-5). In Growth room II. experiment, the leaves of *invh* were significantly smaller than WT at 14 days ($t=5.67$, $n_1= n_2=38$, $P<0.001$) and 21 days ($t=3.42$, $n_1=27$ $n_2=30$, $P=0.001$), but not at 30 days. The plants were also significantly shorter than WT at 30 days ($t=7.41$, $n_1= n_2=27$, $P<0.001$), but not at 56 days. No significant differences were observed in Growth room III. experiment.

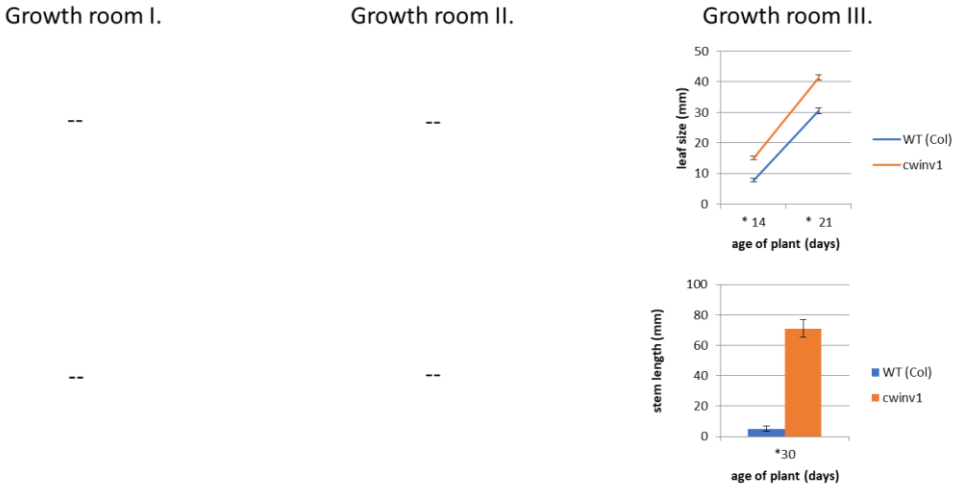

Figure 4-6 Vegetative tissue measurements of *cwinv1* and WT (Col).

Mean values shown +/- standard error. Asterisks indicate significant difference (* P<0.05, ** P<0.001)

Only one set of observations is available for cwinv1 (Fig. 4-6). The leaves of *cwinv1* were significantly larger than WT at 14 days ($n_1=25$ $n_2=31$, $P<0.001$) and 21 days $n_1=23$ $n_2=29$, $P<0.001$). The plants were also significantly taller than WT at 30 days ($n_1= 5$ $n_2=28$, $P<0.001$)

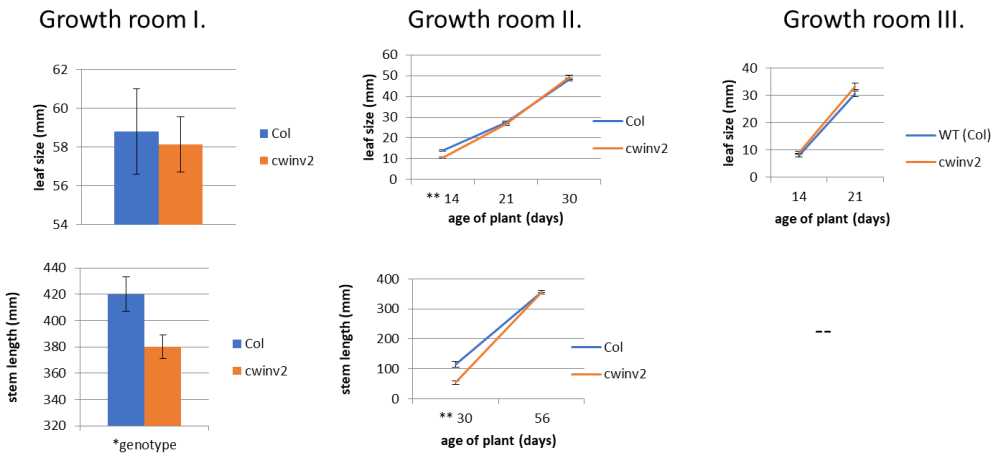

Figure 4-7 Vegetative tissue measurements of *cwinv2* and WT (Col).

Mean values shown +/- standard error. Asterisks indicate significant difference (* P<0.05, ** P<0.001).

cwinv2 was observed in three separate experiments (Fig 4-7). In Growth room I. experiment, the *cwinv2* plants were significantly shorter than WT (t=2.535, $n_1=n_2=16$, P=0.017). Measured at 51 days. In Growth room II. experiment, *cwinv2* plants had significantly smaller leaves at 14 days than WT (t=5.01, $n_1=28$, $n_2=34$, P<0.001) but the leaf sizes did not differ significantly later on. Similarly, at 30 days, *cwinv2* plants were significantly shorter than WT (t=5.69, $n_1=22$, $n_2=24$, P<0.001), but at 56 days, the heights of *cwinv2* and WT were not significantly different. No significant differences were observed in Growth room III. experiment.

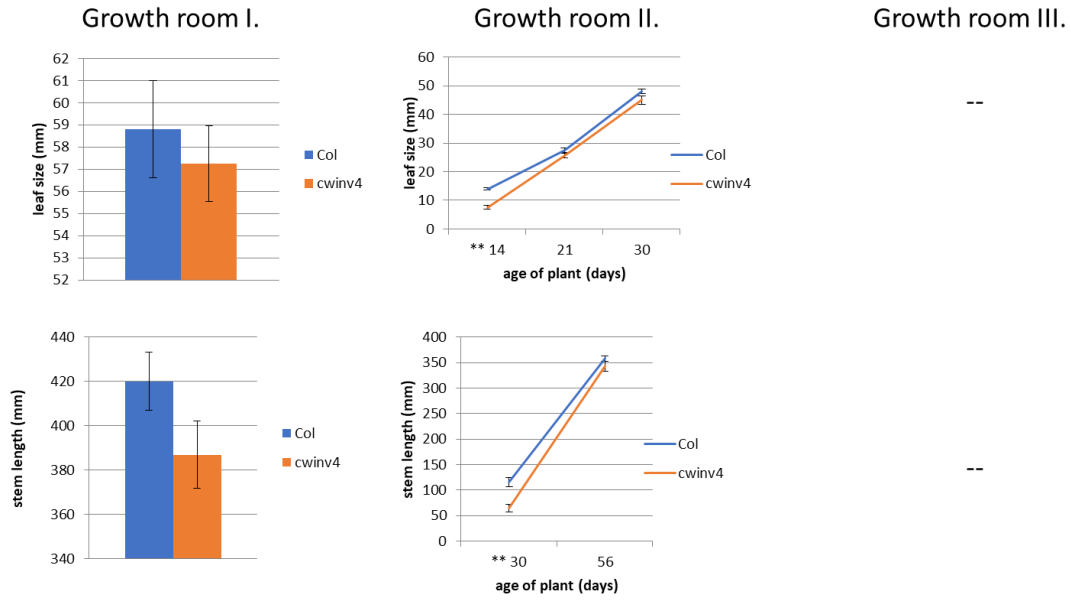

Figure 4-8 Vegetative tissue measurements of *cwinv4* and WT (Col).

Mean values shown +/- standard error. Asterisks indicate significant difference (* P<0.05, ** P<0.001).

No significant differences were observed in *cwinv4* in Growth room I. experiment (Fig 4-8). In Growth room II. experiment, the size of leaves at 14 days was

significantly smaller in *cwinv4* than the control (t=7.779, n_1=34, n_2=27, p>0.001) and the length of the stems was shorter than the control at 30 days (t=4.362, n_1=22, n_2=20, p>0.001), however later the plants equalised and there were no significant differences in these measurements

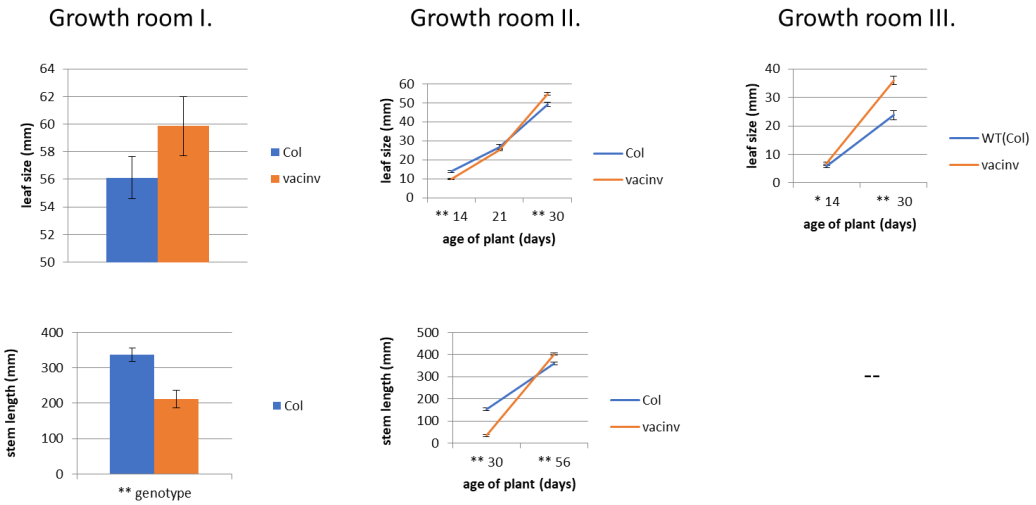

Figure 4-9 Vegetative tissue measurements of *vacinv* and WT (Col).

Mean values shown +/- standard error. Asterisks indicate significant difference (* P<0.05, ** P<0.001).

vacinv was grown in three separate experiments (Fig. 4-9). In Growth room I. experiment, the *vacinv* plants were significantly shorter than the WT (t=3.980, n_1=16, n_2=15, P<0.001) Measured at 43 days. In Growth room II. experiment, The size of *vacinv* leaves was significantly smaller at 14 days (t=5.317, n_1=n_2=33, P<0.001), however at 21 days there was not a significant difference. At 30 days *vacinv* leaves grew significantly larger than WT (t=4.098, n_1=20, n_2=22, P<0.001). At 30 days, *vacinv* plants were significantly shorter than WT (t=15.355, n_1=20, n_2=22, P<0.001), but when the senescing plants were measured at 56 days, *vacinv* were significantly taller (t=5.082, n_1=21, n_2=22, P<0.001). In Growth room III. Experiment, the size of *vacinv* leaves was significantly larger than WT at 14 days (n_1=49 n_2=27, P=0.0162), and at 30 days (n_1=46 n_2=27, P<0.001)

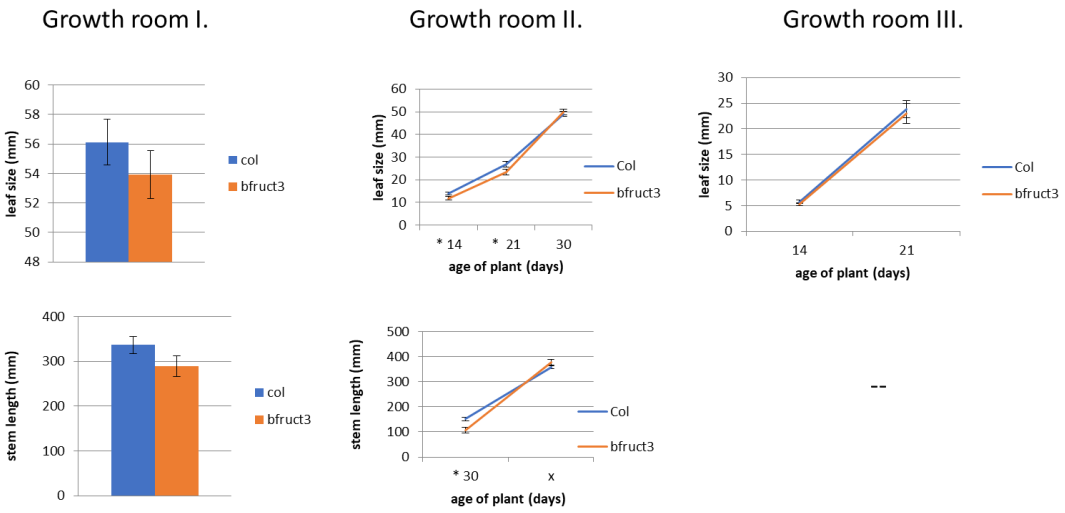

Figure 4-10 Vegetative tissue measurements of *bfruct3* and WT (Col).

Mean values shown +/- standard error. Asterisks indicate significant difference (* P<0.05, ** P<0.001).

In Growth room I. experiment, no significant differences were observed in *bfruct3* measurements (Fig. 4-10). In Growth room II. experiment, the leaves of *bfruct3* were significantly shorter than the control at 14 days (t=2.076, n_1=33, n_2=25, P=0.043) and at 21 days (t=2.012, n_1=25, n_2=24, P=0.05), but the difference in size at 30 days was not significant. Similarly, *bfruct3* plants were significantly shorter at 30 days (t=3.424, n_1=20, n_2=22, P=0.001), but when the senescing plants were measured at 56 days, no significant difference was found between *bfruct3* and Col. No significant differences were observed in Growth room III. experiment.

The observed phenotype data are summarised in Table 4-3. The size of rosette leaf of *inva* was smaller than WT in two out of three experiments, somewhat consistent with the reported growth defect in root and leaf development in a study using an identical T-DNA line (Xiang et al., 2011b). The leaves of *invh* were also smaller on both occasions it was grown. Cell wall invertase mutants have been reported as having normal phenotype (Sherson et al., 2003b), and this is the case here as well, except for *cwinv2* being shorter than WT. *vacinv* plants seemed to develop slower than WT, perhaps due to the root defect reported in *vacinv* seedlings (Sergeeva et al., 2006; Wang et al., 2010), but at maturity had larger rosette leaves.

Table 4-3 Phenotype data for selected invertase KO lines: vegetative tissue measurements.

measurements listed were significantly different from WT ($p<0.05$). Leaf: length of largest rosette leaf; stem: length of main stem from base of plant

genotype	Growth room I. February 2016	Growth room II. June 2016	Growth room III. September 2016	Figure reference
inva SALK_015233	Smaller leaf No significant difference in stem length	Smaller leaf at 21 days but not at 30 days At 56 days: Shorter stem	No significant difference in leaf size	Figure 4-4
invh SALK_016378	--	At 14 and 21 days: Smaller leaf At 30 days: Shorter stem	Smaller leaf	Figure 4-5
cwinv1 SALK_091455	--	--	Larger leaf Longer stem	Figure 4-6
cwinv2 SALK_068113	At 51 days: Shorter stem No significant difference in leaf size	At 14 days: Smaller leaf At 30 days: Shorter stem	No significant difference in leaf or stem size	Figure 4-7
cwinv4 SALK_094878	No significant difference in leaf or stem size	At 14 days: Smaller leaf At 30 days: Shorter stem	--	Figure 4-8
vacinv SAIL_1256_C02	At 43 days: Shorter stem No significant difference in leaf	At 14 days: Smaller leaf At 30 days: Shorter stem Larger leaf At 56 days: Longer stem	Larger leaf	Figure 4-9
bfruct3 SALK_015898	No significant difference in leaf or stem size	At 14 and 21 days: Smaller leaf At 30 days: Shorter stem	No significant difference in leaf size	Figure 4-10

4.2.3.2 KO line fertility

To assess the fertility of invertase KO lines, the plants were grown to maturity and allowed to self-fertilitse and the phenotype of their seeds and siliques was observed. Initially, the number of fertile and sterile (*i.e.,* empty) siliques was planned to be investigated, but since all KO lines produced seeds, the size of silique was recorded also as measure of fertility. In the Growth room III. experiment,

sterility data and silique number per unit of stem length were not included and only sizes were recorded. The measurements are shown below and compiled in Table 4-4.

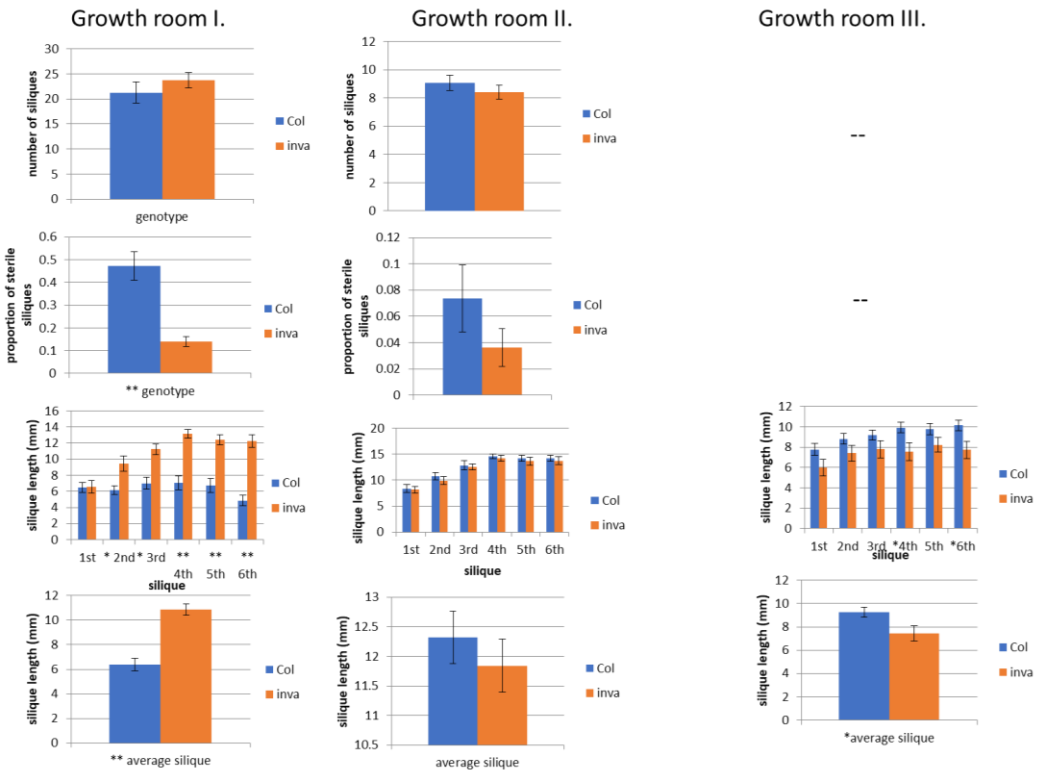

Figure 4-11 Silique measurements of *inva* and WT (Col).

Mean values shown +/- standard error. Asterisks indicate significant difference (* P<0.05, ** P<0.001).

In Growth room I. experiment, the proportion of sterile siliques was significantly smaller in *inva* ($z=4.24$, $n_1=14$, $n_2=16$, $P<0.001$). The average *inva* silique was longer than the average WT silique ($z=4.28$, $n_1=14$, $n_2=16$, $P<0.001$). The sizes of the 1st silique were not significantly different, but the other siliques were significantly longer than WT ($n_1=14$, $n_2=16$. 2nd: $z=2.41$, $P=0.016$; 3rd: $z=3.28$, $P=0.001$; 4th: $z=4.20$, $P<0.001$; 5th: $z=3.87$, $P<0.001$; 6th: $z=4.16$, $P<0.001$). No significant differences were observed in Growth room II. experiment. In Growth room III. experiment, the average *inva* silique was shorter than the average WT silique ($n_1=37$, $n_2=18$, $P= 0.0264$). The sizes 4th and 6th siliques were significantly shorter than WT ($n_1=43$, $n_2=18$ $P<0.05$).

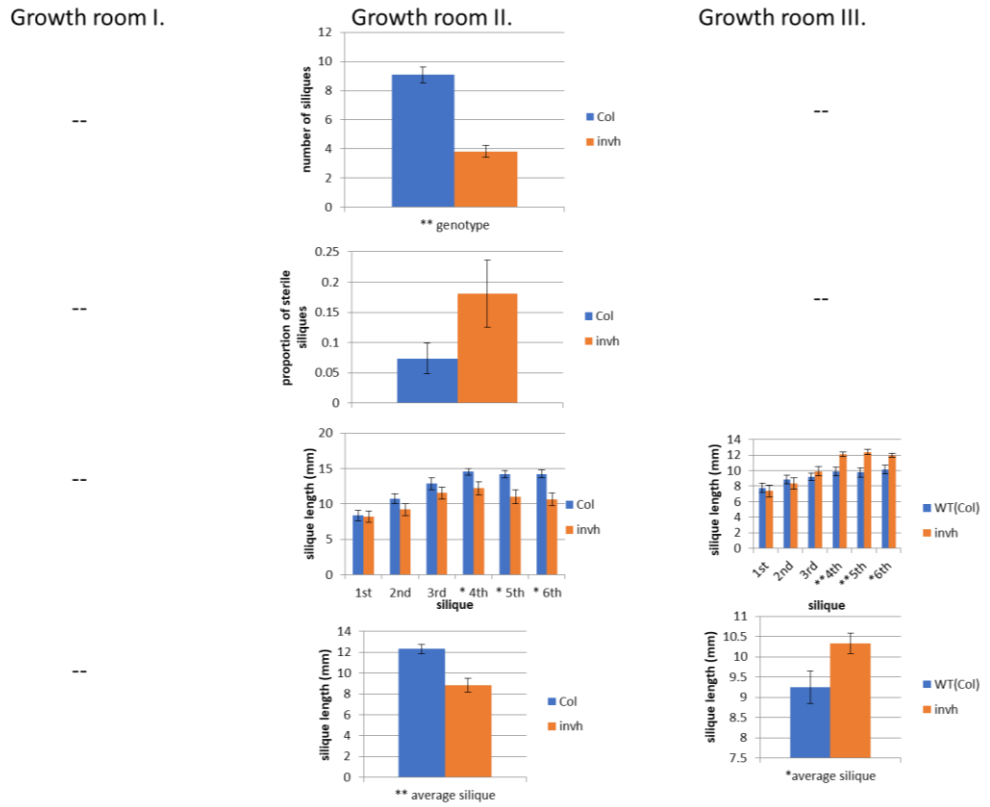

Figure 4-12 Silique measurements of *invh* and WT (Col).

Mean values shown +/- standard error. Asterisks indicate significant difference (* P<0.05, ** P<0.001).

In Growth room II. experiment, the *invh* plants had significantly fewer siliques (t=7.68, n_1=27, n_2=29, P<0.001). There was not a significant difference in the proportion of sterile siliques. The average *invh* silique was significantly shorter than WT (z=3.65, n_1=n_2=27, P<0.001). The 4th, 5th and 6th *invh* siliques were significantly shorter than WT (4th: z=2.43, n_1=27, n_2=15, P=0.015; 5th: z=2.86, n_1=26, n_2=12, P=0.004; 6th: z=2.44, n_1=24, n_2=6, P=0.007). In Growth room III. Experiment, the average *invh* silique was significantly longer than WT (n_1=43 n_2=22, P=0.0281). The 4th, 5th and 6th *invh* siliques were significantly longer than WT (n_1=43 n_2=22, 4th: P<0.001; 5th: P=0.001; 6th: P=0.0038)

Growth room I.	Growth room II.	Growth room III.
--	--	--
--	--	--
--	--	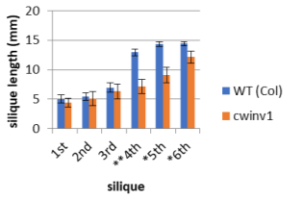
--	--	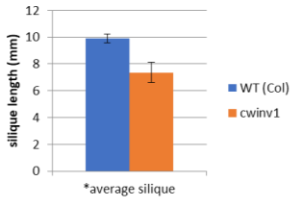

Figure 4-13 Silique measurements of *cwinv1* and WT (Col).

Mean values shown +/- standard error. Asterisks indicate significant difference (* P<0.05, ** P<0.001).

The average *cwinv1* silique was significantly shorter than WT (n_1=19 n_2=17, P=0.0055). The 4th, 5th and 6th *cwinv1* siliques were significantly shorter than WT (4th: n_1=19 n_2=16, P<0.001; 5th: n_1=19 n_2=15, P=0.0012; 6th: n_1=19 n_2=16, P=0.0399)

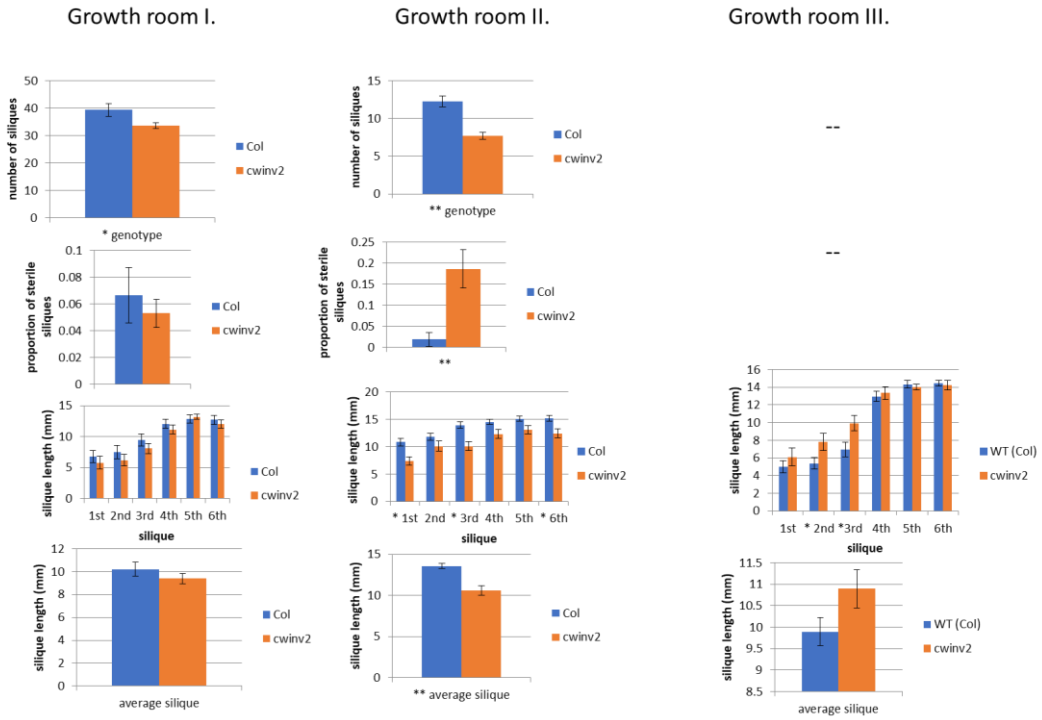

Figure 4-14 Silique measurements of *cwinv2* and WT (Col).

Mean values shown +/- standard error. Asterisks indicate significant difference (* P<0.05, ** P<0.001).

In Growth room I. experiment, the *cwinv2* plants had significantly fewer siliques (t=2.27, n_1=n_2=16, P=0.03). The number of siliques per unit of stem length was not significantly different. No significant differences were found in silique size and sterility. In Growth room II. experiment, *cwinv2* plants had significantly fewer siliques (t=5.45, n_1=21, n_2=25, P<0.001), and a larger proportion of sterile siliques (z=2.999, n_1=21, n_2=25, P=0.003). An average *cwinv2* silique was significantly shorter than an average WT silique (z=3.65, n_1=21, n_2=25, P<0.001), with the 1st, 3rd and 6th silique being significantly shorter than in WT (1st: z=2.75, n_1=21, n_2=25, P=0.006; 3rd: z=3.26, n_1=21, n_2=25, P=0.001; 6th: z=2.16, n_1=21, n_2=21, P=0.03). In Growth room III. Experiment, the 2nd and 3rd *cwinv2* silique was significantly longer than WT silique (2nd: n_1=18, n_2=19, P=0.0469; 3rd n_1=19, n_2=21, P=0.0169)

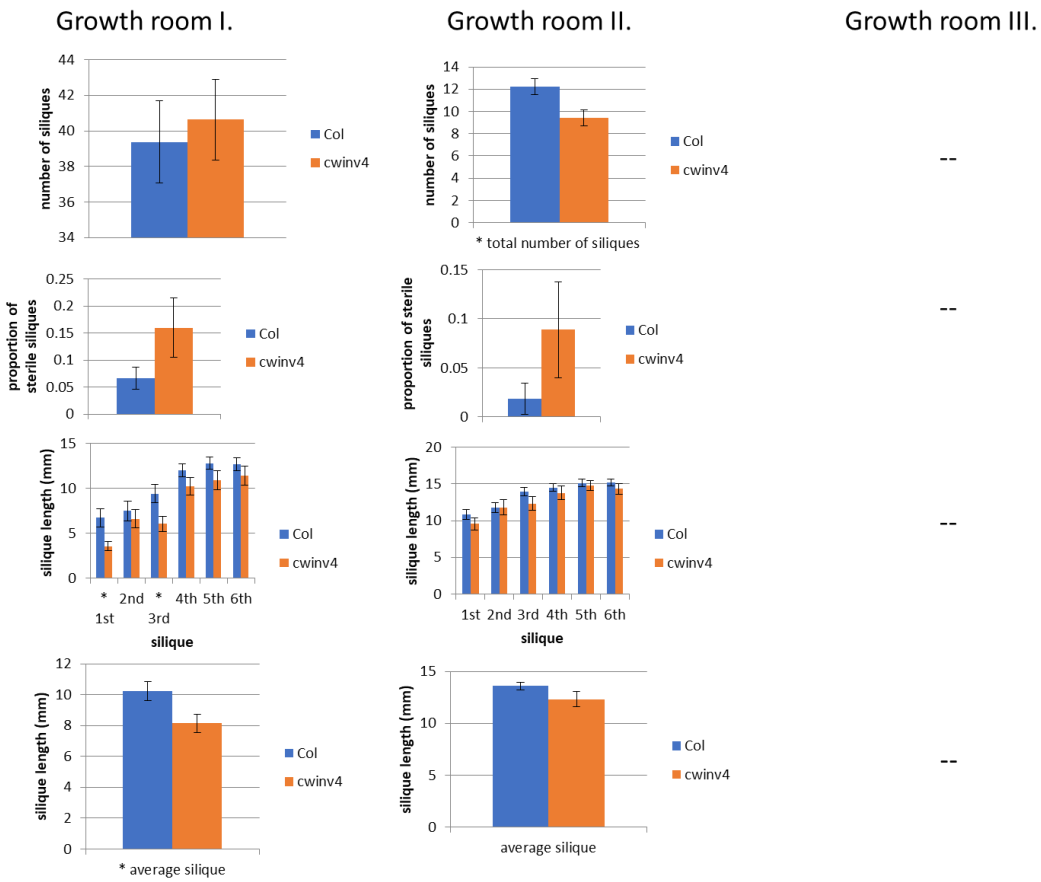

Figure 4-15 Silique measurements of *cwinv4* and WT (Col).

Mean values are shown +/- standard error. Asterisks indicate significant difference (* P<0.05, ** P<0.001).

In Growth room I. experiment, siliques of *cwinv4* were significantly shorter on average ($z=2.506$, $n_1=n_2=16$, $P=0.01$) with the differences being significant in the 1st silique ($z=2.186$, $n_1=n_2=16$, $P=0.03$) and the 3rd silique ($z=2.186$, $n_1=n_2=16$, $P=0.03$). No significant differences were observed in silique number and sterility. In Growth room II. experiment, the number of siliques on each plant at 35 days was significantly lower in *cwinv4* ($t=2.786$, $n_1=21$, $n_2=20$, $P=0.008$), as well as number of siliques per unit of stem length. No significant differences in silique lengths or sterility between *cwinv4* and Col were observed.

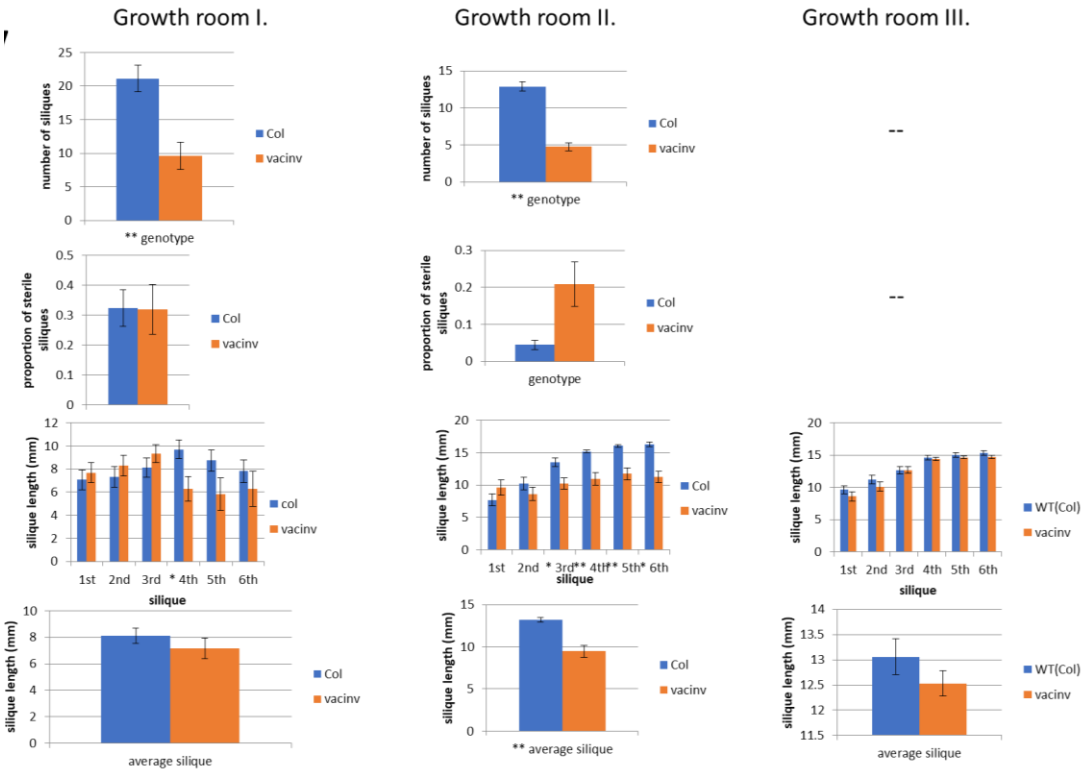

Figure 4-16 Silique measurements of *vacinv* and WT (Col)

Mean values shown +/- standard error. Asterisks indicate significant difference (* P<0.05, ** P<0.001).

In Growth room I. experiment, the *vacinv* plants had significantly fewer siliques (t=4.031, n_1=16, n_2=15, P<0.001). The number of siliques per unit of stem length (to account for *vacinv* being shorter) was also significantly lower (z=2.29, n_1=16, n_2=15, P= 0.02). The 4th silique of *vacinv* was significantly smaller than that of WT (z=2.122, n_1=16, n_2=11, P= 0.03). The sizes of the other siliques and proportion of sterile siliques were not significantly different from WT. In Growth room II. experiment, *vacinv* plants had significantly fewer siliques than WT (t=9.714, n_1=21, n_2=22, P<0.001). The proportion of sterile siliques in *vacinv* was larger, but not significantly different from WT at the 95% confidence level (z=1.89, n_1=21, n_2=20, P= 0.059). The average silique was shorter in *vacinv* compared to WT (z=3.912, n_1=21, n_2=20, P<0.001). In particular, there was a significant difference from WT in the length of the 3rd silique (z= 2.719, n_1=21, n_2=18, P=0.007), 4th silique (z=3.526, n_1=21, n_2=16, P<0.001), 5th silique (z=4.464, n_1=21, n_2=11, P<0.001), and 6th silique (z=3.85, n_1=21, n_2=8, P=0.001). No significant differences were observed in Growth room III. experiment.

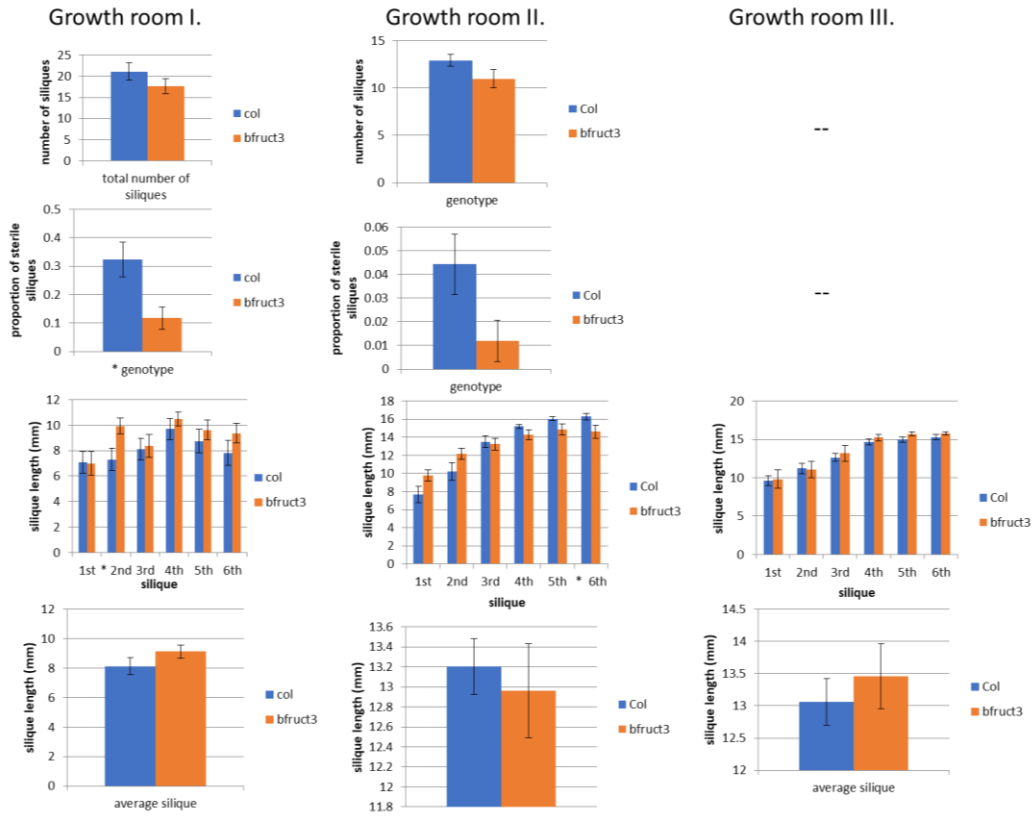

Figure 4-17 Silique measurements of *bfruct3* and WT (Col)

Mean values shown +/- standard error. Asterisks indicate significant difference (* P<0.05, ** P<0.001).

In Growth room I. experiment, *bfruct3* plants had a smaller proportion of sterile siliques than WT (z=2.619, n_1=n_2=16, P=0.009). The 2nd silique in *bfruct3* was significantly longer than in Col (z=2.28, n_1=n_2=16, P=0.023). The number of siliques was not significantly different. In Growth room II. experiment, the average length of the 6th silique was significantly smaller in *bfruct3* (t=2.634, n_1=21, n_2=20, P=0.008). The other siliques were not significantly different from WT. The proportion of sterile siliques, number of siliques, and average silique length were not significantly different from WT. No significant differences were observed in Growth room III. experiment.

Table 4-4 Phenotype data for selected invertase KO lines: silique measurements.

Measurements listed were significantly different from WT ($p<0.05$). Silique length: measured on siliques on main stem, 1st silique being the oldest; sterile siliques: siliques which contain no seeds; Avg: average silique (mean length of the six first siliques).

genotype	Growth room I. February 2016	Growth room II. June 2016	Growth room III. September 2016	Figure reference
inva SALK_015233	Fewer sterile siliques Longer siliques (avg., 2nd, 3rd, 4th, 5th, 6th)	No significant difference in silique number or size	Shorter silique (avg, 4th and 6th)	Figure 4-11
invh SALK_016378	--	Fewer siliques Shorter siliques (avg., 4th, 5th, 6th)	Longer siliques (avg, 4th, 5th, 6th)	Figure 4-12
cwinv1 SALK_091455	--	--	Shorter siliques (avg, 4th, 5th, 6th)	Figure 4-13
cwinv2 SALK_068113	Fewer siliques, but no significant difference in number of siliques per unit of stem length. No significant difference in silique size or sterility	At 35 days: Fewer siliques More sterile siliques Shorter siliques (avg., 1st, 3rd, 6th)	Longer siliques (2nd, 3rd)	Figure 4-14
cwinv4 SALK_094878	At 51 days: Shorter siliques (avg., 1st, 3rd) No significant difference silique number	At 35 days: Fewer siliques (and siliques per unit of stem length) No significant difference in silique size	--	Figure 4-15
vacinv SAIL_1256_C02	Fewer siliques (and siliques per unit of stem length) At 43 days: 4th silique shorter	At 35 days: Fewer siliques Shorter siliques (avg., 3rd, 4th, 5th, 6th)	No significant difference in silique size	Figure 4-16
bfruct3 SALK_015898	At 43 days: Fewer sterile siliques 2nd silique longer	At 35 days: 6th silique shorter No significant difference silique number or proportion of sterile siliques	No significant difference in silique size	Figure 4-17

The only KO line which had a consistent phenotype in multiple experiments was *vacinv*, which had fewer siliques which were smaller than WT.

4.2.3.3 Flowering time

The proportion of KO plants and corresponding WT plants with at least one open flower was observed in two separate experiments, to determine whether there is delay in flowering. The only KO line which had consistently delayed flowering was *vacinv* (Table 4-5. Experiment 1: 23% of *vacinv* (n=31) and 83% of WT (n=30) were flowering at 28 days. Experiment 2: 40% of *vacinv* (n=22) and 100% of WT (n=20) were flowering at 30 days.)

Table 4-5 The proportion of plants with at least one open flower.

Experiment 1, plants sown 12/2016, observed at 28 days; Experiment 2, plants sown 07/2016, observed at 30 days.

	Experiment 1				**Experiment 2**			
genotype	proportion KO plants flowering	n (KO plants)	proportion WT control flowering	n (WT plants)	proportion KO plants flowering	n (KO plants)	proportion WT control flowering	n (WT plants)
bfruct3	61%	28	83%	30	95%	22	100%	20
cwinv1	100%	25	70%	23	95%	22	100%	22
cwinv2	76%	29	70%	23	71%	24	100%	22
cwinv4	90%	30	70%	23	80%	20	100%	22
inva	-	-	-	-	100%	24	93%	25
invh	92%	26	43%	28	33%	27	93%	25
vacinv	23%	31	83%	30	41%	22	100%	20

4.2.3.4 Flower phenotype

In order to investigate the phenotype of the floral organs of invertase KO plants, flowers were collected from three different plants of each genotype at three different stages: “stage 4 buds” (oldest unopened bud, anther stage 12 (Sanders et al., 1999)), “before dehiscence” (petals protruding, anther stage 12-13 (Sanders et al., 1999)) and “after dehiscence” (first fully open flower, anther stage 13(-14) (Sanders et al., 1999)). The measurements were made using ZEN 2.3 Lite from photographs. The length of one of the medial stamens was measured base of the filament to the top of the anther. The lengths of the pistil, sepal, and petal were also measured.

The differences in these measurements between samples were, however, very subtle and more samples would be needed to assess whether they are statistically significant (Fig. 4-18).

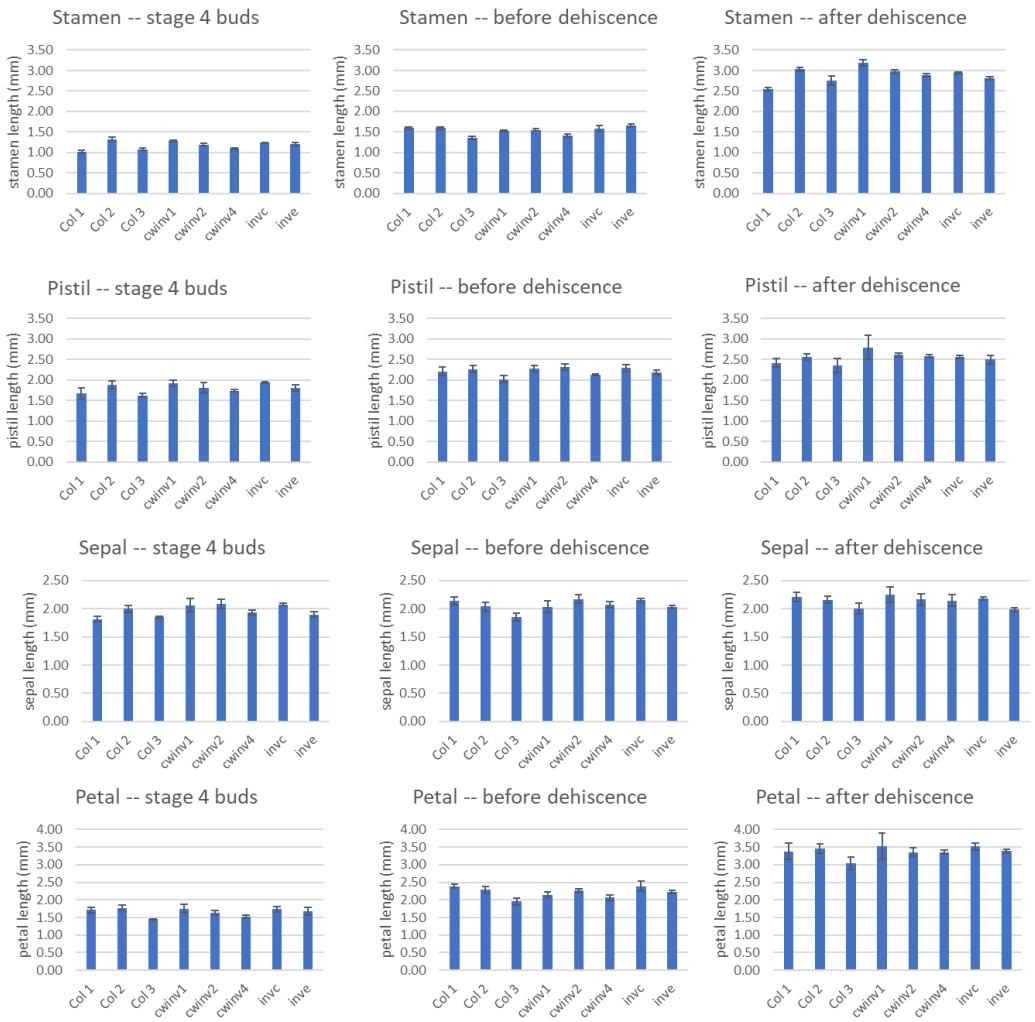

Figure 4-18. Floral organ length in invertase KO lines and WT (Columbia).

n=3. The mean length +/- S.E. is shown. The plants were grown in the growth room in 3x4 trays which were rotated in position weekly to minimize environmental impact on the differences in phenotype, however the three control trays (Col 1-3) show more noticeable differences than the KO lines.

4.2.4 Multiple KO

4.2.4.1 cwinv2cwinv4 double KO

CWINV2 and CWINV4 were found to be among the top invertase isoforms of interest for potential roles in anther dehiscence (Chapter 3 Section 3.3), and they also seem to be complementary (Figure 4-3). To explore their functions further, a knockout in both genes was generated.

A *cwinv2cwinv4* double KO mutant was generated by crossing *cwinv2* (SALK_068113) with *cwinv4* (SALK_094878). First filial generation (F1) plants were allowed to self-fertilise to produce the second filial generation (F2). F2 plants were checked by PCR for presence of both T-DNA inserts (Fig. 4-5). The *cwinv2cwinv4* plants were fertile and appeared identical to WT. However, their phenotype has not been assessed in detail.

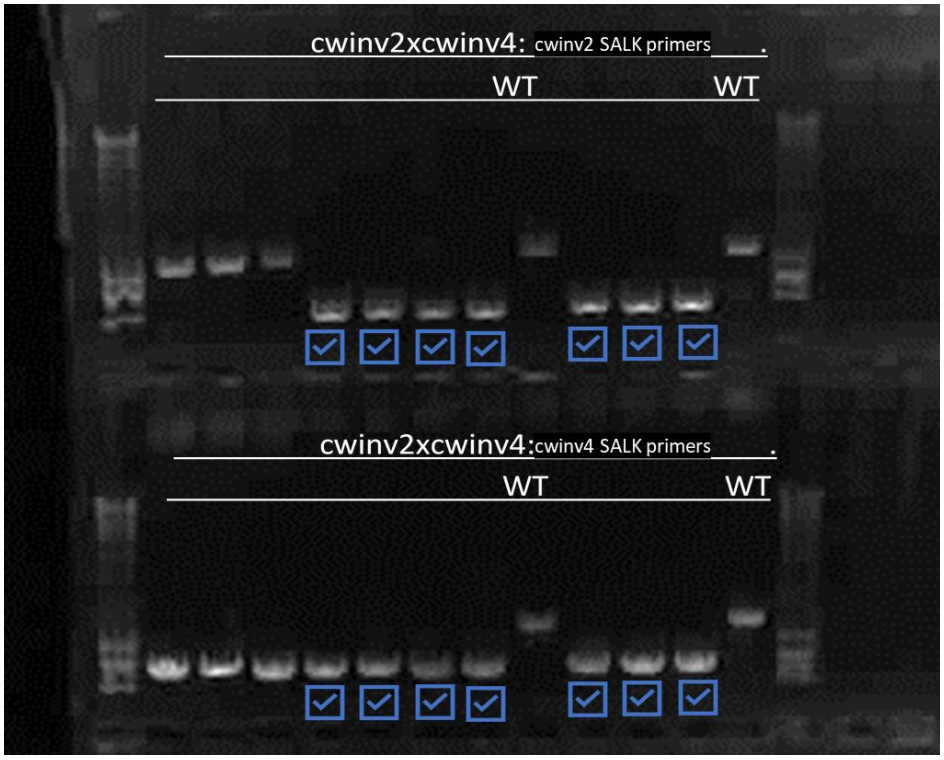

Figure 4-19 Genotyping PCR of *cwinv2cwinv4* double KO mutant.

Upper row: primers detecting T-DNA in *CWINV2*; bottom row: primers detecting T-DNA in *CWINV4*. Blue checkmarks indicate plants in which both T-DNA inserts are present. This figure is not representative of allele segregation in F2 overall.

4.2.5 CRISPR/Cas9

CRISPR/Cas9 gene editing was investigated as an approach to make knock-out mutants for additional invertase genes. Target sequences with minimal off-target potential were identified for future use (Table 4-6)

Table 4-6 Target design using the CRISPOR guide RNA selection tool (Haeussler et al., 2016)

Gene	target	target sequence	target name	Enzymes usable for screening
BFRUCT3	BFRUCT3 exon 1	ACGGGTCTCCGGGATCTGGT CGG	bfruct3_1	BspPI, MflI, Hpy188I, NdeII, BslI
	BFRUCT3 exon 1	TCCGACGGGTCTCCGGGATC TGG	bfruct3_2	NdeII, BspPI, Hpy188I, PfoI, MflI, BslI
CWINV1	CWINV1 exon 1	CGGTAGGGCTGGTTTACGGA AGG	cwinv1_1	TspGWI
	CWINV1 exon 3	GAACCCGAAAGGAGCCGTGT GGG	cwinv1_2	MaeIII
CWINV2	CWINV2 exon 4	AGACACCGGGACTGACGCCA AGG	cwinv2_1	ErhI, HgaI, BslI, AcyI, BseDI
	CWINV2 exon 3	CCATGTCTTGAGGTATGGGT CGG	cwinv2_2	Hpy188I
CWINV4	CWINV4 exon 3	TAGAGACCTTTGTAGTATAC TGG	cwinv4_1	Bse1I, Hpy166II, PspPI, Bme18I, BstZ17I, FblI
	CWINV4 exon 3	AGACGGGCATTGGAGAACCG TGG	cwinv4_2	BstDSI, BslI, HpyCH4III, BseDI
CWINV5	CWINV5 exon 2	CAACGACCGTTATAACCGCC AGG	cwinv5_1	Bme18I, StyD4I, SsiI, BstNI, PspPI
	CWINV5 exon 2	CCGATCCATATCTACGGCAC TGG	cwinv5_2	BceAI, Bme18I, Bse1I, PspPI, TspRI
VACINV	VACINV exon 1	AGAGACCAAATGAGACGGCG AGG	vacinv_1	BceAI, BseRI
	VACINV exon 1	TTCCGGTGATCGGAACACGC CGG	vacinv_2	MspI, Cfr10I, NaeI, SgrAI, MreI, BstC8I

4.3 Discussion

4.3.1 Observed phenotype of KO lines

None of the observed phenotypes in KO lines seems to be consistent with published data, despite some knockouts being reported as having severe impairment to growth (Table 4-1). However, the observed phenotypes did not show similar trends between separate experiments, except for *vacinv.*

vacinv plants develop slower than WT, perhaps due to the root defect reported in *vacinv* seedlings (Sergeeva et al., 2006; Wang et al., 2010), but at maturity had larger rosette leaves. They also had fewer siliques which were smaller in comparison to WT, and their flowering was delayed.

4.3.2 Redundancy

CWINV1, *CWINV2* and *CWINV4* seem to be acting in a complementary way: when one is knocked out, the other two are upregulated. These genes are quite closely related (Fig. 3-1), along with *CWINV5*. Complementation has been reported in other sets of closely related invertase isoforms. Loss of *CINV1* expression increases *CINV2* transcript levels (Barratt et al., 2009).

Both *CWINV2* and *CWINV4* are highly expressed in flowers and reported to have functions in reproduction in studies using tissue-specific silencing. Anther-specific silencing of *CWINV2* disrupted carbohydrate supply for pollen development leading

to sterility (Hirsche et al., 2009a). Ovule-specific silencing of *CWIN2* and *CWIN4* impacted ovule initiation by disrupting sugar signalling (Liao et al., 2020). It would be interesting to analyse the effect of silencing *CWINV2* and *CWINV4* simultaneously in the anther. However, since *cwinv2cwinv4* plants were fertile, knocking out all four cell wall invertase genes may be necessary to see an effect. Due to the proximity of *CWINV1* and *CWINV5* on chromosome 3, crossing available T-DNA lines to produce quadruple mutant is not a viable option. CRISPR/Cas9 gene editing was instead explored, and target sequences identified which could be used to produce a multiple knock out mutant.

Chapter 5: Hormonal regulation of anther dehiscence

5.1 Introduction

Jasmonic acid (JA) is a lipid-derived signalling compound know to regulate many plant processes, including flower opening and floral organ development in *Arabidopsis* (Ishiguro et al., 2001a) Tomato (Niwa et al., 2018), and Chrysanthemum (Fei et al., 2016).

Auxin and giberellin may have an indirect role in activation of jasmonate synthesis in *Arabidopsis* (Acosta and Przybyl, 2019).

Jasmonate signalling in the Arabidopsis root upon inoculation with a mutualistic fungus *Phomopsis liquidambari* at the flowering stage, through inhibition of sugar transport and soluble invertase activity was identified as a likely mechanism for flowering-mediated root sugar depletion upon fungal inoculation, perhaps to direct resources toward flower development (Zhang et al., 2019).

The water transport out of the anthers in *Arabidopsis* is thought to be regulated by jasmonic acid synthesized in the filaments, which drives water uptake into, and elongation of, filaments and petals (Ishiguro et al., 2001b).

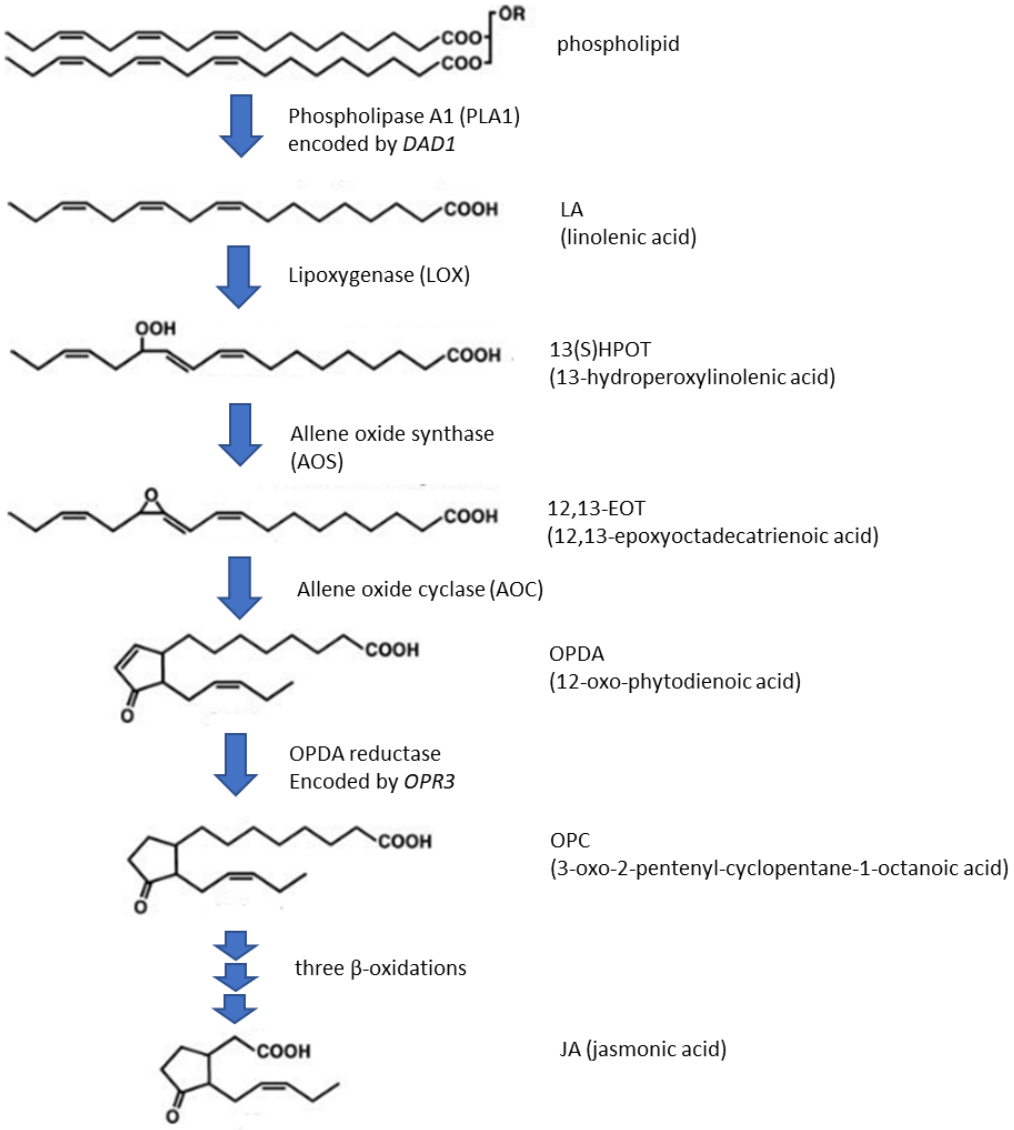

Figure 5-1. Biosynthesis of jasmonic acid from phospholipid precursor.

Adapted from (Ishiguro et al., 2001a; Stintzi and Browse, 2000)

Ishiguro et al. describe the *A. thaliana* Phospholipase A1 (PLA1), encoded by *DAD1*, which catalyses the initial step of JA biosynthesis (Fig. 5-1). *DAD1* is expressed in stamen filaments in middle and late-stage buds. In *dad1* KO mutant plants, anther dehiscence does not occur even after flower opening, and the anthers remain hydrated. This dehiscence defect can be rescued by application of exogenous methyl jasmonate (derivative of JA). It has been proposed that jasmonic acid regulates the water transport from anthers by inducing the expression of relevant genes (Ishiguro et al., 2001b), and it is possible that some invertase isoforms are among them.

Other indehiscent KO mutants in the JA biosynthesis pathway have been characterised. 12-oxophytodienoate (OPDA) reductase activity is disrupted in *delayed dehiscence1* mutant, which releases pollen too late for pollination to occur

(Sanders et al., 2000). Another member of the OPDA reductase family is *OPR3*, whose KO mutant *opr3* is fully indehiscent (Stintzi and Browse, 2000).

5.2 Results

5.2.1 Analysis of invertase expression in *opr3* background

Information available about *A. thaliana* invertases through FlowerNet (Pearce et al. 2015) was used to identify invertases whose expression is altered in jasmonic acid treatment time course. This data was obtained from experiments using *opr3* mutant plants. *opr3* plants do not produce OPDA reductase, one of the enzymes required in the final steps of JA biosynthesis (Fig. 5-1). The plants were treated with exogenous JA, and OPDA as control. Stage 12 (refer to Table 1-1) stamens were collected at several timepoints after a single treatment application (Mandaokar et al., 2006). The plots of individual timecourses, produced through FlowerNet, are shown in Fig. 5-2.

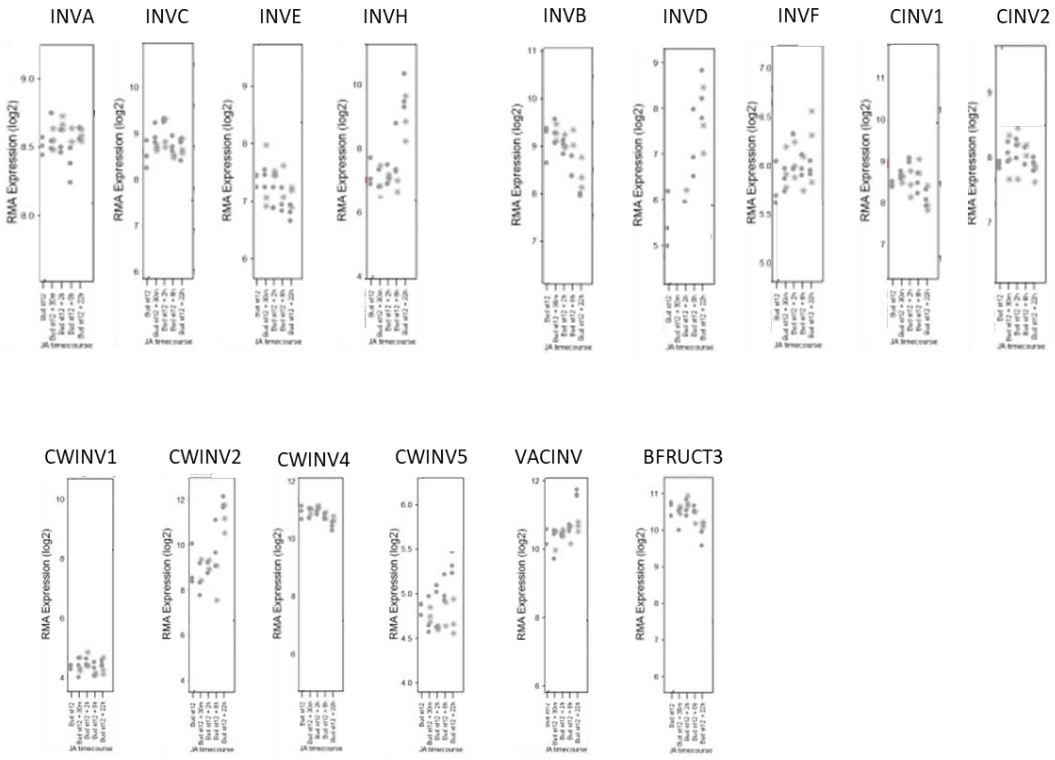

Figure 5-2 JA timecourse showing changes to gene expression in stamens in *opr3* mutant background after treatment with JA (circles) and OPDA (stars).

Adapted from (Mandaokar et al., 2006; Pearce et al., 2015).

Among the invertase isoforms, the expression of *INVE, INVB, CWINV4* and *BFRUCT3* was decreased following JA treatment, and the expression of *INVH, INVD, CWINV2, CWINV5* and *VACINV* was increased (Table 5-1).

Table 5-1 *A. thaliana* invertases with data on expression in stamen in response to JA treatment (data from FlowerNet (Pearce et al., 2015))

		Locus	Name	Response to JA timecourse (Fig.5-2)
Alkaline/ Neutral invertases	α (mitochon-drion or plastid-targeted)	AT1G56560	*INVA*	no
		AT3G06500	*INVC*	no
		AT5G22510	*INVE*	decrease
		AT3G05820	*INVH*	increase
	β (cytosolic)	AT4G34860	*INVB*	decrease
		AT1G22650	*INVD*	increase
		AT1G72000	*INVF*	no
		AT1G35580	*CINV1*	no
		AT4G09510	*CINV2*	no
Acid invertases	Extra-cellular	AT3G13790	*CWINV1*	no
		AT3G52600	*CWINV2*	increase
		AT2G36190	*CWINV4*	decrease
		AT3G13784	*CWINV5*	increase
	Vacuolar	AT1G12240	*VACINV*	increase
		AT1G62660	*BFRUCT3*	decrease

5.2.2 Expression of invertases in *dad1* background

To investigate which invertases may regulated by JA, their expression was investigated in the *dad1* KO line SALK_138439. The *dad1* mutant does not produce JA which leads to lack of anther dehiscence and sterility. *DAD1* is expressed in middle and late-stage buds (Ishiguro et al., 2001b), therefore the expression of invertases in stage 4 buds (Chapter 2 Section 2.1.3) from *dad1* compared to WT was investigated.

To obtain homozygous *dad1* plants more easily without the need to screen a segregating population, *dad1* plants were treated with methyl jasmonate to restore

their fertility and produce homozygous *dad1* seeds (method adapted from (Ishiguro et al., 2001a; Sanders et al., 2000) and described in Chapter 2 Section 2.1.5).

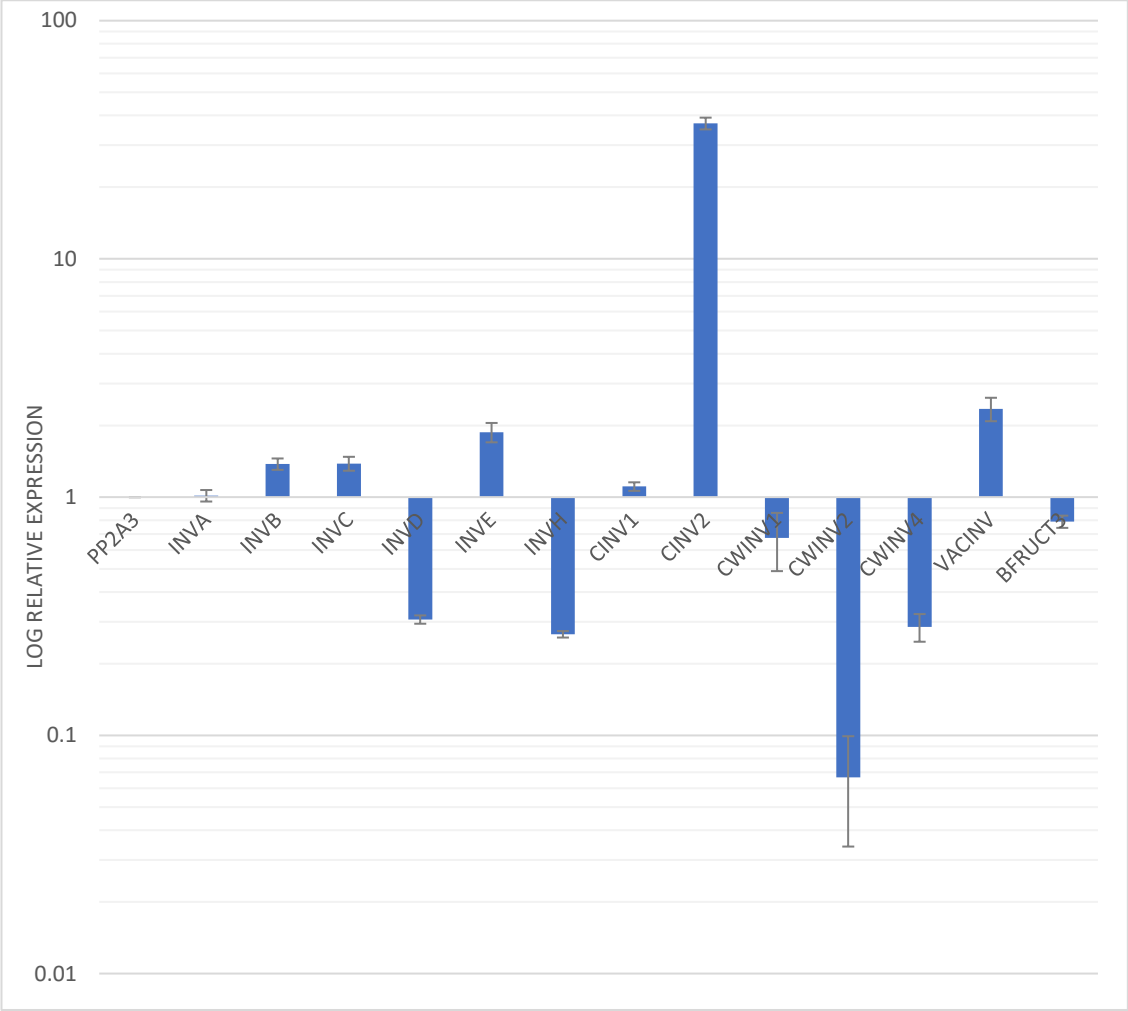

Figure 5-3. Expression of invertases in jasmonic acid deficient mutant.

Expression was assessed by qRT-PCR in *A. thaliana* mutant *dad1,* which does not produce jasmonic acid, and in wild-type (ecotype *Landsberg erecta*) buds at stage 4 (containing mature pollen, before dehiscence (Chapter 2 Section 2.1.3)). Expression in *dad1* is shown relative to expression in WT +/- standard error of the mean. The values are normalized to the expression of the house-keeping gene *PP2A3*.

The expression of *INVE, VACINV* and especially *CINV2* is upregulated in *dad1* plants compared to WT, while *INVD, INVH, CWINV2* and *CWINV4* are downregulated (Fig. 5-3). This suggests their involvement in facilitating JA-mediated water transport during anther dehiscence.

5.3 Discussion

INVD, INVH CWINV2 and *CWINV4* had increased expression in the late stages of flower development in WT background (Chapter 3, Section 3.2.3), but not in the

dad1 background (Section 5.2.2), suggesting they may be regulated by JA. Additionally, the fact that *CINV2* and *VACINV* were upregulated in *dad1* (Fig. 5-3) warrants further investigation as well.

However, the expression analysis presented in Section 5.2.2 has only been replicated once. Ideally, at least three biological replicates should be performed to confirm the results. Another improvement to be made in expression analysis is using the ecotype Col-0 (*Columbia*), rather than *Landsberg erecta,* as the control for expression in KO lines (including *dad1*), as the background of the *dad1* KO line SALK_138439 is Col-0. Samples of late stage 4 buds (Chapter 2 Section 2.1.3) of *dad1* and Col-0 plants from three independent biological replicates have been collected, but their analysis has not been completed (Appendix Section 8.1).

For further analysis of invertase expression in *dad1,* promoter-GUS fusion constructs described in Chapter 3 Section 3.2.4 could be utilised.

Chapter 6: General discussion

The aim of this project was to investigate the role of invertases in establishing the osmotic gradient required for dehydration of the anther during anther dehiscence.

Several invertase isoforms (*INVH, INVD, CWINV2,* and *CWINV4*) were detected by qRT-PCR analysis to be upregulated in *A. thaliana* buds during late stages of bud development (Chapter 3 Section 3.2.3) but downregulated in the absence of JA, a known regulator of water transport out of the anthers (Chapter 5 Section 5.2.2). This suggests that these isoforms may be involved in facilitating JA-mediated water transport during anther dehiscence.

The promoter sequences of the genes with potential role in anther water transport were used to prepare β-glucuronidase (GUS) reporter constructs to investigate their localization (Chapter 3 Section 3.2.4). In particular, the localization of *CINV2* and *VACINV* gene products in *dad1* (JA-deficient) background is of interest, as these genes are upregulated in *dad1.* The reporter constructs could also be used to investigate the upregulated expression in KO lines of closely related genes, such as *CWINV2* and *CWINV4* in *cwinv1* (Chapter 4 Section 4.2.2.2).

Analysis of the phenotype of KO mutants did not uncover a striking phenotype in any of the mutants, as the observations were not replicable. *vacinv* plants developed slower than WT, had fewer siliques which were smaller in comparison to WT, and their flowering was delayed, indicating a possible slight effect of *VACINV* on fertility (Chapter 4 Section 4.3.1).

The phylogenic tree (Chapter 3, Fig.3-1) reveals that several of the invertase isoforms are evolutionarily close, so one of the pair may be redundant. Indeed, it has been reported that while single mutations in *CINV1* and *CINV2* did not affect the plant phenotype, double mutants *cinv1/cinv2* were drastically affected (Barratt et al., 2009). *CINV1* is the primary cytosolic invertase isoform, but *CINV2* can compensate for loss of *CINV1* (Meng et al., 2021; Pignocchi et al., 2021).

CWINV2 and *CWINV4* may have complementary or additive roles in ovule initiation (Liao et al., 2020). Vacuolar invertases can also compensate for loss of one isoform to some degree. While *VACINV* provides the majority of vacuolar invertase activity, both genes need to be suppressed to achieve significant alteration to vacuolar sugar homeostasis (Vu et al., 2020; Weiszmann et al., 2018). Deficiency in vacuolar invertase does not seem to be compensated cytosolic invertase (Weiszmann et al., 2018).

This is also in consistent with the results of expression analysis in KO lines. Especially in extracellular invertases, in lines where one gene is knocked out the others are upregulated (Chapter 4 Section 4.2.2.2). A cross of *cwinv2cwinv4* KO lines has been produced, however it did not seem to show an impaired phenotype (Chapter 4 Section 4.2.4.1). It may be the case that all of the extracellular invertases

need to be knocked out for an effect to be seen. *CWINV1* and *CWINV5* are located on the same chromosome, approximately 2 kb apart, and producing a quadruple mutant *cwinv1cwinv2cwinv4cwinv5* by crossing is therefore not likely to be feasible. CRISPR/Cas9 gene editing was instead explored as an option to produce a multiple knock out mutant.

Antisense repression has been used to target an invertase by (Hirsche et al., 2009b). The RNAi construct they used was targeting *CWINV2*, and its success was assessed by measuring invertase activity in pollen. Transformed plants showed impaired silique development and pollen viability. The T-DNA insertional mutant line *cwinv2* does not share this phenotype, so it is possible that the RNAi construct is repressing the other extracellular invertases (which are upregulated in *cwinv2*) as well. Using RNAi could be a good alternative to multiple crossing.

Most of the results presented here have only been replicated once or twice. At least three biological replicates should be performed for expression analysis and phenotyping, to confirm the results.

A detailed understanding of pollen formation and release has profound implications for selective crop breeding. Hybrid vigour (heterosis) conveys superior traits to hybrids compared to inbred parent lines, but the production of hybrids usually requires either labour-intensive manual emasculation or existence of male-sterile parent line. To maintain this line, a rescue of fertility is needed. Targeting dehiscence, instead of pollen formation or viability, offers the possibility of blocking the release of pollen reversibly. This would enable engineering the rescue of fertility in response to an external trigger (for example temperature).

Another agricultural impact could be the prevention of transgenic pollen release into wild populations. The release of pollen in the field and crossing with wild relatives is a growing concern due to the risk of passing favourable traits onto wild weedy relatives of commercial crops. Here, a more complex understanding of the factors which trigger dehiscence could be applied to time the release of pollen in crops so that the chance of outcrossing is decreased.

Research into the importance of water transport in flowering could additionally be useful in breeding crops for climate change. Manipulation of water transport pathways in drought resistant crops to ensure more efficient water use may also affect water transport in dehiscence. As this would affect the crop yield, it is necessary to expand our understanding of dehiscence and avoid such unexpected effects.

6.1 Conclusion

Several invertase isoforms were detected by qRT-PCR analysis which are upregulated in *A. thaliana* buds during late stages, but downregulated in the absence of jasmonic acid, suggesting a role in anther dehiscence. Single KO mutant plants do not show a phenotype alteration, and data on expression of invertases in selected KO lines and analysis of phylogeny suggest some of the invertases are complementary. Crosses of some of these lines have been produced, however using CRISPR/Cas9 or RNAi to target multiple genes may be a better option. Reporter constructs have been prepared to investigate the localization of selected invertases. In the investigation of the molecular mechanisms governing water transport in anther dehiscence, the genes identified here can be subject for further study.

References

Acosta, I.F., and Przybyl, M. (2019). Jasmonate Signaling during Arabidopsis Stamen Maturation. Plant and Cell Physiology *60*, 2648–2659. https://doi.org/10.1093/pcp/pcz201.

Alonso, J.M., Stepanova, A.N., Leisse, T.J., Kim, C.J., Chen, H., Shinn, P., Stevenson, D.K., Zimmerman, J., Barajas, P., Cheuk, R., et al. (2003). Genome-wide insertional mutagenesis of Arabidopsis thaliana. Science (1979) *301*, 653–657. https://doi.org/10.1126/science.1086391.

Åstrand, J., Knight, C., Robson, J., Talle, B., and Wilson, Z.A. (2021). Evolution and diversity of the angiosperm anther: trends in function and development. Plant Reproduction *34*, 307–319. https://doi.org/10.1007/s00497-021-00416-1.

Barnes, W.J., and Anderson, C.T. (2018). Cytosolic invertases contribute to cellulose biosynthesis and influence carbon partitioning in seedlings of Arabidopsis thaliana. Plant Journal *94*, 956–974. https://doi.org/10.1111/tpj.13909.

Barratt, D.H.P.P., Derbyshire, P., Findlay, K., Pike, M., Wellner, N., Lunn, J., Feil, R., Simpson, C., Maule, A.J., and Smith, A.M. (2009). Normal growth of Arabidopsis requires cytosolic invertase but not sucrose synthase. Proc Natl Acad Sci U S A *106*, 13124–13129. https://doi.org/10.1073/pnas.0900689106.

Bassil, E., Tajima, H., Liang, Y.C., Ohto, M. aki, Ushijima, K., Nakano, R., Esumi, T., Coku, A., Belmonte, M., and Blumwald, E. (2011). The arabidopsis Na+/H+ antiporters NHX1 and NHX2 control vacuolar ph and K+ homeostasis to regulate growth, flower development, and reproduction. Plant Cell *23*, 3482–3497. https://doi.org/10.1105/tpc.111.089581.

Beauzamy, L., Nakayama, N., and Boudaoud, A. (2014). Flowers under pressure: Ins and outs of turgor regulation in development. Annals of Botany *114*, 1517–1533. https://doi.org/10.1093/aob/mcu187.

Berardini, T.Z., Reiser, L., Li, D., Mezheritsky, Y., Muller, R., Strait, E., and Huala, E. (2015). The arabidopsis information resource: Making and mining the “gold standard” annotated reference plant genome. Genesis *53*, 474–485. https://doi.org/10.1002/dvg.22877.

Berendzen, K., Searle, I., Ravenscroft, D., Koncz, C., Batschauer, A., Coupland, G., Somssich, I.E., and Ülker, B. (2005). A rapid and versatile combined DNA/RNA extraction protocol and its application to the analysis of a novel DNA marker set polymorphic between Arabidopsis thaliana ecotypes Col-0 and Landsberg erecta. Plant Methods *1*, 4. https://doi.org/10.1186/1746-4811-1-4.

Bonner, L.J., and Dickinson, H.G. (1990). Anther dehiscence in Lycopersicon esculentum II. Water relations. New Phytologist *115*, 367–375. https://doi.org/10.1111/j.1469-8137.1990.tb00463.x.

Bots, M., Vergeldt, F., Wolters-Arts, M., Weterings, K., Van As, H., and Mariani, C. (2005). Aquaporins of the PIP2 class are required for efficient anther dehiscence in tobacco. Plant Physiology *137*, 1049–1056. https://doi.org/10.1104/pp.104.056408.

de Coninck, B., le Roy, K., Francis, I., Clerens, S., Vergauwen, R., Halliday, A.M., Smith, S.M., van Laere, A., and van den Ende, W. (2005). Arabidopsis AtcwINV3 and 6 are not invertases but are fructan exohydrolases (FEHs) with different substrate specificities. Plant, Cell and Environment *28*, 432–443. https://doi.org/10.1111/j.1365-3040.2004.01281.x.

Dawson, J., Sözen, E., Vizir, I., van Waeyenberge, S., Wilson, Z.A., and Mulligan, B.J. (1999). Characterization and genetic mapping of a mutation (ms35) which prevents anther dehiscence in Arabidopsis thaliana by affecting secondary wall thickening in the endothecium. New Phytologist *144*, 213–222. https://doi.org/10.1046/j.1469-8137.1999.00507.x.

Dennis, R. (2017). Analysis of anther dehydration ; a process required for anther dehiscence and pollen release. University of Nottingham.

Dereeper, A., Guignon, V., Blanc, G., Audic, S., Buffet, S., Chevenet, F., Dufayard, J.F., Guindon, S., Lefort, V., Lescot, M., et al. (2008). Phylogeny.fr: robust phylogenetic analysis for the non-specialist. Nucleic Acids Res *36*, W465-9. https://doi.org/10.1093/nar/gkn180.

Fei, J., Tan, S., Zhang, F., Hua, L., Liao, Y., Fang, W., Chen, F., and Teng, N. (2016). Morphological and physiological differences between dehiscent and indehiscent anthers of Chrysanthemum morifolium. Journal of Plant Research *129*, 1069–1082. https://doi.org/10.1007/s10265-016-0854-8.

Ferguson, A.C., Pearce, S., Band, L.R., Yang, C., Ferjentsikova, I., King, J., Yuan, Z., Zhang, D., and Wilson, Z.A. (2017). Biphasic regulation of the transcription factor ABORTED MICROSPORES (AMS) is essential for tapetum and pollen development in Arabidopsis. New Phytologist *213*, 778–790. https://doi.org/10.1111/nph.14200.

García, C.C., Nepi, M., and Pacini, E. (2006). Structural aspects and ecophysiology of anther opening in Allium triquetrum. Annals of Botany *97*, 521–527. https://doi.org/10.1093/aob/mcl015.

Ge, Y.X., Angenent, G.C., Wittich, P.E., Peters, J., Franken, J., Busscher, M., Zhang, L.M., Dahlhaus, E., Kater, M.M., Wullems, G.J., et al. (2000). NEC1, a novel gene, highly expressed in nectary tissue of Petunia hybrida. Plant Journal *24*, 725–734. https://doi.org/10.1046/j.1365-313X.2000.00926.x.

Ge, Y.X., Angenent, G.C., Dahlhaus, E., Franken, J., Peters, J., Wullems, G.J., and Creemers-Molenaar, J. (2001). Partial silencing of the NEC1 gene results in early opening of anthers in Petunia hybrida. Molecular and General Genetics *265*, 414–423. https://doi.org/10.1007/s004380100449.

Guo, X., Li, L., Liu, X., Zhang, C., Yao, X., Xun, Z., Zhao, Z., Yan, W., Zou, Y., Liu, D., et al. (2022). MYB2 Is Important for Tapetal PCD and Pollen Development by Directly Activating Protease Expression in Arabidopsis. International Journal of Molecular Sciences *23*. https://doi.org/10.3390/ijms23073563.

Haeussler, M., Schönig, K., Eckert, H., Eschstruth, A., Mianné, J., Renaud, J.B., Schneider-Maunoury, S., Shkumatava, A., Teboul, L., Kent, J., et al. (2016). Evaluation of off-target and on-target scoring algorithms and integration into the guide RNA selection tool CRISPOR. Genome Biology *17*, 425–428. https://doi.org/10.1186/s13059-016-1012-2.

Haouazine-Takvorian, N., Tymowska-Lalanne, Z., Takvorian, A., Tregear, J., Lejeune, B., Lecharny, A., and Kreis, M. (1997). Characterization of two members of the Arabidopsis thaliana gene family, Atβfruct3 and Atβfruct4, coding for vacuolar invertases. Gene *197*, 239–251. https://doi.org/10.1016/S0378-1119(97)00268-0.

Heslop-Harrison, Y., and Heslop-Harrison, J.S. (1996). Lodicule function and filament extension in the grasses: Potassium ion movement and tissue specialization. Annals of Botany *77*, 573–582. https://doi.org/10.1006/anbo.1996.0072.

Hirsche, J., Engelke, T., Völler, D., Götz, M., and Roitsch, T. (2009a). Interspecies compatibility of the anther specific cell wall invertase promoters from Arabidopsis and tobacco for generating male sterile plants. Theoretical and Applied Genetics *118*, 235–245. https://doi.org/10.1007/s00122-008-0892-2.

Hirsche, J., Engelke, T., Völler, D., Götz, M., Roitsch, T., Voller, D., Gotz, M., and Roitsch, T. (2009b). Interspecies compatibility of the anther specific cell wall invertase promoters from Arabidopsis and tobacco for generating male sterile plants. Theoretical and Applied Genetics *118*, 235–245. https://doi.org/10.1007/s00122-008-0892-2.

Ishiguro, S., Kawai-Oda, A., Ueda, J., Nishida, I., and Okada, K. (2001a). The DEFECTIVE IN ANTHER DEHISCENCE1 Gene Encodes a Novel Phospholipase A1 Catalyzing the Initial Step of Jasmonic Acid Biosynthesis, Which Synchronizes Pollen Maturation, Anther Dehiscence, and Flower Opening in Arabidopsis . The Plant Cell *13*, 2191–2209. https://doi.org/10.1105/tpc.010192.

Ishiguro, S., Kawai-Oda, A., Ueda, J., Nishida, I., and Okada, K. (2001b). The DEFECTIVE IN ANTHER DEHISCENCE1 Gene Encodes a Novel Phospholipase A1 Catalyzing the Initial Step of Jasmonic Acid Biosynthesis, Which Synchronizes Pollen Maturation, Anther Dehiscence, and Flower Opening in Arabidopsis . The Plant Cell *13*, 2191–2209. https://doi.org/10.1105/tpc.010192.

Keijzer, C.J.J. (1987). the Processes of Anther Dehiscence and Pollen Dispersal: I. the Opening Mechanism of Longitudinally Dehiscing Anthers. New Phytologist *105*, 487–498. https://doi.org/10.1111/j.1469-8137.1987.tb00886.x.

Li, J., Foster, R., Ma, S., Liao, S.J., Bliss, S., Kartika, D., Wang, L., Wu, L., Eamens, A.L., and Ruan, Y.L. (2021). Identification of transcription factors controlling cell wall invertase gene expression for reproductive development via bioinformatic and transgenic analyses. Plant Journal *106*, 1058–1074. https://doi.org/10.1111/tpj.15218.

Liao, S., Wang, L., Li, J., and Ruan, Y.L. (2020). Cell wall invertase is essential for ovule development through sugar signaling rather than provision of carbon nutrients. Plant Physiology *183*, 1126–1144. https://doi.org/10.1104/pp.20.00400.

Lou, Y., Gou, J.Y., and Xue, H.W. (2007). PIP5K9, an Arabidopsis phosphatidylinositol monophosphate kinase, interacts with a cytosolic invertase to negatively regulate sugar-mediated root growth. Plant Cell *19*, 163–181. https://doi.org/10.1105/tpc.106.045658.

Lou, Y., Zhou, H.S., Han, Y., Zeng, Q.Y., Zhu, J., and Yang, Z.N. (2018). Positive regulation of AMS by TDF1 and the formation of a TDF1–AMS complex are required for anther development in Arabidopsis thaliana. New Phytologist *217*, 378–391. https://doi.org/10.1111/nph.14790.

Mandaokar, A., Thines, B., Shin, B., Markus Lange, B., Choi, G., Koo, Y.J., Yoo, Y.J., Choi, Y.D., Choi, G., and Browse, J. (2006). Transcriptional regulators of stamen development in Arabidopsis identified by transcriptional profiling. The Plant Journal *46*, 984–1008. https://doi.org/10.1111/j.1365-313X.2006.02756.x.

Martín, M.L., Lechner, L., Zabaleta, E.J., and Salerno, G.L. (2013a). A mitochondrial alkaline/neutral invertase isoform (A/N-InvC) functions in developmental energy-demanding processes in Arabidopsis. Planta *237*, 813–822. https://doi.org/10.1007/s00425-012-1794-8.

Martín, M.L., Lechner, L., Zabaleta, E.J., and Salerno, G.L. (2013b). A mitochondrial alkaline/neutral invertase isoform (A/N-InvC) functions in developmental energy-demanding processes in Arabidopsis. Planta *237*, 813–822. https://doi.org/10.1007/s00425-012-1794-8.

Maruta, T., Otori, K., Tabuchi, T., Tanabe, N., Tamoi, M., and Shigeoka, S. (2010). New insights into the regulation of greening and carbon-nitrogen balance by sugar metabolism through a plastidic invertase. Plant Signaling and Behavior *5*, 1131–1133. https://doi.org/10.4161/psb.5.9.12568.

Meng, L.S., Wei, Z.Q., Cao, X.Y., Tong, C., Lv, M.J., Yu, F., and Loake, G.J. (2020). Cytosolic invertase-mediated root growth is feedback regulated by a glucose-dependent signaling loop. Plant Physiology *184*, 895–908. https://doi.org/10.1104/pp.20.00778.

Meng, L.S., Bao, Q.X., Mu, X.R., Tong, C., Cao, X.Y., Huang, J.J., Xue, L.N., Liu, C.Y., Fei, Y., and Loake, G.J. (2021). Glucose- and sucrose-signaling modules regulate the

Arabidopsis juvenile-to-adult phase transition. Cell Reports *36*, 109348. https://doi.org/10.1016/j.celrep.2021.109348.

Mercier, R.W., and Gogarten, J.P. (1995). A second cell wall acid invertase gene in Arabidopsis thaliana. Plant Physiol *107*, 659–660. https://doi.org/10.1104/pp.107.2.659.

Mitsuda, N., Seki, M., Shinozaki, K., and Ohme-Takagi, M. (2005). The NAC transcription factors NST1 and NST2 of Arabidopsis regulate secondary wall thickenings and are required for anther dehiscence. Plant Cell *17*, 2993–3006. https://doi.org/10.1105/tpc.105.036004.

Mitsuhashi, W., Sasaki, S., Kanazawa, A., Yang, Y.Y., Kamiya, Y., and Toyomasu, T. (2004). Differential expression of acid invertase genes during seed germination in Arabidopsis thaliana. Bioscience, Biotechnology and Biochemistry *68*, 602–608. https://doi.org/10.1271/bbb.68.602.

Nelson, M.R., Band, L.R., Dyson, R.J., Lessinnes, T., Wells, D.M., Yang, C., Everitt, N.M., Jensen, O.E., and Wilson, Z.A. (2012). A biomechanical model of anther opening reveals the roles of dehydration and secondary thickening. New Phytologist *196*, 1030–1037. https://doi.org/10.1111/j.1469-8137.2012.04329.x.

Ni, D.A. (2012a). Role of vacuolar invertase in regulating Arabidopsis stomatal opening. Acta Physiologiae Plantarum *34*, 2449–2452. https://doi.org/10.1007/s11738-012-1036-5.

Ni, D.A. (2012b). Role of vacuolar invertase in regulating Arabidopsis stomatal opening. Acta Physiologiae Plantarum *34*, 2449–2452. https://doi.org/10.1007/s11738-012-1036-5.

Niwa, T., Suzuki, T., Takebayashi, Y., Ishiguro, R., Higashiyama, T., Sakakibaraa, H., and Ishiguro, S. (2018). Jasmonic acid facilitates flower opening and floral organ development through the upregulated expression of SlMYB21 transcription factor in tomato. Bioscience, Biotechnology and Biochemistry *82*, 292–303. https://doi.org/10.1080/09168451.2017.1422107.

O'Malley, R.C., Barragan, C.C., and Ecker, J.R. (2015). A User ' s Guide to the Arabidopsis T-DNA Insertional Mutant Collections. Methods in Molecular Biology 323–342. .

Pearce, S., Ferguson, A., King, J., and Wilson, Z.A. (2015). FlowerNet: A gene expression correlation network for anther and pollen development. Plant Physiology *167*, 1717–1730. https://doi.org/10.1104/pp.114.253807.

Pignocchi, C., Ivakov, A., Feil, R., Trick, M., Pike, M., Wang, T.L., Lunn, J.E., and Smith, A.M. (2021). Restriction of cytosolic sucrose hydrolysis profoundly alters development, metabolism, and gene expression in Arabidopsis roots. Journal of Experimental Botany *72*, 1850–1863. https://doi.org/10.1093/jxb/eraa581.

Qi, X., Wu, Z., Li, J., Mo, X., Wu, S., Chu, J., and Wu, P. (2007). AtCYT-INV1, a neutral invertase, is involved in osmotic stress-induced inhibition on lateral root growth in Arabidopsis. Plant Molecular Biology *64*, 575–587. https://doi.org/10.1007/s11103-007-9177-4.

Quilliam, R.S., Swarbrick, P.J., Scholes, J.D., and Rolfe, S.A. (2006). Imaging photosynthesis in wounded leaves of Arabidopsis thaliana. In Journal of Experimental Botany, pp. 55–69.

Robles, P., and Pelaz, S. (2005). Flower and fruit development in Arabidopsis thaliana. International Journal of Developmental Biology *49*, 633–643. https://doi.org/10.1387/ijdb.052020pr.

Roitsch, T., Balibrea, M.E., Hofmann, M., Proels, R., and Sinha, A.K. (2003). Extracellular invertase: Key metabolic enzyme and PR protein. Journal of Experimental Botany *54*, 513–524. https://doi.org/10.1093/jxb/erg050.

Ruhlmann, J.M., Kram, B.W., and Carter, C.J. (2010a). Cell wall invertase 4 is required for nectar production in Arabidopsis. Journal of Experimental Botany *61*, 395–404. https://doi.org/10.1093/jxb/erp309.

Ruhlmann, J.M., Kram, B.W., and Carter, C.J. (2010b). Cell wall invertase 4 is required for nectar production in Arabidopsis. Journal of Experimental Botany *61*, 395–404. https://doi.org/10.1093/jxb/erp309.

Sanders, P.M., Bui, A.Q., Weterings, K., McIntire, K.N., Hsu, Y.C., Lee, P.Y., Truong, M.T., Beals, T.P., and Goldberg, R.B. (1999). Anther developmental defects in Arabidopsis thaliana male-sterile mutants. Sexual Plant Reproduction *11*, 297–322. https://doi.org/10.1007/s004970050158.

Sanders, P.M., Lee, P.Y., Biesgen, C., Boone, J.D., Beals, T.P., Weiler, E.W., and Goldberg, R.B. (2000). The Arabidopsis DELAYED DEHISCENCE1 gene encodes an enzyme in the jasmonic acid synthesis pathway. Plant Cell *12*, 1041–1061. https://doi.org/10.1105/tpc.12.7.1041.

Schindelin, J., Arganda-Carreras, I., Frise, E., Kaynig, V., Longair, M., Pietzsch, T., Preibisch, S., Rueden, C., Saalfeld, S., Schmid, B., et al. (2012). Fiji: An open-source platform for biological-image analysis. Nature Methods *9*, 676–682. https://doi.org/10.1038/nmeth.2019.

Schwebel-Dugue, N., el Mtili, N., Krivitzky, M., Jean-Jacques, I., Williams, J.H.H., Thomas, M., Kreis, M., and Lecharny, A. (1994). Arabidopsis gene and cDNA encoding cell-wall invertase. Plant Physiology *104*, 809–810. https://doi.org/10.1104/pp.104.2.809.

Sergeeva, L.I., Keurentjes, J.J.B., Bentsink, L., Vonk, J., van der Plas, L.H.W., Koornneef, M., and Vreugdenhil, D. (2006). Vacuolar invertase regulates elongation of Arabidopsis thaliana roots as revealed by QTL and mutant analysis. Proc Natl Acad Sci U S A *103*, 2994–2999. https://doi.org/10.1073/pnas.0511015103.

Sherson, S.M., Alford, H.L., Forbes, S.M., Wallace, G., and Smith, S.M. (2003a). Roles of cell-wall invertases and monosaccharide transporters in the growth and development of Arabidopsis. Journal of Experimental Botany *54*, 525–531. https://doi.org/10.1093/jxb/erg055.

Sherson, S.M., Alford, H.L., Forbes, S.M., Wallace, G., and Smith, S.M. (2003b). Roles of cell-wall invertases and monosaccharide transporters in the growth and development of Arabidopsis. Journal of Experimental Botany *54*, 525–531. https://doi.org/10.1093/jxb/erg055.

Slawinski, L., Israel, A., Artault, C., Thibault, F., Atanassova, R., Laloi, M., and Dédaldéchamp, F. (2021). Responsiveness of Early Response to Dehydration Six-Like Transporter Genes to Water Deficit in Arabidopsis thaliana Leaves. Frontiers in Plant Science *12*, 1–21. https://doi.org/10.3389/fpls.2021.708876.

Smyth, D.R., Bowman, J.L., and Meyerowitz, E.M. (1990). Early Flower Development in Arabidopsis. The Plant Cell *2*, 755. https://doi.org/10.2307/3869174.

Stadler, R., Truernit, E., Gahrtz, M., and Sauer, N. (1999). The AtSUC1 sucrose carrier may represent the osmotic driving force for anther dehiscence and pollen tube growth in Arabidopsis. Plant Journal *19*, 269–278. https://doi.org/10.1046/j.1365-313X.1999.00527.x.

Stintzi, A., and Browse, J. (2000). The Arabidopsis male-sterile mutant, opr3, lacks the 12-oxophytodienoic acid reductase required for jasmonate synthesis. Proc Natl Acad Sci U S A *97*, 10625–10630. https://doi.org/10.1073/pnas.190264497.

Tamoi, M., Tabuchi, T., Demuratani, M., Otori, K., Tanabe, N., Maruta, T., and Shigeoka, S. (2010). Point mutation of a plastidic invertase inhibits development of the photosynthetic apparatus and enhances nitrate assimilation in sugar-treated Arabidopsis seedlings. Journal of Biological Chemistry *285*, 15399–15407. https://doi.org/10.1074/jbc.M109.055111.

Tarkowski, L.P., Tsirkone, V.G., Osipov, E.M., Beelen, S., Lammens, W., Vergauwen, R., van den Ende, W., and Strelkov, S. v. (2020). Crystal structure of Arabidopsis thaliana neutral invertase 2. Acta Crystallographica Section F: Structural Biology Communications *76*, 152–157. https://doi.org/10.1107/S2053230X2000179X.

Thorneycroft, D., Sherson, S.M., and Smith, S.M. (2001). Using gene knockouts to investigate plant metabolism. Journal of Experimental Botany *52*, 1593–1601. https://doi.org/10.1093/jxb/52.361.1593.

Tong, Z., Li, Q., Yang, Y., Dai, F., Gao, J., and Hong, B. (2013). Isolation and expression analysis of LoPIP2, a lily (Lilium Oriental Hybrids) aquaporin gene involved in desiccation-induced anther dehiscence. Scientia Horticulturae *164*, 316–322. https://doi.org/10.1016/j.scienta.2013.09.022.

Vargas, W.A., and Salerno, G.L. (2010). The Cinderella story of sucrose hydrolysis: Alkaline/neutral invertases, from cyanobacteria to unforeseen roles in plant cytosol

and organelles. Plant Science *178*, 1–8. https://doi.org/10.1016/j.plantsci.2009.09.015.

Vargas, W., Cumino, A., and Salerno, G.L. (2003). Cyanobacterial alkaline/neutral invertases. Origin of sucrose hydrolysis in the plant cytosol? Planta *216*, 951–960. https://doi.org/10.1007/s00425-002-0943-x.

Vargas, W.A., Pontis, H.G., and Salerno, G.L. (2008). New insights on sucrose metabolism: Evidence for an active A/N-Inv in chloroplasts uncovers a novel component of the intracellular carbon trafficking. Planta *227*, 795–807. https://doi.org/10.1007/s00425-007-0657-1.

Vu, D.P., Rodrigues, C.M., Jung, B., Meissner, G., Klemens, P.A.W., Holtgräwe, D., Fürtauer, L., Nägele, T., Nieberl, P., Pommerrenig, B., et al. (2020). Vacuolar sucrose homeostasis is critical for plant development, seed properties, and night-time survival in Arabidopsis.

Wang, L., Li, X.R., Lian, H., Ni, D.A., He, Y.K., Chen, X.Y., and Ruan, Y.L. (2010). Evidence that high activity of vacuolar invertase is required for cotton fiber and arabidopsis root elongation through osmotic dependent and independent pathways, respectively. Plant Physiology *154*, 744–756. https://doi.org/10.1104/pp.110.162487.

Wei, D., Liu, M., Chen, H., Zheng, Y., Liu, Y., Wang, X., Yang, S., Zhou, M., and Lin, J. (2018). INDUCER OF CBF EXPRESSION 1 is a male fertility regulator impacting anther dehydration in Arabidopsis.

Weiszmann, J., Fürtauer, L., Weckwerth, W., and Nägele, T. (2018). Vacuolar sucrose cleavage prevents limitation of cytosolic carbohydrate metabolism and stabilizes photosynthesis under abiotic stress. FEBS Journal *285*, 4082–4098. https://doi.org/10.1111/febs.14656.

Wilson, Z.A., Song, J., Taylor, B., and Yang, C. (2011). The final split: The regulation of anther dehiscence. Journal of Experimental Botany *62*, 1633–1649. https://doi.org/10.1093/jxb/err014.

Xiang, L., le Roy, K., Bolouri-Moghaddam, M.R., Vanhaecke, M., Lammens, W., Rolland, F., and van den Ende, W. (2011a). Exploring the neutral invertase-oxidative stress defence connection in Arabidopsis thaliana. Journal of Experimental Botany *62*, 3849–3862. https://doi.org/10.1093/jxb/err069.

Xiang, L., Li, Y., Rolland, F., and van den Ende, W. (2011b). Neutral invertase, hexokinase and mitochondrial ROS homeostasis: Emerging links between sugar metabolism, sugar signaling and ascorbate synthesis. Plant Signaling and Behavior *6*, 1567–1573. https://doi.org/10.4161/psb.6.10.17036.

Xiang, L., le Roy, K., Bolouri-Moghaddam, M.R., Vanhaecke, M., Lammens, W., Rolland, F., and van den Ende, W. (2011c). Exploring the neutral invertase-oxidative

stress defence connection in Arabidopsis thaliana. Journal of Experimental Botany *62*, 3849–3862. https://doi.org/10.1093/jxb/err069.

Xu, J., Ding, Z., Vizcay-Barrena, G., Shi, J., Liang, W., Yuan, Z., Werck-Reichhart, D., Schreiber, L., Wilson, Z.A., and Zhang, D. (2014a). Aborted microspores acts as a master regulator of pollen wall formation in Arabidopsis. Plant Cell *26*, 1544–1556. https://doi.org/10.1105/tpc.114.122986.

Xu, Y., Iacuone, S., Li, S.F., and Parish, R.W. (2014b). MYB80 homologues in Arabidopsis, cotton and Brassica: Regulation and functional conservation in tapetal and pollen development. BMC Plant Biology *14*, 1–14. https://doi.org/10.1186/s12870-014-0278-3.

Yang, C., Vizcay-Barrena, G., Conner, K., and Wilson, Z.A. (2007a). Male Sterility1 is required for tapetal development and pollen wall biosynthesis. Plant Cell *19*, 3530–3548. https://doi.org/10.1105/tpc.107.054981.

Yang, C., Song, J., Ferguson, A.C., Klisch, D., Simpson, K., Mo, R., Taylor, B., Mitsuda, N., and Wilson, Z.A. (2017). Transcription factor MYB26 is key to spatial specificity in anther secondary thickening formation. Plant Physiology *175*, 333–350. https://doi.org/10.1104/pp.17.00719.

Yang, X.Y., Li, J.G., Pei, M., Gu, H., Chen, Z.L., and Qu, L.J. (2007b). Over-expression of a flower-specific transcription factor gene AtMYB24 causes aberrant anther development. Plant Cell Reports *26*, 219–228. https://doi.org/10.1007/s00299-006-0229-z.

Yoshida, T., Anjos, L. dos, Medeiros, D.B., Araújo, W.L., Fernie, A.R., and Daloso, D.M. (2019). Insights into ABA-mediated regulation of guard cell primary metabolism revealed by systems biology approaches. Progress in Biophysics and Molecular Biology *146*, 37–49. https://doi.org/10.1016/j.pbiomolbio.2018.11.006.

Yuan, C., Zhang, S., Hu, R., Wei, D., Tang, Q., Wang, Y., Tian, S., Niu, Y., and Wang, Z. (2021). Comparative transcriptome analysis provides insight into the molecular mechanisms of anther dehiscence in eggplant (Solanum melongena L.). Genomics *113*, 497–506. https://doi.org/10.1016/j.ygeno.2020.12.032.

Zhang, W., Yuan, J., Cheng, T., Tang, M.J., Sun, K., Song, S.L., Xu, F.J., and Dai, C.C. (2019). Flowering-mediated root-fungus symbiosis loss is related to jasmonate-dependent root soluble sugar deprivation. Plant Cell and Environment *42*, 3208–3226. https://doi.org/10.1111/pce.13636.

Zhu, E., You, C., Wang, S., Cui, J., Niu, B., Wang, Y., Qi, J., Ma, H., and Chang, F. (2015). The DYT1-interacting proteins bHLH010, bHLH089 and bHLH091 are redundantly required for Arabidopsis anther development and transcriptome. Plant Journal *83*, 976–990. https://doi.org/10.1111/tpj.12942.

Appendix

8.1 Material for expression analysis

Table 8-1 Material collected for analysis of changes in invertase expression between wild type buds of increasing ages.

Biological rep.	Flash-frozen samples (buds staged 1-4)	RNA	cDNA	qRT-PCR
Preliminary (*Ler* background)	done	done	done	13/11/15, 07/01/16 07/01/16
BR1Col	22/07/16	13/05/19	-	-
BR2Col	26/08/16	-	-	-
BR3Col	18/06/19	-	-	-

Table 8-2 Material collected for expression analysis of invertases in JA-deficient mutant *dad1*

Biological rep.	Corresponding WT control	Flash-frozen samples (buds staged 1-4)	RNA	cDNA	qRT-PCR
preliminary	*Ler*	done	done	done	15/01/16 22/02/16
BR1dad	BR1Col	22/07/16	13/05/19	-	-
BR2dad	BR2Col	26/08/16	-	-	-
BR3dad	BR3Col	18/06/19	-	-	-

Table 8-3 Material collected for expression analysis of invertase genes in single KO lines

Biological rep.	Flash-frozen samples (whole inflorescence)	RNA	cDNA	qRT-PCR
preliminary	done	done	done	10/12/15 and 20/05/16
BR1ko	22/07/16	-	-	-
BR2ko	16/10/16	-	-	-
BR3ko	19/12/16	03/09/18	5/21	

8.2 Gene maps

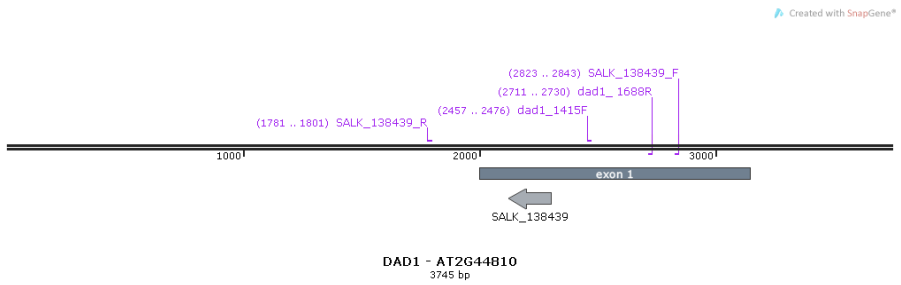

Figure 8-1. Map of *DAD1* showing the location of primers used and the location of the T-DNA insert in the available KO line.

Figure created with SnapGene software (from GSL Biotech; available at snapgene.com)

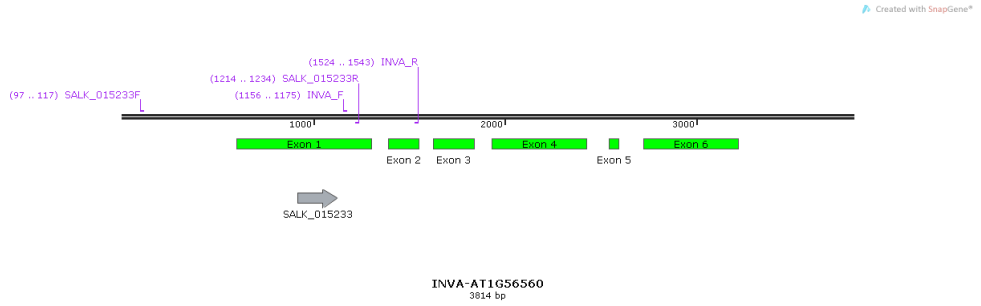

Figure 8-2. Map of *INVA* showing the location of primers used and the location of the T-DNA insert in the available KO line.

Figure created with SnapGene software (from GSL Biotech; available at snapgene.com)

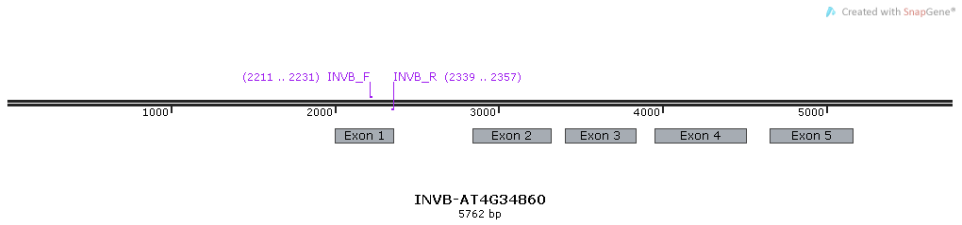

Figure 8-3. Map of *INVB* showing the location of primers used.

Figure created with SnapGene software (from GSL Biotech; available at snapgene.com)

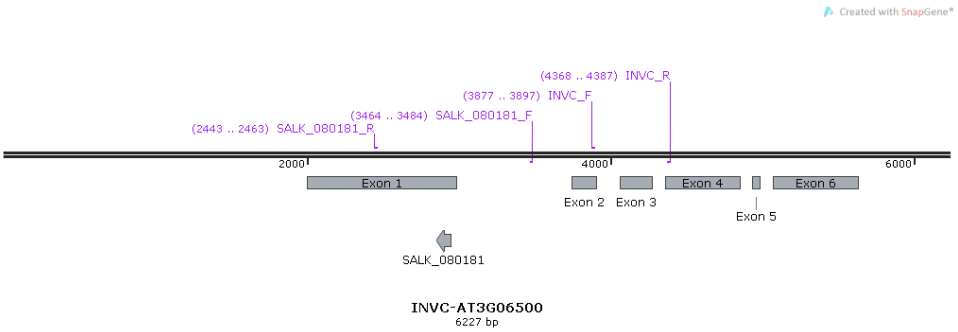

Figure 8-4. Map of *INVC* showing the location of primers used and the location of the T-DNA insert in the available KO line.

Figure created with SnapGene software (from GSL Biotech; available at snapgene.com)

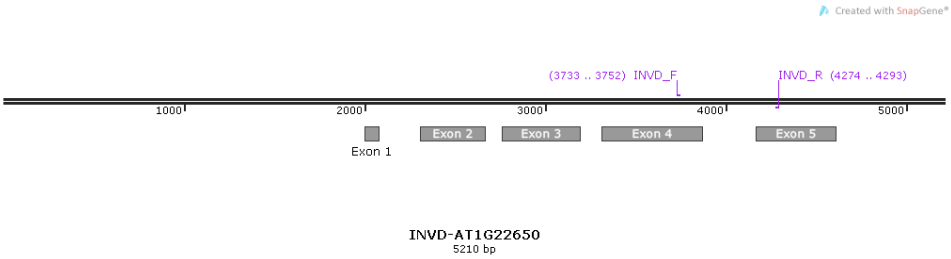

Figure 8-5. Map of *INVD* showing the location of primers used.

Figure created with SnapGene software (from GSL Biotech; available at snapgene.com)

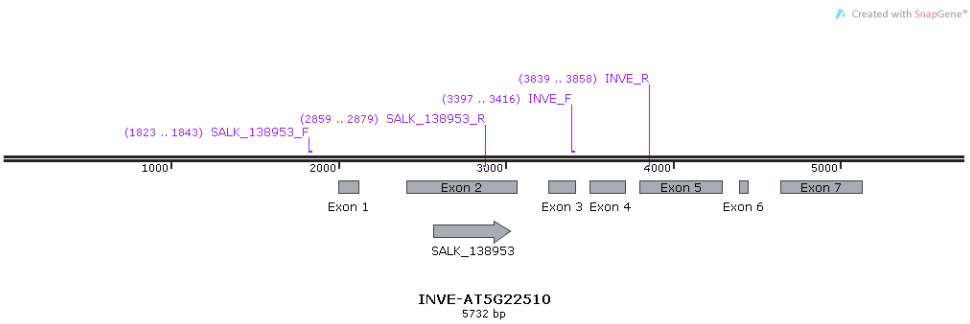

Figure 8-6. Map of *INVE* showing the location of primers used and the location of the T-DNA insert in the available KO line.

Figure created with SnapGene software (from GSL Biotech; available at snapgene.com)

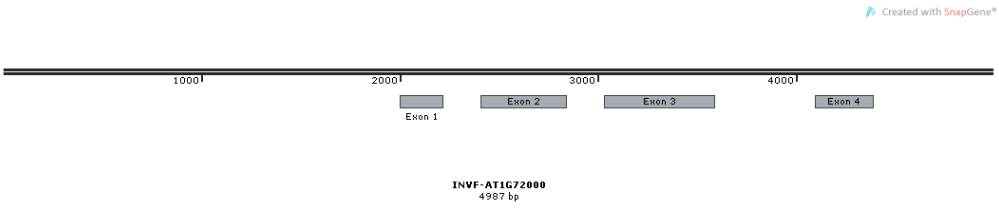

Figure 8-7. Map of *INVF*.

Figure created with SnapGene software (from GSL Biotech; available at snapgene.com)

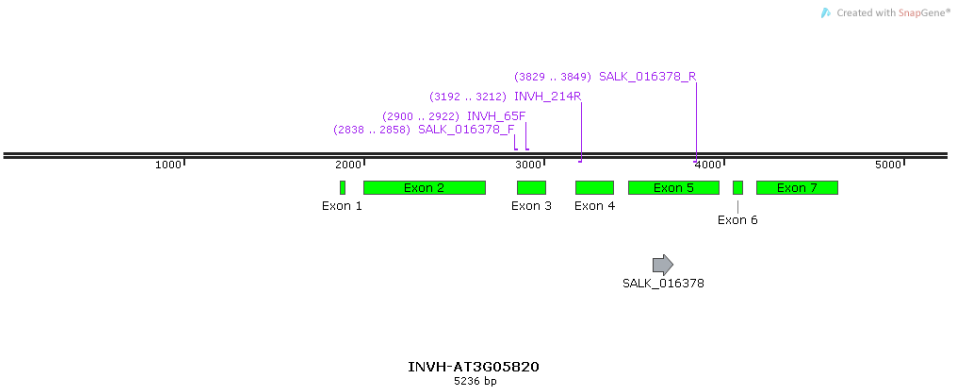

Figure 8-8. Map of *INVH* showing the location of primers used and the location of the T-DNA insert in the available KO line.

Figure created with SnapGene software (from GSL Biotech; available at snapgene.com)

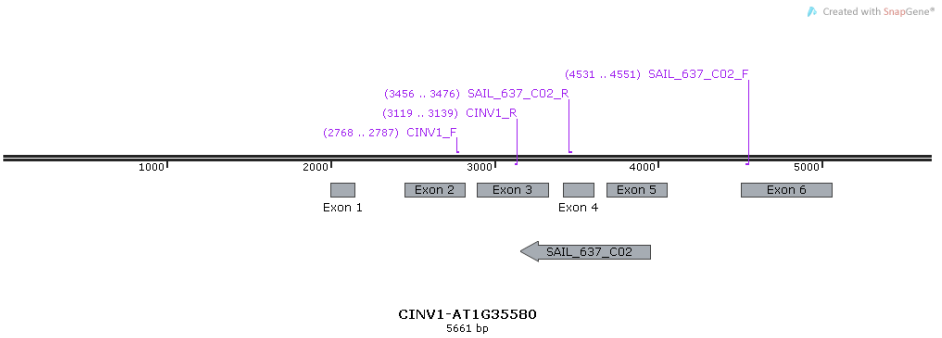

Figure 8-9. Map of *CINV1* showing the location of primers used and the location of the T-DNA insert in the available KO line.

Figure created with SnapGene software (from GSL Biotech; available at snapgene.com)

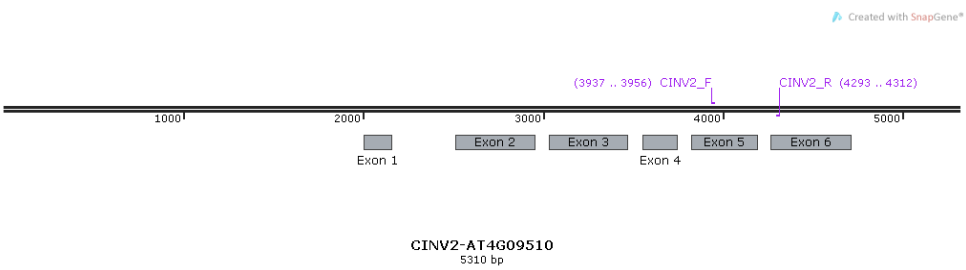

Figure 8-10. Map of *CINV2* showing the location of primers used.

Figure created with SnapGene software (from GSL Biotech; available at snapgene.com)

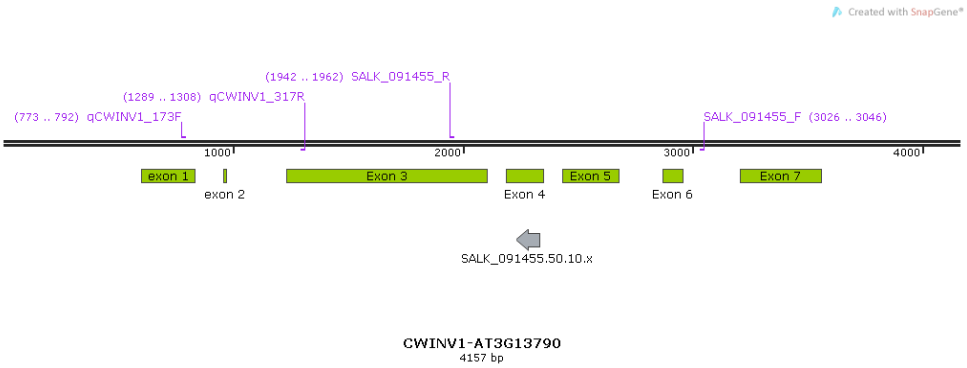

Figure 8-11. Map of *CWINV1* showing the location of primers used and the location of the T-DNA insert in the available KO line.

Figure created with SnapGene software (from GSL Biotech; available at snapgene.com)

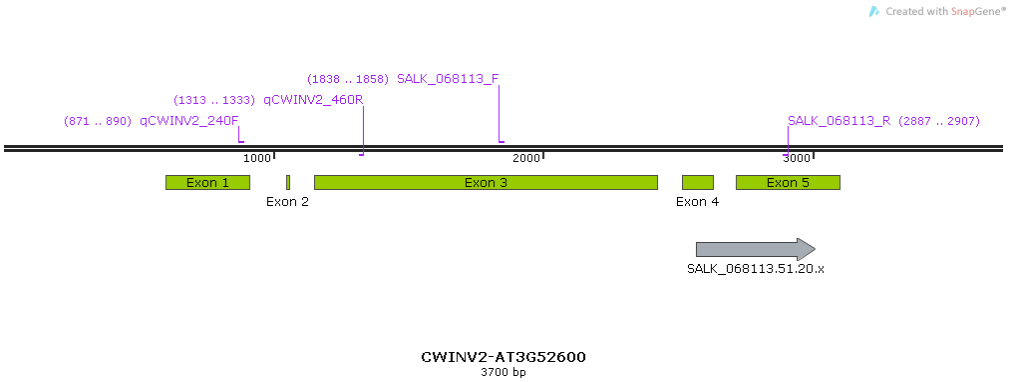

Figure 8-12. Map of *CWINV2* showing the location of primers used and the location of the T-DNA insert in the available KO line.

Figure created with SnapGene software (from GSL Biotech; available at snapgene.com)

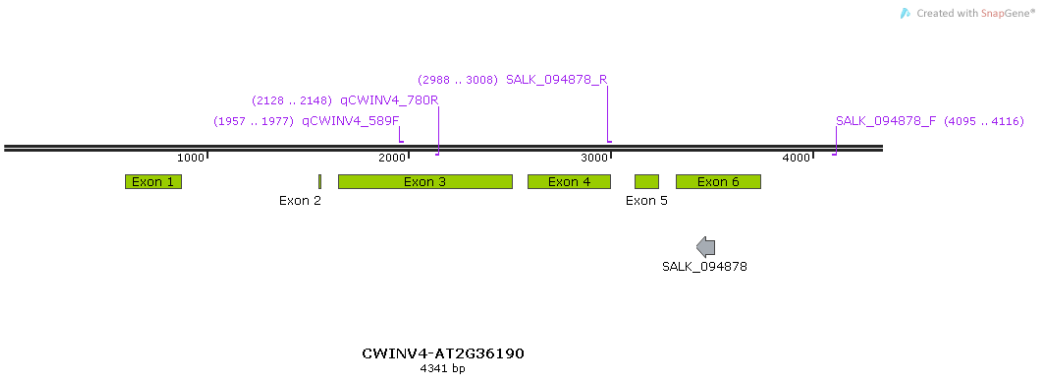

Figure 8-13. Map of *CWINV4* showing the location of primers used and the location of the T-DNA insert in the available KO line.

Figure created with SnapGene software (from GSL Biotech; available at snapgene.com)

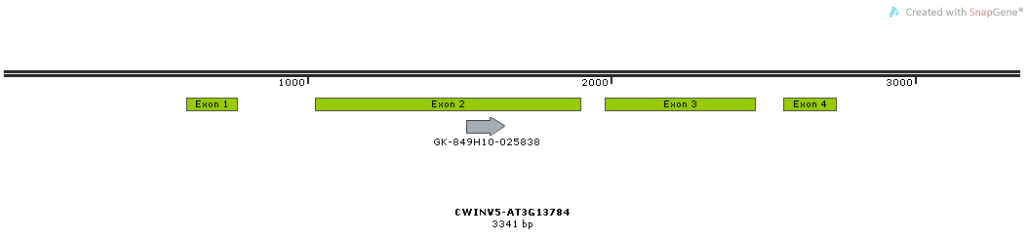

Figure 8-14. Map of *CWINV5* showing the location of the T-DNA insert in the available KO line.

Figure created with SnapGene software (from GSL Biotech; available at snapgene.com)

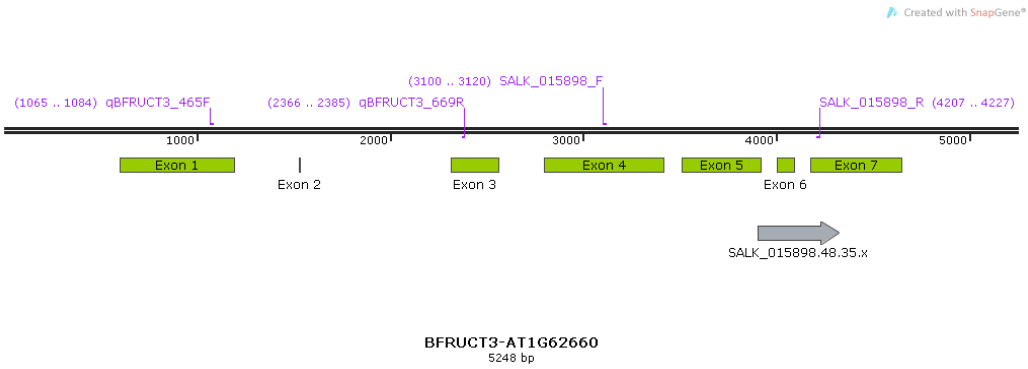

Figure 8-15. Map of *BFRUCT3* showing the location of primers used and the location of the T-DNA insert in the available KO line.

Figure created with SnapGene software (from GSL Biotech; available at snapgene.com)

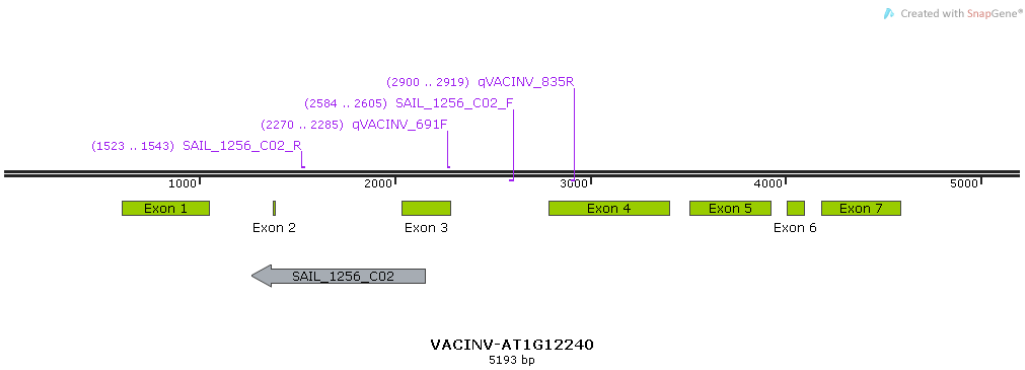

Figure 8-16. Map of *VACINV* showing the location of primers used and the location of the T-DNA insert in the available KO line.

Figure created with SnapGene software (from GSL Biotech; available at snapgene.com)

8.3 Construct Maps

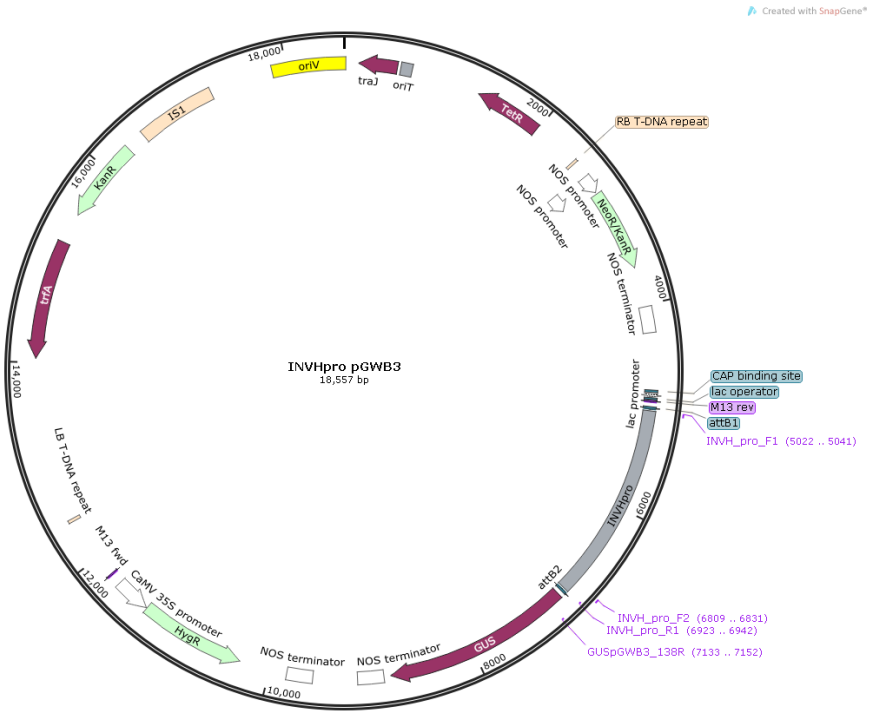

Figure 8-17. Map of pGWB3 destination vector containing the INVH promoter.

Figure created with SnapGene software (from GSL Biotech; available at snapgene.com)

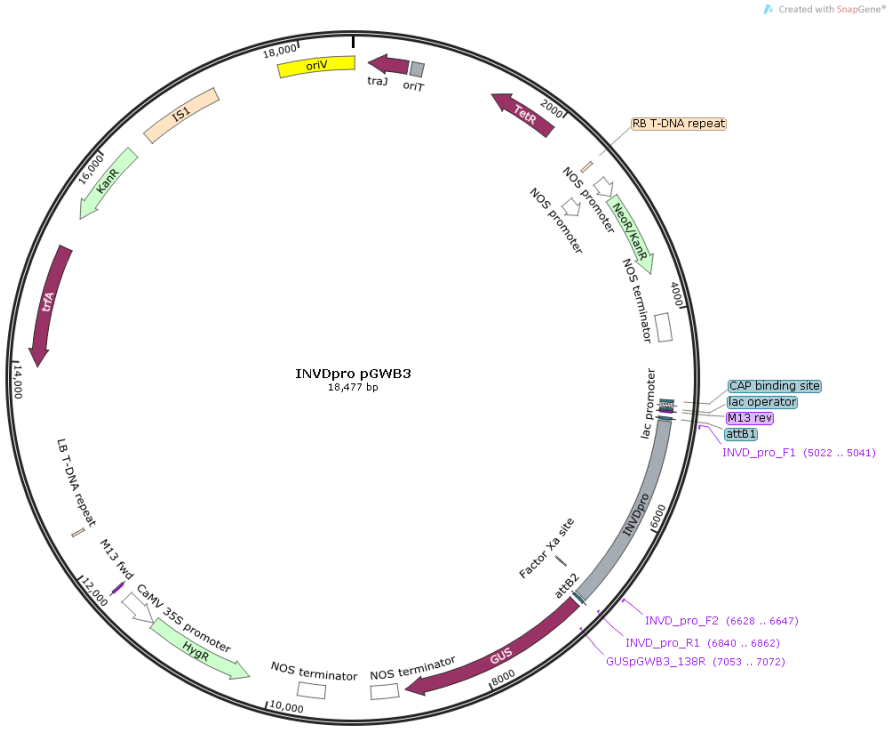

Figure 8-18. Map of pGWB3 destination vector containing the INVD promoter.

Figure created with SnapGene software (from GSL Biotech; available at snapgene.com)

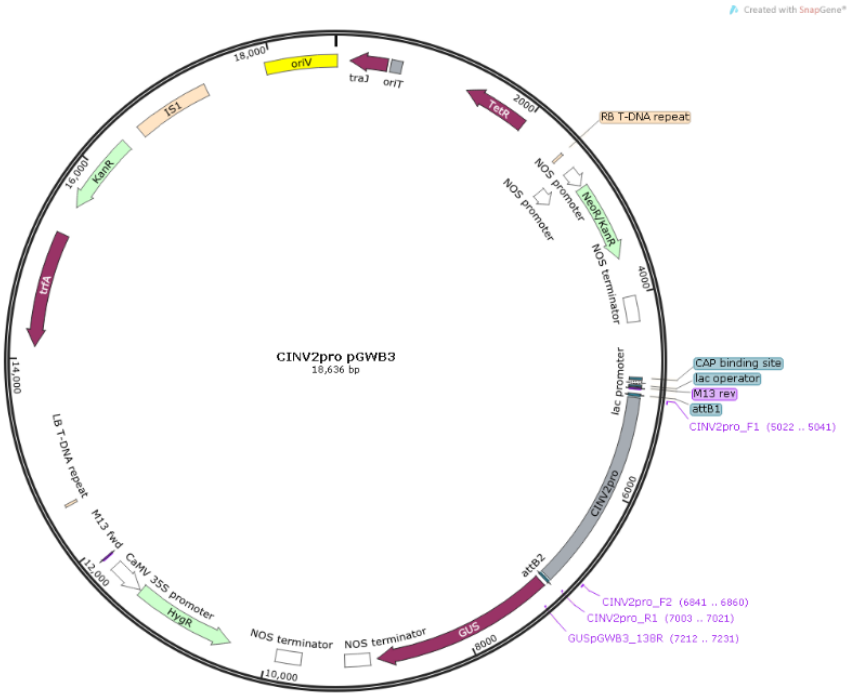

Figure 8-19. Map of pGWB3 destination vector containing the CINV2 promoter.

Figure created with SnapGene software (from GSL Biotech; available at snapgene.com)

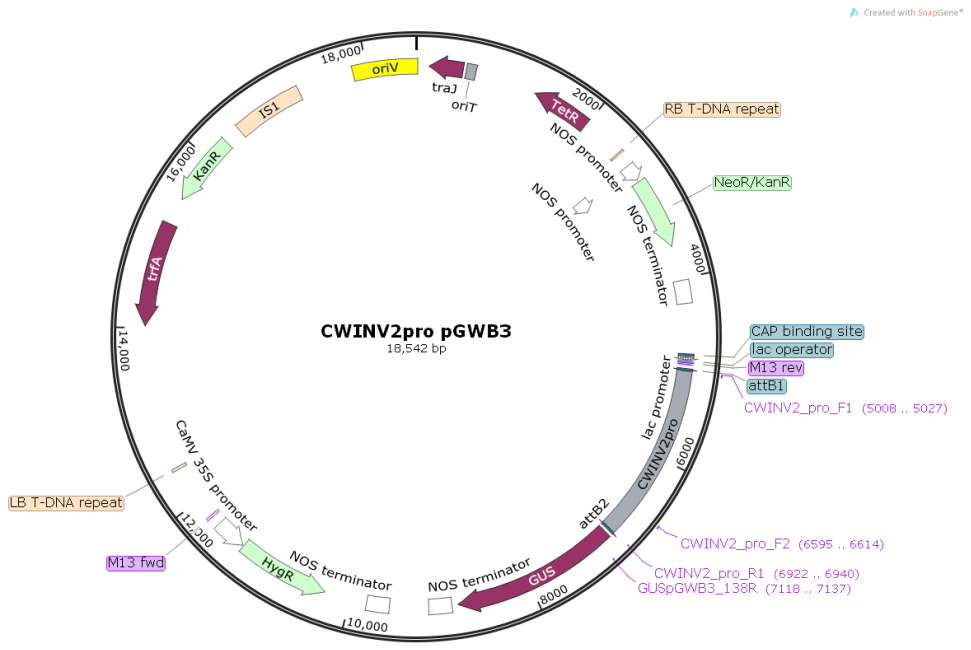

Figure 8-20. Map of pGWB3 destination vector containing the CWINV2 promoter.

Figure created with SnapGene software (from GSL Biotech; available at snapgene.com)

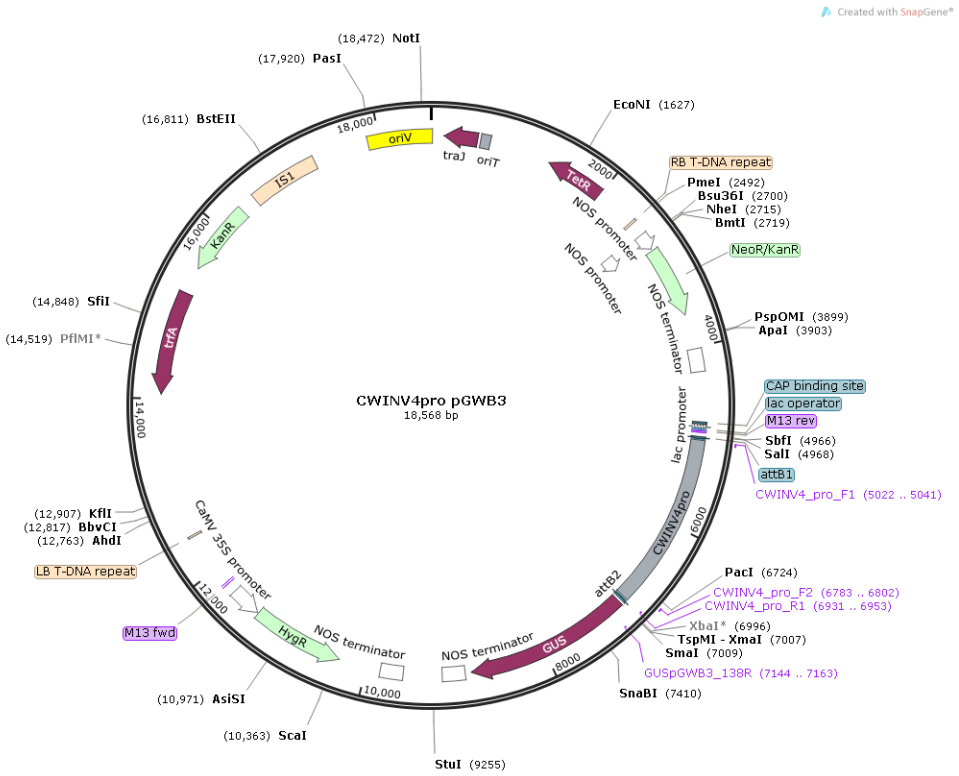

Figure 8-21. Map of pGWB3 destination vector containing the CWINV4 promoter.

Figure created with SnapGene software (from GSL Biotech; available at snapgene.com)

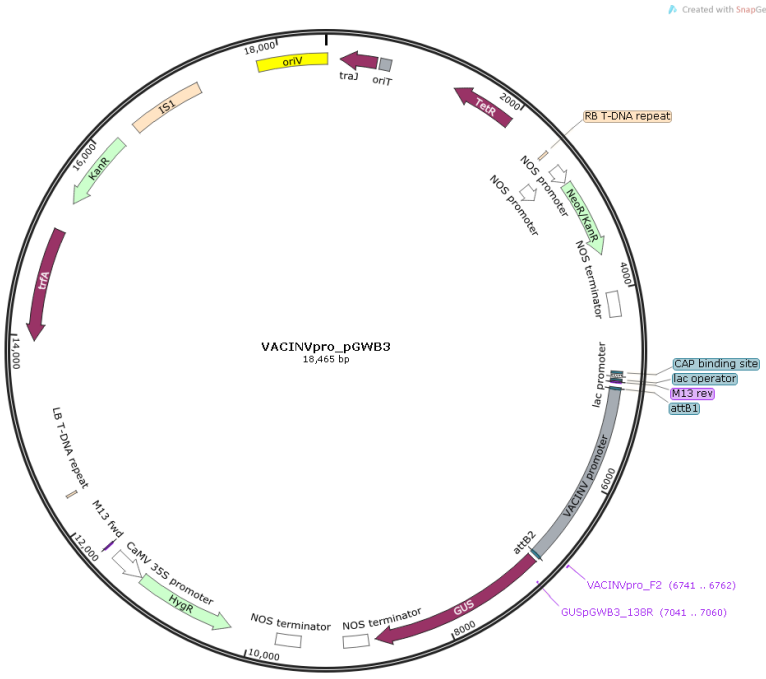

Figure 8-22. Map of pGWB3 destination vector containing the VACINV promoter.

Figure created with SnapGene software (from GSL Biotech; available at snapgene.com)